



**SCIENTIFIC COMMITTEE
ELEVENTH REGULAR SESSION**
Pohnpei, Federated States of Micronesia
5–13 August 2015

Standardized CPUE for south Pacific albacore tuna (*Thunnus alalunga*) from
operational longline data

WCPFC-SC11-2015/SA-IP-03

L. Tremblay-Boyer¹, S. McKechnie, S. J. Harley

¹Oceanic Fisheries Programme, Secretariat of the Pacific Community

Contents

1	Introduction	4
2	Methods	5
2.1	Description of dataset and initial cleaning	5
2.2	Clustering	6
2.3	Data filtering for GLM	7
2.4	GLMs	8
2.4.1	Error distributions	8
2.4.2	Negative binomial error distribution	8
2.4.3	Delta-lognormal/hurdle models	8
2.5	Model fit and comparison	9
2.6	Model selection	10
2.7	Calculation of standardized indices of relative abundance for the negative binomial and delta-lognormal models	10
2.8	Estimation of coefficients of variation	11
3	Results	11
3.1	Cluster analysis	11
3.2	Standardized indices	12
4	Discussion	13
4.1	Data used in the analysis	14
4.2	Improvements on standardization	15
4.2.1	Cluster analysis	15
4.2.2	Vessel effects	15
4.2.3	Uneven sampling of cells over time	16
4.2.4	Additional avenues for research	17
A	Appendix	89

Executive summary

This report documents the estimation of standardised catch-per-unit-effort (CPUE) indices that are used in the 2015 stock assessment of South Pacific Albacore. The analyses are performed on an extensive, operational-level, longline fishing dataset, that combines records provided by distant water fishing nations and records held by SPC (including those for fleets and EEZs of the Pacific Island Countries and Territories). This has provided considerably higher temporal and spatial coverage of data than the datasets used for previous standardisations of albacore CPUE.

The standardisation process involved; grooming the dataset to remove missing data, erroneous data and data from vessels that were only present in the dataset for a very short period of time, using clustering analyses to identify records targeting albacore, filtering out data where the clustering predicted significant non-albacore-targeting activity, fitting generalised linear models to the filtered dataset to estimate relative abundance of albacore, and checking the fit and assumptions of the modelling and exploring alternative indices with differing assumptions.

Clustering analyses identified significant changes in putative targeting practices over time in most of the stock assessment regions. In general, the temperate regions were dominated by albacore targeting with some targeting of alternative species such as swordfish or yellowfin. Fishing in the tropical regions was largely attributed to yellowfin and bigeye targeting with some albacore targeting on the southern boundaries.

The nominal indices of relative abundance display significant, rapid declines in abundance early in the 1960s–70s before stabilising latter in the time series when trends become more region-specific and range from slight increases to moderate declines in abundance. Standardised indices were often substantially different from the nominal indices with the nature of the differences being region-specific.

We discuss several avenues of research that will likely improve the estimation of CPUE indices for use in future stock assessments of South Pacific Albacore. These include addressing variation in spatio-temporal trends within regions, which could have a significant influence on abundance indices, if present, particularly in the early part of the time series where spatial coverage of the dataset is poor. Furthermore, we recommend investigation of the relationship between the occurrence of fishing and CPUE, as there is wide-spread evidence of vessels in some fleets remaining in-port during periods of low CPUE, and only fishing once CPUE of other vessels attains economically favourable levels. This phenomenon can potentially lead to hyper-stability of estimated CPUE indices, and if it is occurring for albacore, then methods to alleviate the problem are required.

1 Introduction

Catch-per-unit-effort (CPUE) data provide our main insight into historical trends in the abundance of tuna populations in the Pacific, and as such play a key role in stock assessments. Several factors can introduce bias in the relationship between CPUE and abundance, especially in the Pacific where there has been ongoing improvements in fishing techniques, as well as changes in the composition of fishing fleets and their targeting strategies. Here we present standardized CPUE indices for south Pacific albacore (*Thunnus alalunga*) derived from operational longline catch-and-effort data for national and distant-water fleets, using a new expanded dataset.

For this process, operational-level fisheries data, where observations are provided at the scale of individual fishing sets, are preferred to data at coarser resolutions as they allow analyses to better account for sources of bias when producing standardized indices of abundance. For instance it is easier to identify a species targeted in a set with operational-level data than with data aggregated at the month \times 5-degree cell level. This is important because we typically want to retain fishing sets that target the focal species, as indices built from a mixture of targeting and non-targeting sets may not reflect true trends in abundance, especially if the proportion of sets targeting the focal species changes over space or time, as is often seen in the Pacific.

In previous assessments for South Pacific Albacore, a limited amount of operational-level data were available to the SPC, such that standardizations were based on either a subset of the operational set data available (Bigelow and Hoyle, 2012) or a mixture of operational and aggregated data (Hoyle and Okamoto, 2011). At the WCPFC Scientific committee in 2014, the distant water fishing nations (DWFNs) of China, Chinese Taipei, Korea, Japan, and the United States agreed to give the SPC access to the operational-level data for their fleets for the Pacific-wide bigeye assessment (McKechnie et al., 2015a). Subsequently, during the data workshop (OFP, 2015b), China, Chinese Taipei, Korea, and the United States extended data access to include the albacore CPUE standardization. The standardized indices presented here thus come from the operational set data provided by these countries, combined with SPC holdings (including those for fleets and EEZs of the Pacific Island Countries and Territories—PICTs).

This year’s albacore stock assessment implements many different features to the assessment model used in 2012 (Hoyle et al., 2012), most notably we define 8 new model regions for which CPUE indices are estimated separately (see map in Figure 1). Corresponding to previous analyses, we attempt to account for changes in targeting as well as control for individual vessel performance.

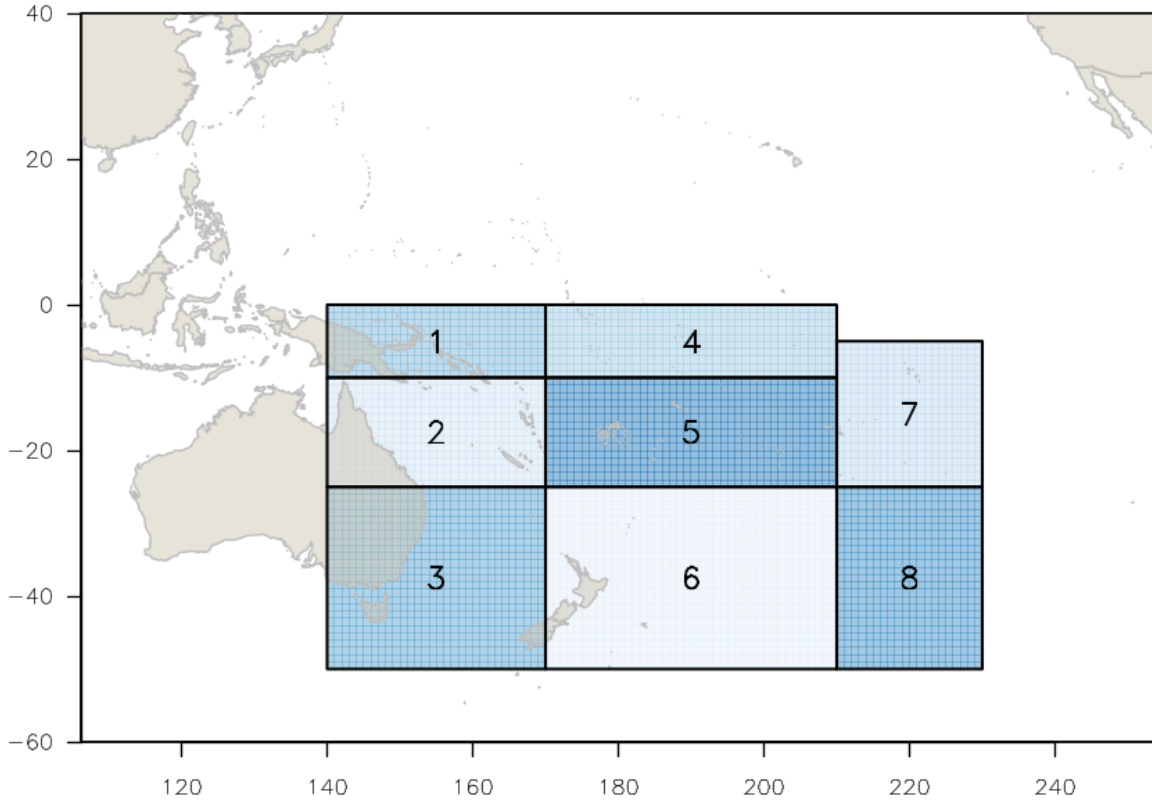


Figure 1: Region definitions for the 2015 South Pacific albacore stock assessment. CPUE indices are standardized for each region separately

2 Methods

2.1 Description of dataset and initial cleaning

We use the term operational-level longline data to refer to records of fishing activity at the scale of the longline set, characterized by the date and location of that set, the vessel, the effort deployed (here in number of hooks), the catch in numbers by species that resulted from this longline set, and, when available, relevant operational characteristics of the longline set such as the number of hooks-between-floats (HBF). The dataset includes catches of the four species most likely to be targeted in longline operations: albacore tuna (ALB), bigeye tuna (BET), yellowfin tuna (YFT), and swordfish (SWO). We are deriving CPUE for albacore tuna, but having access to the catches of all four species yields insight into the vessel’s targeting behaviour, and can inform the exclusion, or retention, of the set in the standardization analyses. Table 1 summarizes the variables present in the dataset.

The first level of data grooming was applied to remove sets outside of the temporal or spatial span

of the analysis, or with improbable records. Sets with missing logdates, sets with 0 hooks, sets where there were more albacore caught than the number of hooks, sets from years before 1960, sets outside of the regions defined for the stock assessment, and sets where there was not at least one individual of alb, bet, yft or swo caught, were all excluded from the dataset. After this initial cleaning we were left with 2,115,139 records and the availability of potential predictor variables for use in GLMs is shown in Table 1.

Table 1: Summary and coverage of potential explanatory variables available in the dataset

Variable	% records	Retained in GLM	Note
Date of set	100	No	
Year	100	Yes	Used in clustering
Quarter	100	Yes	
Month	100	No	Used in clustering
Geographic coordinate (1° or 5°)	100	Yes	
Vessel identification	100	Yes	Used in clustering
Hooks-between-floats, HBF	49	No	
Set start time	38	No	
Effort in hooks	100	Yes	

2.2 Clustering

The first step of the analysis was to assign individual longline sets to a species targeting group, so that non-albacore targeting sets could be excluded from the standardization. We used clustering to classify sets, assuming that in general, sets that target a specific species should have a higher proportion of that species in their catch. Cluster analysis has been recommended by several authors to formally generate this set-wise classification (He et al., 1997; Hoyle et al., 2014), and has been used in previous standardization of bigeye and albacore CPUE in the WCPO (Bigelow and Hoyle, 2012). The clustering analysis relied on the aggregated proportion of the four available species (ALB, BET, SWO and YFT) caught by the same vessel in a given month-year in a region (considered to be a ‘trip’ for the purpose of clustering). Unlike previous CPUE standardization analyses for South Pacific ALB (Bigelow and Hoyle, 2012), we had access to swordfish catches and chose to include these as there appeared to be significant swordfish targeting events within the dataset. Set composition was aggregated at the trip-level (i.e. vessel \times month) to remove between sets variations in catch, and better reflect the vessel’s overall targeting strategy. We used this level of aggregation instead of actual fishing trips as some these can extend over multiple months and target switching may occur over this period (see McKechnie et al. (2015b) for more details on the choice of “trip” for clustering).

Based on previous analyses on these data by (McKechnie et al., 2015a), we used k-means clustering with the Hartigan-Wong algorithm from the R package stats, which is efficient when working with large datasets. We note, however, that numerous alternative clustering algorithms can be used in

such analyses and changes in the assignment of sets to targeting clusters under different algorithms cannot be ruled out.

The k-means algorithm assigns observations to a pre-set, user-defined number of groups (“clusters”) to maximize the Euclidean distance between the group means (“cluster centre”, the mean proportion of each species in the catch of sets belonging to the cluster). For each region we ran the algorithm with 2, 3 and 4 clusters since we only had 4 variables (one for each target species).

There is no formal criterion to select the “best” number of individual clusters for a dataset. Instead, we based our region-wise selection of cluster numbers on the following considerations:

1. Visual inspection of the relationship between the number of clusters and the proportion of variance explained by including an additional cluster. The point where the increasing curve shows evidence of inflection indicates where the addition of new clusters has little impact on improving the fit to the data.
2. Careful examination of overall, temporal and spatial trends in cluster composition to ensure all key targeting activities over time and space were adequately represented by the chosen number of clusters, while maximizing the number of records available to the standardization (Figures 3–34). Albacore targeting clusters were defined as either having a clear signal of ALB targeting based on the target species composition (>60% albacore in the catch of the cluster centre), or a consistent presence (>20%) of albacore in the catch. In regions where tropical tunas are the main targets, clusters with lower proportions of albacore catch were allowed. If multiple clusters were selected for a region, cluster identity was used as an explanatory categorical factor in the standardization process (see Table 2).

2.3 Data filtering for GLM

As defined in section 2.2, only sets belonging to albacore targeting clusters were used for the GLM analyses (see Table 2). We then applied three layers of filtering to identify, for each region, levels of year-quarters, $5 \times 5^\circ$ cells and vessels that had sufficient sample size to retain for the standardization:

1. Core fleet: Vessels active for at least 4 quarters with a minimum of 20 sets over their activity time-span. This value was chosen to maximize the amount of catch and effort retained over time and space (see Figures 3 to 18), but still have data available to enough quarters to reliably estimate a vessel coefficient. We note that in most regions a high number of vessels were excluded (Figure 2), even with a value of 4 quarters, which is the minimum number of quarters we felt was enough to justify estimating an effect for a given vessel. In contrast, for the CPUE standardization used for the 2015 Pacific-wide bigeye assessment, values of 10 and 15 quarters were used as thresholds to estimate vessel effects (McKechnie et al., 2015b).
2. $5 \times 5^\circ$ cells: A minimum of 20 sets per 5° cell was required to retain sets occurring in this cell and estimating a corresponding cell effect.

3. Year-quarters: A minimum of 50 sets per year-quarter was required to retain sets occurring during this year-quarter and estimating a corresponding year-quarter effect.

We subsequently refer to the sets remaining after these levels of filtering as the core fleet/dataset.

Due to low sample sizes and consequent uncertainty in standardised indices in the early period of the time series we also investigated a truncated time period as a sensitivity analysis. The truncated datasets were simply constructed by filtering out all records before the first quarter of 1976.

2.4 GLMs

Models were fitted using Template Model Builder launched from R (TMB, [Kristensen et al., 2014](#)), as this approach yielded considerable improvements in run-time for large datasets compared to previous CPUE standardizations that relied on R alone.

2.4.1 Error distributions

We used two general models to estimate the relationship between CPUE and explanatory variables: the delta-lognormal (DLN, or hurdle approach) and the negative binomial GLM. In contrast to [McKechnie et al. \(2015a\)](#), we did not also fit the delta-gamma model as they found that it was always outperformed by the DLN for very similar datasets.

2.4.2 Negative binomial error distribution

Albacore catch-in-numbers, n_i , is modelled with effort as an explanatory variable with

$$n_i \sim \text{NegBin}(\mu_i, \theta) \tag{1}$$

$$\log(\mu_i) = \beta_0 + \beta_{yq[i]} + \dots + \beta_H \log h_i \tag{2}$$

where μ_i is the mean albacore catch in count for set i , θ is the size parameter, β_{yq} are the year-quarter coefficients, and ‘...’ are coefficients for the levels of additional factor variables included for set i . Parameter β_H is the coefficient for a linear relationship between log mean count and $\log h_i$, the logarithm of hooks (divided by 100) fished for set i . We parameterize the negative binomial likelihood based on the mean μ_i and variance $V_i = \mu_i + \mu_i^2/\theta$.

2.4.3 Delta-lognormal/hurdle models

The probability of having a set with non-zero catch and the CPUE of the catch when positive are modelled separately using a binomial and a log-normal distribution, respectively. The binomial GLM uses a binary response variable (y_i ; $1 = \geq 1$ fish caught, or a $0 =$ zero fish caught in set i)

$$y_i \sim \text{Bernoulli}(p_i) \tag{3}$$

$$\log\left(\frac{p_i}{1-p_i}\right) = \beta_0 + \beta_{yq[i]} + \dots + \beta_H h_i \tag{4}$$

where p_i is probability of at least one albacore individual being caught in set i , the logit link function is used to express this probability in terms of the linear predictor and the model coefficients have the same interpretation as in section 2.4.2. β_H is the coefficient for the continuous variable of hooks fished (divided by 100) for set i on the natural, rather than log-scale used above for the Negative binomial.

$$\log c_i \sim \text{Normal}(\log \mu_i, \sigma^2) \tag{5}$$

$$\log \mu_i = \beta_0 + \beta_{yq[i]} + \dots \tag{6}$$

where \log is the log-CPUE of ALB (number caught divided by hundred hooks) and the parameters in the linear predictor are interpreted as above.

Because we only retained sets belonging to albacore clusters, in some regions there were very few sets with zero albacore catch, preventing the binomial component of the model from converging. To circumvent this we only used a full hurdle model approach on regions that had a minimum of 10% sets with zero albacore catch in at least 10% of quarters once filtering was applied. For the others, we removed all sets with zero catch and only modelled the positive component of hurdle models, as described in Equation 5.

Table 2: Cluster settings retained for each region for data filtering and GLM analyses

Region	Specified # of cluster	Cluster kept	Cluster added as factor?
1	3	<i>alb1</i>	No
2	3	<i>alb1</i>	No
3	3	<i>alb1</i>	No
4	4	<i>alb1, alb2</i>	Yes
5	3	<i>alb1, alb2</i>	Yes
6	2	<i>alb1</i>	No
7	2	<i>alb1</i>	No
8	2	<i>alb1</i>	No

2.5 Model fit and comparison

Model fit was assessed based on traditional approaches as recommended in Hoyle et al. (2014). We also included new diagnostics not previously utilized for WCPO CPUE analyses. Most notably, the use of quantile residuals (Dunn and Smyth, 1996) instead of Pearson’s or deviance residuals,

Table 3: Final GLM model structure for CPUE standardization by region

Region	Model structure	% deviance
1	yrqtr + cell + vessel + log(hook)	26.3
2	yrqtr + cell + vessel + log(hook)	16.6
3	yrqtr + cell + vessel + log(hook)	60.4
4	yrqtr + cell + cluster + vessel + log(hook)	36.9
5	yrqtr + cell + cluster + vessel + log(hook)	29.5
6	yrqtr + cell + vessel + log(hook)	32.3
7	yrqtr + cell + vessel + log(hook)	33.9
8	yrqtr + cell + vessel + log(hook)	41.1

allows us to generate interpretable residuals from binary or count data used to verify the fit of binomial and negative binomial GLMs. We also simulated data from the fitted GLM models and compared the distribution of the simulated and observed data. If the model is adequate then the simulated data will be similar to those observed, at least for the characteristics of the data that are considered to be important for standardizing CPUE indices.

2.6 Model selection

Apart from year-quarter, the candidate explanatory variables available in the dataset for use in the GLMs are geographic coordinates at the 5° resolution, vessel identification, set start time, hooks-between-floats (HBF) and cluster (for regions where multiple albacore targeting clusters were retained). Set start time and HBF were only available for about 38% and 49% of the pre-filtered data, with uneven coverage in space and time, so were not considered. Given the limited number of explanatory variables available, we elected to retain all of the remaining variables. We verified that these were relevant by fitting a complete model, removing each one of the variables at a time and comparing the proportion of variance explained, AIC values and diagnostics for the model, with and without the variable. Table 3 details the final model structure used for each region.

2.7 Calculation of standardized indices of relative abundance for the negative binomial and delta-lognormal models

Indices were estimated by predicting CPUE for each year-quarter, setting the value of model covariates to the modal level for categorical variables and the mean value for continuous variables. CPUE indices were then normalized by dividing them by their mean across the time period over which they were calculated. Note that for the negative binomial this process yields identical indices to those produced by using only the back-transformed year effects.

2.8 Estimation of coefficients of variation

Current implementations of stock assessments in MFCL are based on user-defined, time-variant, coefficients of variation (CVs) for the relative abundance component of the likelihood (e.g., for bigeye, [Harley et al., 2014](#)). Calculation of these CVs partly relies on the uncertainty in the year-quarter effects of the standardized indices of abundance. The absolute values of these SEs are deemed unimportant since correlation structures in the records of the operational-level longline data are not well accounted for, such that the actual SEs estimated from the GLMs under-represent the true amount of variation in the data. In addition, observation error is only one component of the uncertainty represented in the likelihood. That being said, the *relative* variation between years is considered to be informative. As there are issues with the standard method of estimating year-specific SEs from GLM ([Ianelli et al., 2012](#)), we used an alternative method developed by [Francis \(1999\)](#).

3 Results

3.1 Cluster analysis

The cluster analyses were used to allocate sets to a main target species, with the goal of removing non-albacore targeting sets and ensure that albacore catchability was the same across sets retained for the analysis. This approach is further justified by examining trends in regional nominal CPUE by cluster, which shows important contrasts between albacore and non-albacore targeting clusters (Figures 41 to 48). We include here mean species composition for a set belonging to a given cluster for scenarios with 2, 3 and 4 clusters (Figures 19–33), as well as temporal trends in cluster membership by region (Figures 20–34). These were all examined to decide (1) how many targeting strategies would be allowed by region, and (2) whether cluster would be included as a factor (see Table 2). We give a brief description of key targeting trends by region below, and also display maps of cluster distribution over time under the chosen number of clusters, by region (Figures 35–40).

- Region 1 shows bigeye and yellowfin clusters with no clear trends in membership over time when we assumed two targeting clusters. Adding a third cluster assigns some of the sets from the bigeye cluster to an albacore targeting cluster. Membership in the albacore cluster shows no clear trend over time except for a decline in prevalence before the 1970s. For this region we retained the single albacore targeting cluster identified when allowing 3 targeting strategies (Figures 19 and 20).
- Region 2 shows a high proportion of sets targeting albacore, with a decrease in membership in the 1990s. An additional yellowfin targeting cluster gets separated into a secondary albacore targeting cluster when allowing three clusters, and an additional, smaller, bigeye targeting cluster appears when 4 clusters are used. For this region we kept the main albacore targeting

cluster identified with 3 clusters (Figures 21 and 22).

- Region 3 shows three main target species: yellowfin, albacore and swordfish. Swordfish-targeting emerges when 3 or 4 centres are specified. After a sudden decrease in the proportion of sets targeting albacore around 1985 (but also when there were the fewest trips), the proportion of trips targeting albacore increases slowly over time. For this region we kept the main albacore targeting cluster created when 3 clusters are allowed (Figures 23 and 24).
- Albacore are not a main target species in region 4 which is located in tropical waters. This becomes especially true from the mid-1975s onwards, with bigeye and yellowfin targeting becoming dominant. As such, a clear albacore targeting cluster only emerges when 4 centres are allowed, and sets in this cluster occur mostly in the southern parts of the region. To increase the number of sets available to the analysis, we used 4 centres with the two albacore clusters (*alb1* and *alb2*), and included cluster as a factor in the GLM (Figures 25 and 26).
- Region 5 has a dominant albacore targeting cluster throughout the time-series, as well as a less prevalent yellowfin cluster. Having 3 clusters allows us to distinguish a primary and secondary albacore cluster (*alb1* and *alb2* – the later having a higher proportion of yellowfin). We retained this clustering configuration and included cluster as a factor in subsequent GLMs (Figures 27 and 28).
- Region 6 has clearly defined albacore targeting throughout, with the primary albacore targeting cluster *alb1* having a high proportion of albacore. There is also a swordfish cluster which emerges in the mid-1990s under all configurations. We used 2 clusters and retained the albacore targeting cluster (Figures 29 and 30).
- Region 7 has a mix of albacore, bigeye and, when 3 or more clusters were specified, yellowfin targeting. There is a drop in albacore targeting at the end of the 1980s but it increases again as catches increase in this region in the 1990s. For this region we retained the albacore targeting cluster identified when specifying two targeting strategies (Figures 31 and 32).
- Region 8 had the lowest number of sets among regions. They consist almost entirely of albacore targeting, except for an important swordfish cluster that appears in the mid-2000s. For this region we retained the albacore targeting cluster identified when allowing two targeting clusters (Figures 33 and 34).

3.2 Standardized indices

We applied multiple levels of filtering to improve the quality and reliability of the records included in the dataset before estimating year, cell and vessel effects (see Methods, section 2.3). The temporal trends in nominal CPUE were impacted by this filtering, except for regions 5 and 6 for which the nominal CPUE remained essentially unchanged (Figure 49). As expected, removing non-albacore targeting clusters generally had the most impact on relative trends (see also nominal CPUE by

cluster, Figures 41 to 48). Selecting a core fleet based on a minimum of 4 quarters activity impacts the nominal CPUE, but to a lesser extent. Even with this low threshold for the time-span of vessel fishing activity, a considerable number of vessels were removed from the dataset for each region, especially for regions 1 and 8 (Figure 2). However, the spatial and temporal representation of the remaining vessels matches that of the catch and effort data (spatial: Figures 4 to 18; temporal: Figures 3 to 17).

Step plots (Figures 51 to 58) show the relative change in standardized year-quarter effects by the sequential addition of new explanatory factors to the GLM model. Vessel effects tend to impact the standardized indices the most across regions, and also tend to explain the highest proportion of variation in the data. Residual diagnostic plots and influence/coefficient estimates for the negative binomial distribution are shown in Figures 59 to 74. This distribution performed well across regions and was used to calculate the final standardized indices.

In general, there was a steep decline in nominal CPUE across regions from the 1960s to the mid-1970s (Figure 50). Standardization reduces this trend in some instances (e.g. regions 3, 4, 5 and 7) and can also decrease declines in CPUE in years where the effort increased (e.g. regions 4 and 7). The filters applied to define the core dataset can also result in standardized indices spanning a small portion of the years for which we have records in a region (e.g. Region 1). In general, the relative trends match those seen in previous analyses of South Pacific albacore CPUE (Bigelow and Hoyle, 2012; Hoyle and Okamoto, 2011) though the use of different region definitions prevent more in-depth comparison. The truncation of the dataset from 1976 and subsequent refitting of the standardisation models produced indices with almost identical trends to those from the full time series (Figure 50).

4 Discussion

This analysis develops standardized CPUE indices for South Pacific albacore for the 8 regions used in the 2015 stock assessment. These indices attempt to account for changes in targeting in space and time using clustering, as well as partially controls for technological improvements in fishing efficiency through the inclusion of vessel effects. In general, the trends in the indices shown here are similar to those reported in the 2012 analysis of similar data (Bigelow and Hoyle, 2012), that is, a sharp decline between 1960 and 1975 followed by a levelling off in recent decades, despite a pronounced increase in fishing effort (Williams and Terawasi, 2014).

As a first attempt to correct for the steep, early declines in CPUE being observed in a small number of cells only, we produced an alternative CPUE scenario where regional indices are adjusted over time based on the proportion of cells that have yet to be explored by the fishery. These indices were not retained in final MFCL runs and are described in Section A for reference.

4.1 Data used in the analysis

This is the first time that we have access to an operational dataset of this temporal and spatial extent for the standardization of South Pacific albacore CPUE. Its coverage in the high seas, in particular, is a valuable feature, as SPC holdings tend to only have high coverage within EEZ waters. The access to this dataset resulted from a collaborative effort in data provision between WCPFC member countries as outlined in [OFP \(2015b\)](#). This dataset provides great opportunities to explore how the complex behaviour of longline fishing fleets in the Pacific impact relative trends in abundance derived from catch-and-effort data, an input to which stock assessments in the Pacific can be highly sensitive. The detailed nature of the dataset promotes the development of new approaches to improve the robustness of standardized indices. The size of the dataset, however, also implies that, in the six months we have had available for its study, and together with other contractual obligations by the OFP-SAM team at SPC, there has been little time to try new methods to analyse the data. The use of new approaches requires considerable testing before being considered robust enough to be included in an analysis presented to the WCPFC Scientific Community and/or used to inform management decisions. In addition, the large size of the dataset means that standard analyses like GLMs take much longer to run (or, in some instance, cannot be run altogether with the computers available at the SPC), such that different software approaches have to be used, which may themselves require additional work to implement (e.g. TMB). We give a further overview of the opportunities and challenges provided by this dataset in the discussion of [McKechnie et al. 2015b](#) and argue for the importance of maintaining continuous access to the complete version of the distant-water fleet operational dataset in [OFP 2015a](#).

While the dataset used here was a considerable improvement over those previously available—e.g., the number of sets is about twice what was available for previous standardizations of CPUE for this species (see [Bigelow and Hoyle 2012](#))—there were still important components missing which may have hindered the estimation of robust indices of abundance. Most notably, we did not have access to non-SPC-held Japanese operational data, which make up most of the effort in many of the stock assessments regions early in the time-series. Given the issues in the relative trends observed early in the time-series we stress that it is key to have access to as much of the fisheries data for this period as possible. This would also improve temporal and spatial coverage, as for less fished regions, many levels of variables like cells and year-quarter had to be removed due to lack of sufficient sampling for the estimation of GLM coefficients. In addition, hook-between-floats and set time information is still missing for enough records that they had to be completely ignored in the analysis despite their potential usefulness in explaining fine-scale variations in catch rates.

4.2 Improvements on standardization

4.2.1 Cluster analysis

The use of cluster analysis to identify targeting relies on the assumption that the proportion of species in the catch reflects target strategy. This assumption is more reliable with albacore, which is the main tuna target species in temperate waters, than with yellowfin and bigeye which can both be found in similar conditions, and for which targeting decisions can be confounded with trends in relative abundance. This step of the analysis is important as trends in CPUE over time can change between targeting clusters. Similarly, if vessels only target albacore in periods where they know albacore CPUE will be high, we over-estimate albacore relative abundance by only retaining those sets. Using the unit of the vessel-month, instead of vessel-set, to identify albacore targeting, allowed us to retain in the model sets with poor albacore CPUE that are related to random variation rather than targeting (e.g. otherwise the clustering would only assign sets with high albacore catch to albacore targeting clusters). Any information about gear configuration would allow us to expand the definition of albacore targeting cluster. We calculate total catch as the catch of all target species (ALB, BET, YFT and SWO) but knowing the catch of other species would allow us to expand the definition of an albacore targeting cluster, since specific species tend to be caught together and species often caught along with albacore would help us identify sets that were targeting albacore but where albacore catch was low.

4.2.2 Vessel effects

The inclusion of vessel effects in standardization allows us to partially account for changes in fleet efficiency over time, and is often the categorical variable with the greatest impact on the standardized indices. As such, it is a priority to ensure that the estimated vessel coefficients are sound. This involves filtering the data to select a ‘core fleet’ with enough sets per vessel over space and time to justify the estimation of individual effects (see Methods section 2.3). The 4 year-quarter threshold for minimum fishing activity used here excluded a high proportion of vessels from most of the regions, yet we felt that 4 was the very minimum number of year-quarters from which we could estimate an individual vessel effect for it not to be confounded with a year-quarter effect. As expected, fitted coefficients for vessel effects tended to increase with the year the vessel entered the fishery, and in most regions fleets showed a distinct signature (Figures 59 to 74). In some regions, many of the excluded vessels only entered in the fishery in recent years, especially distant-water vessels in regions with seasonal fisheries. This period has also seen a steep increase in investment by foreign fleets in the fisheries for south Pacific albacore, such that we would expect that accounting for these vessels might alter the standardized indices for the last years.

GLM model structure is the other main component impacting vessel coefficients. In previous standardizations, fixed effects were assumed for vessels such that estimated effects were not constrained

in any way, resulting in sometimes very high (or very low) effects estimated for individual vessels. In contrast, it would make sense that vessels belonging to the same fleet would be more similar and, while some vessels might perform better than others due to, for instance, skipper experience, we would expect that only few vessels could achieve a performance much higher than the mean performance. In other words, barring a few exceptions, most vessels should be close to the mean performance. In the current analysis we explored the use of random vessel effects as a means to constrain estimated vessel coefficients to a mean fleet value. Fitted random effects in the current analysis were very close to the estimated coefficients but more challenging to produce computationally, so we retained fixed effects in the final indices. The current attempt was, however, preliminary and future work will more adequately explore the potential of using random effects for vessels, for instance by accounting for the expected increase in fleet performance. From a practical point of view, using random effects would allow for a lower year-quarter cut-off for the core fleet as vessel effects would be constrained to realistic values by the model structure.

4.2.3 Uneven sampling of cells over time

The biggest—and virtually unaddressed—challenge in CPUE standardization for Pacific tuna is biased sampling by fishing fleets over space and time. For instance, in early years of our dataset there is very low spatial coverage but the sharp decline in CPUE gets attributed to the entire region. Alternatively, including records that target albacore based on species composition implies that, if abundance is declining, we end up excluding records for trips made in cells where albacore is no longer abundant, resulting in hyperstable indices. Even more advanced geostatistical approaches that account for spatial and/or correlation structures between cells rely on the assumption that the intensity of sampling is independent from the response variable, which is not the case in most fisheries systems. In addition, these analyses work well on small datasets but have not been applied to large, long-term datasets such as those common for Pacific tunas. Methods of addressing this preferential sampling have yet to be applied in fisheries systems and would require adaptation to these situations, together with appropriate simulation models to demonstrate their efficacy.

Accounting for spatio-temporal trends could result in significant changes in standardized indices by accounting for the different causes behind un-fished cells during the history of the fishery. For instance un-fished cells at the start of the time-series potentially have high biomass but have not been explored yet. Un-fished cells at the end could either have had low productivity all along, or have been depleted. The first and third cases are important to identify. Accounting for the first case could balance out the steep declines in CPUE often observed early in CPUE time-series and, in the third case, not accounting for depleted cells promotes hyperstable CPUE indices and over-estimates of relative abundance.

4.2.4 Additional avenues for research

Because of the size of the dataset and the limited time we had available, we used a basic clustering algorithm ('k-means'), after verifying that results were similar to those of algorithms previously used ('hierarchical'). Given the impact of using cluster variables in standardisation models, the clustering method should be a priority branch of exploration, most notably in the three following areas: (i) the type of clustering algorithm; (ii) the inclusion of explanatory variables such as hooks-between-floats, time of set, or catch of representative non-target species to expand the definition of an albacore targeting cluster; (iii) correlation structures between the observed sets, for instance to account for the fact that trips belonging to the same vessel are more similar. Other approaches to quantify targeting should also be reviewed, for example those based on PCA (Winker et al., 2013).

A feature of albacore targeting activity in many EEZs in recent years has been a pattern of fishing effort being conditional on abundance (e.g. Brouwer et al. 2015). In these cases vessels will remain in-port until CPUE of other vessels increases to the point of economic viability. This can have substantial impacts on CPUE indices if it is not accounted for, as CPUE will appear to remain high in years of low abundance through the targeting of time periods of high abundance. We recommend further investigation of these processes to determine the validity of our current approaches.

References

- Bigelow, K. A. and Hoyle, S. D. (2012). Standardized CPUE for South Pacific albacore. WCPFC-SC8-2012/SA-IP-14, Busan, Republic of Korea, 7–15 August 2012.
- Brouwer, S., Harley, S. J., and Pilling, G. (2015). The influence of catch rate on fishing effort – an investigation using south Pacific albacore as an example. WCPFC-SC11-2015/SA-IP-04, Pohnpei, Federated States of Micronesia, 5–13 August 2015.
- Dunn, K. P. and Smyth, G. K. (1996). Randomized quantile residuals. *Journal of Computational and Graphical Statistics*, 5:1–10.
- Francis, R. I. C. C. (1999). The impact of correlations in standardised CPUE indices. NZ Fisheries Assessment Research Document 99/42, National Institute of Water and Atmospheric Research. (Unpublished report held in NIWA library, Wellington.).
- Harley, S. J., Davies, N., Hampton, J., and McKechnie, S. (2014). Stock assessment of bigeye tuna in the Western and Central Pacific Ocean. WCPFC-SC10-2014/SA-WP-01, Majuro, Republic of the Marshall Islands, 6–14 August 2014.
- He, X., Bigelow, K. A., and Boggs, C. H. (1997). Cluster analysis of longline sets and fishing strategies within the hawaii-based fishery. *Fisheries Research*, 31:144–158.

- Hoyle, S., Hampton, J., and Davies, N. (2012). Stock assessment of albacore tuna in the South Pacific Ocean. WCPFC-SC8-2012/SA-WP-04, Busan, Republic of Korea, 7–15 August 2012.
- Hoyle, S. D., Langley, A. D., and Campbell, R. A. (2014). Recommended approaches for standardizing CPUE data from pelagic fisheries. WCPFC-SC10-2014/SA-IP-10, Majuro, Republic of the Marshall Islands, 6–14 August 2014.
- Hoyle, S. D. and Okamoto, H. (2011). Analyses of Japanese longline operational catch and effort for Bigeye and Yellowfin Tuna in the WCPO. WCPFC-SC7-2011/SA-IP-01, Pohnpei, Federated States of Micronesia, 9–17 August 2011.
- Ianelli, J., Maunder, M. N., and Punt, A. E. (2012). Independent review of the 2011 WCPO bigeye tuna assessment. WCPFC-SC8-2012/SA-WP-01, Busan, Republic of Korea, 7–15 August 2012.
- Kristensen, K., Thygesen, U. H., Andersen, K. H., and Beyer, J. E. (2014). Estimating spatio-temporal dynamics of size-structured populations. *Canadian Journal of Fisheries and Aquatic Sciences*, 71:326–336.
- McKechnie, S., Hampton, J., Abascal, F., Davies, N., and Harley, S. J. (2015a). Sensitivity of WCPO stock assessment results to the inclusion of EPO dynamics within a Pacific-wide analysis. WCPFC-SC11-2015/SA-WP-04, Pohnpei, Federated States of Micronesia, 5–13 August 2015.
- McKechnie, S., Tremblay-Boyer, L., and Harley, S. J. (2015b). Analysis of Pacific-wide operational longline CPUE data for bigeye tuna. WCPFC-SC11-2015/SA-WP-03, Pohnpei, Federated States of Micronesia, 5–13 August 2015.
- OFP (2015a). Continued use of longline operational-level data provided by fishing nations to support WCPFC stock assessments. Technical Report WCPFC-SC11-2015/SA-WP-07, Pohnpei, Federated States of Micronesia, 5–13 August 2015.
- OFP (2015b). Report of the workshop on operational longline data. Technical Report WCPFC-SC11-2015/SA-IP-01, Pohnpei, Federated States of Micronesia, 5–13 August 2015.
- Williams, P. and Terawasi, P. (2014). Overview of tuna fisheries in the western and central Pacific Ocean, including economic conditions - 2013. WCPFC-SC10-2014/GN-WP-01, Majuro, Republic of the Marshall Islands, 6–14 August 2014.
- Winker, H., Kerwath, S. E., and Attwood, C. G. (2013). Comparison of two approaches to standardize catch-per-unit-effort for targeting behaviour in a multispecies hand-line fishery. *Fisheries Research*, 139:118–131.

Year-quarter in fleet, by vessels and flag

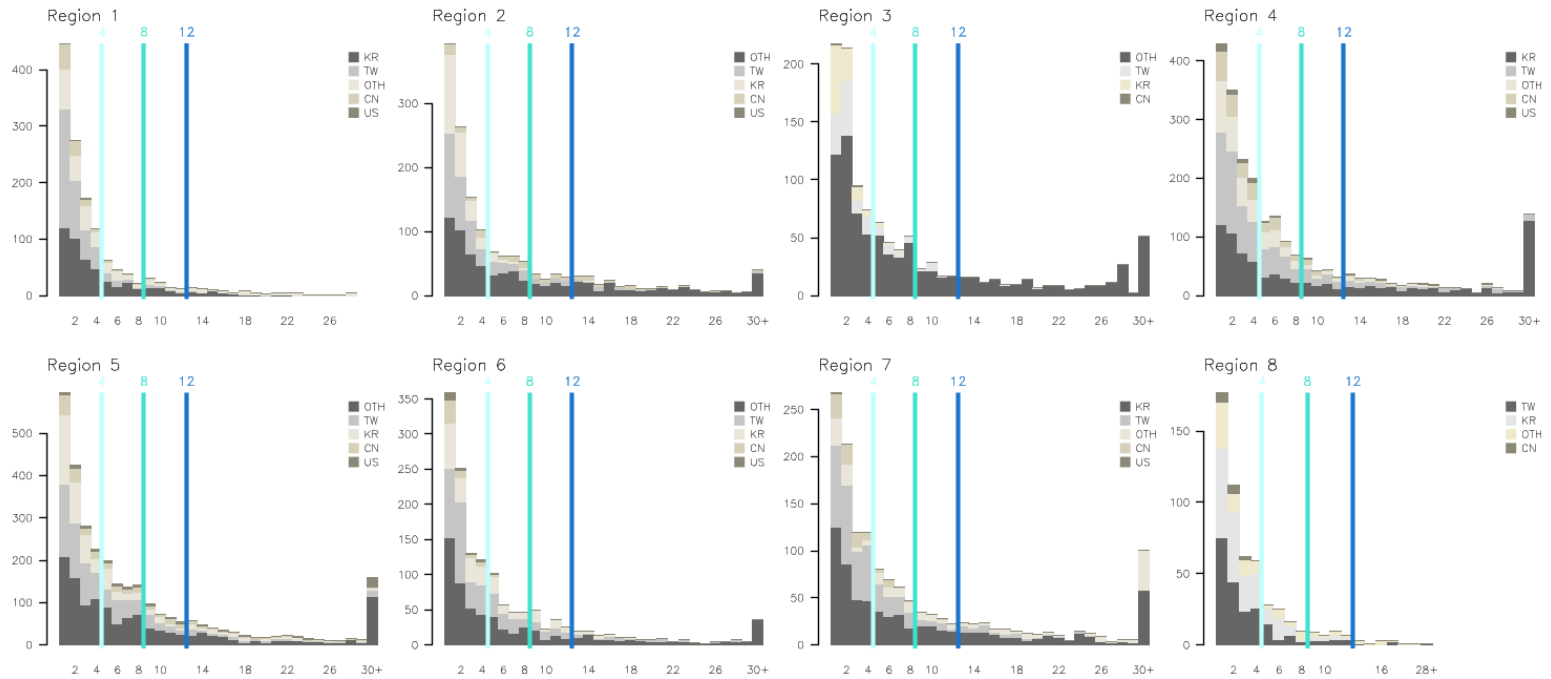


Figure 2: Frequency of the length of fishing activity by vessel in year-quarters, by region, with bars colour-coded for flags. The vertical blue lines show candidate cut-offs for minimal activity length for inclusion in the core fleet.

Vessel filtering by decade // Region 1

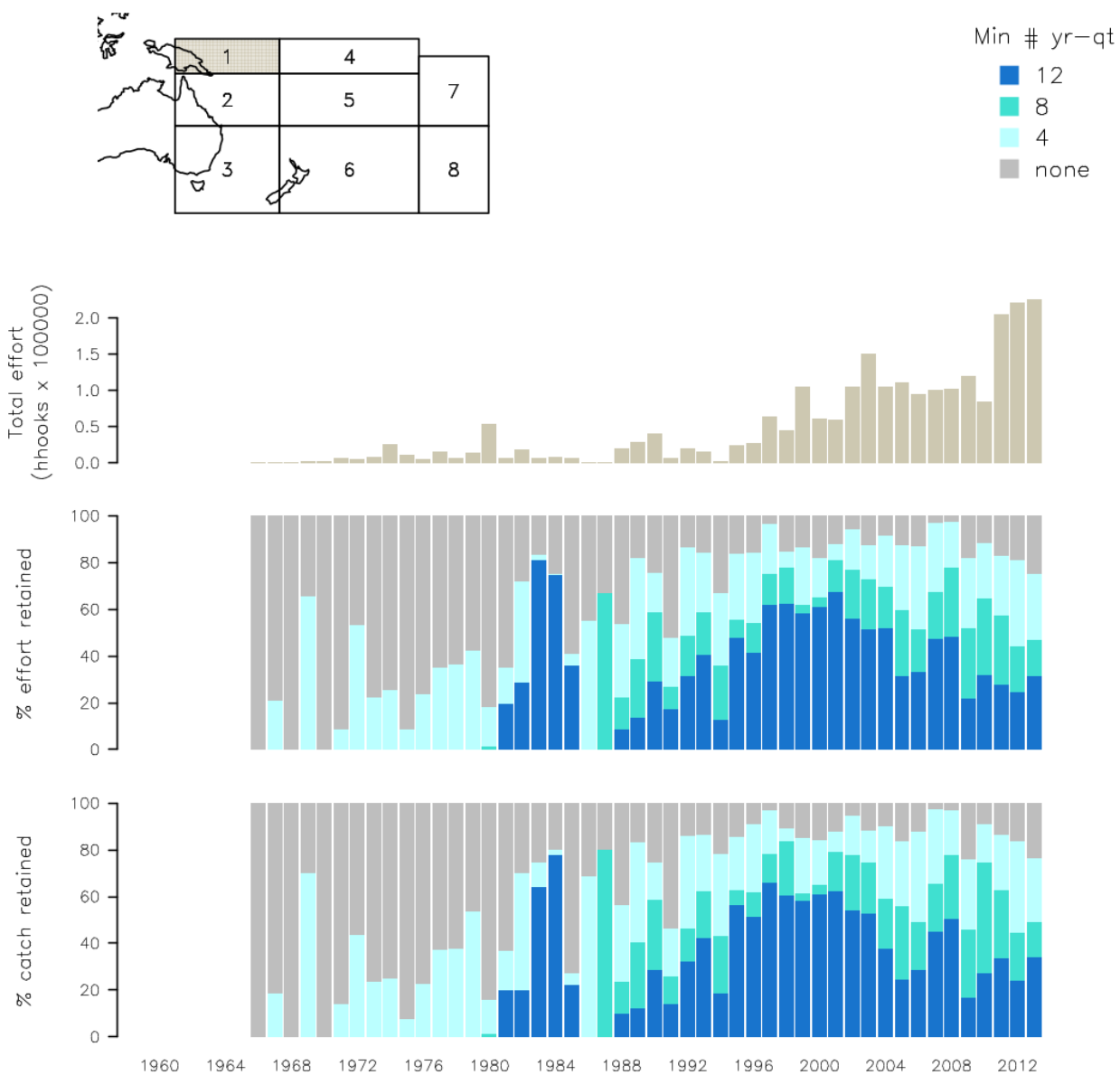


Figure 3: Effect of thresholds of minimal year-quarter presence for core fleet membership on the temporal trends in catch and effort retained for the CPUE analysis.

Vessel filtering // Region 1

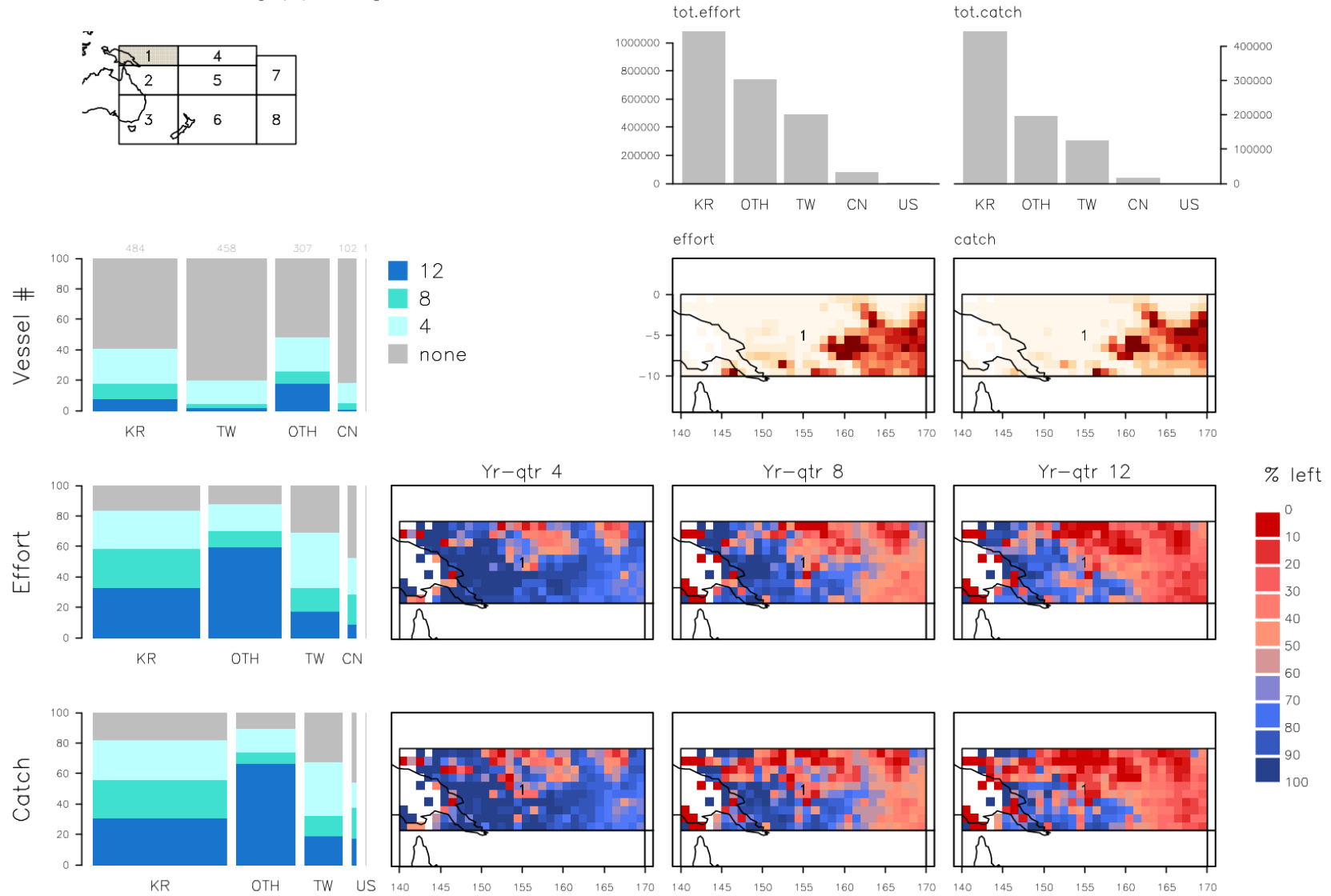


Figure 4: Effect of thresholds of minimal year-quarter presence for core fleet membership on the proportion of vessels remaining by fleet, and the spatial distribution of retained effort and catch.

Vessel filtering by decade // Region 2

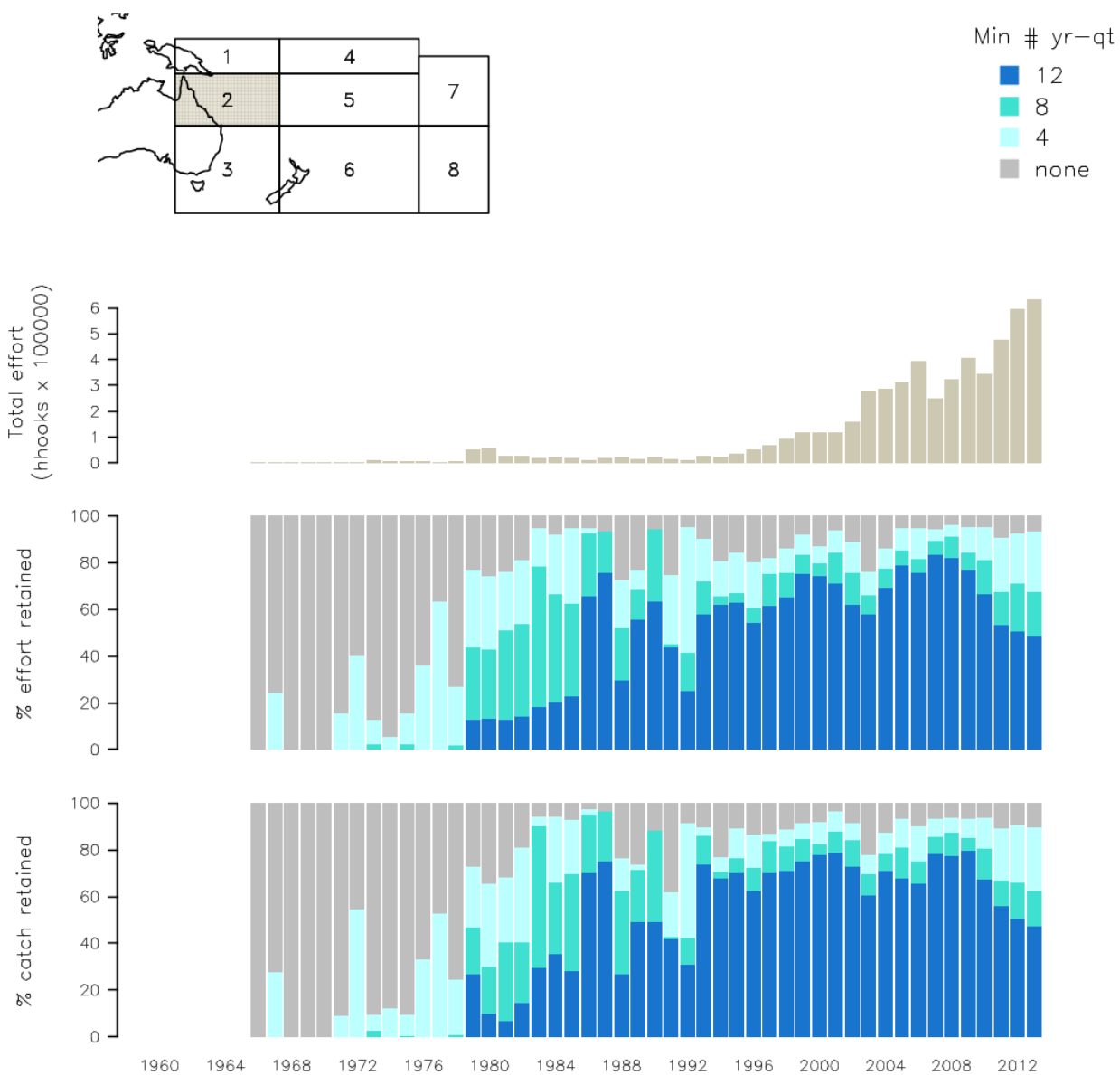


Figure 5: Effect of thresholds of minimal year-quarter presence for core fleet membership on the temporal trends in catch and effort retained for the CPUE analysis.

Vessel filtering // Region 2

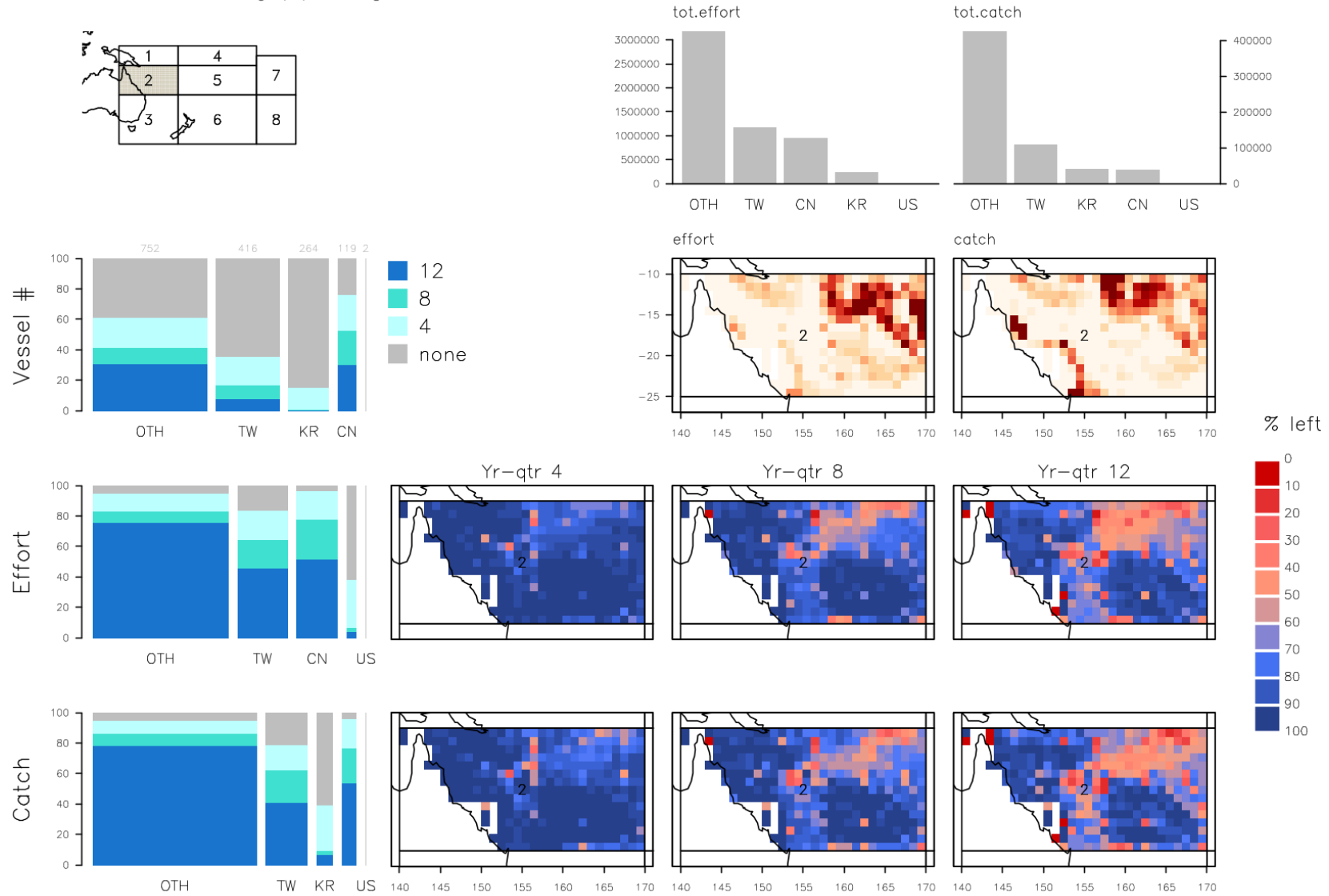


Figure 6: Effect of thresholds of minimal year-quarter presence for core fleet membership on the proportion of vessels remaining by fleet, and the spatial distribution of retained effort and catch.

Vessel filtering by decade // Region 3

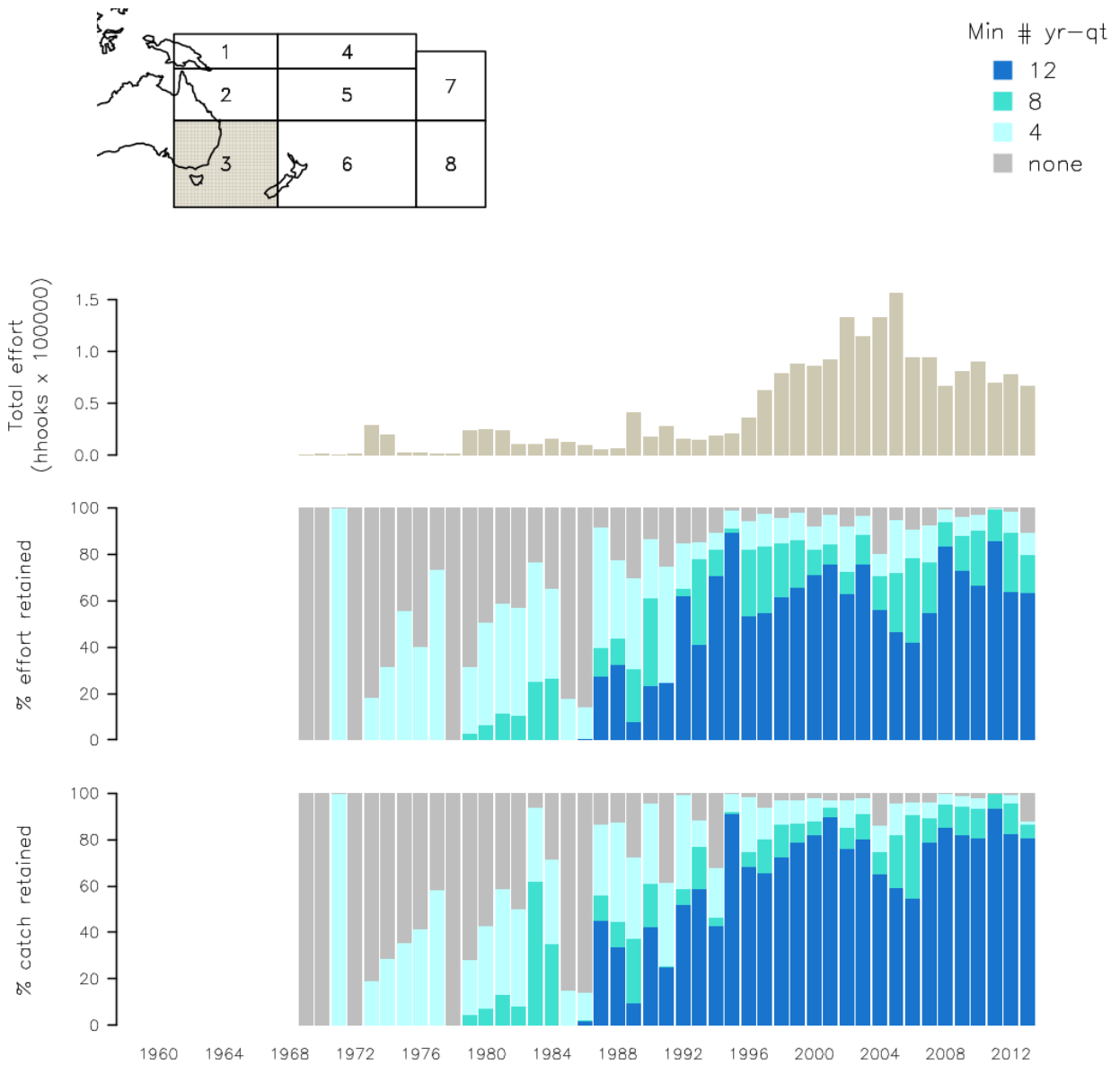


Figure 7: Effect of thresholds of minimal year-quarter presence for core fleet membership on the temporal trends in catch and effort retained for the CPUE analysis.

Vessel filtering // Region 3

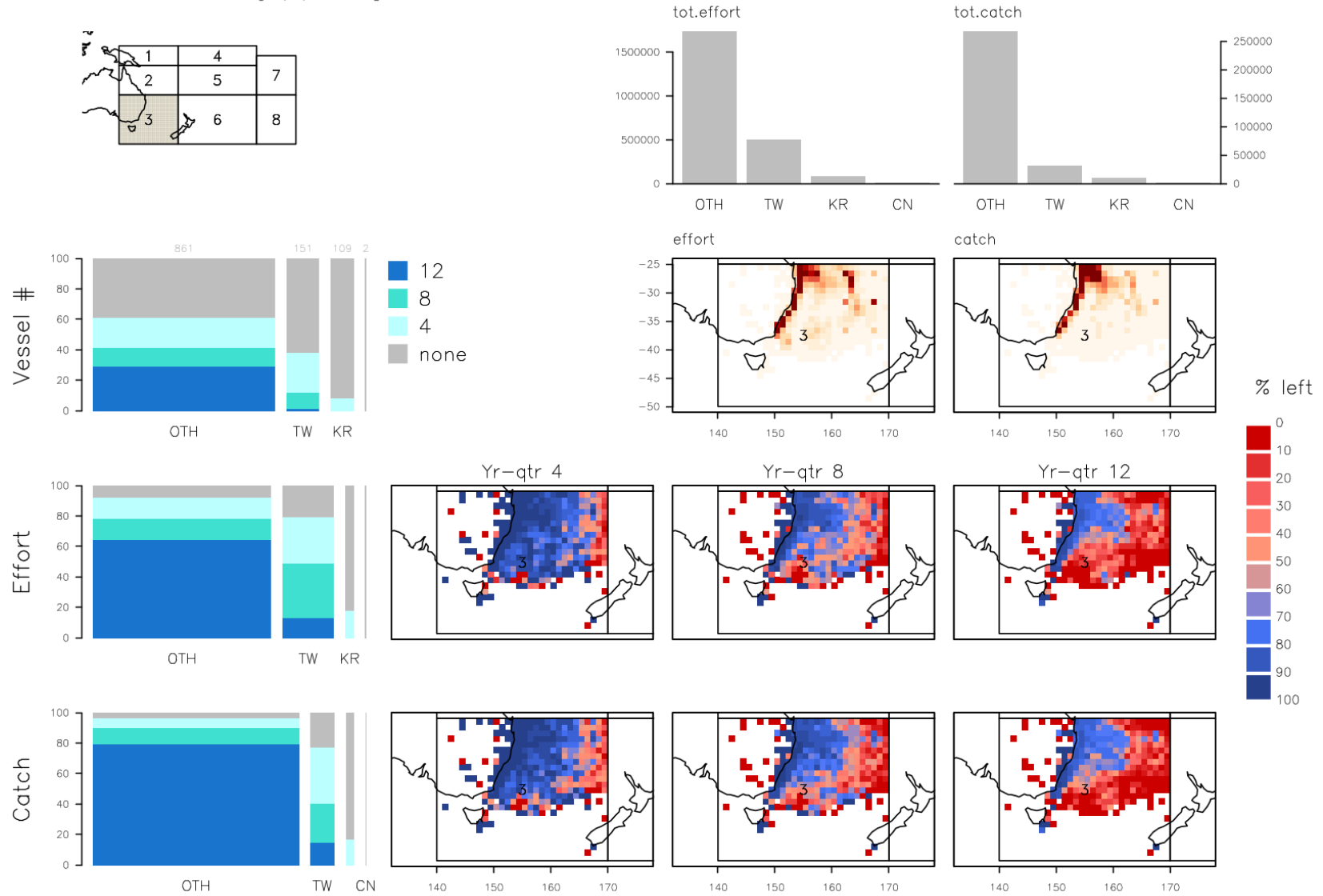


Figure 8: Effect of thresholds of minimal year-quarter presence for core fleet membership on the proportion of vessels remaining by fleet, and the spatial distribution of retained effort and catch.

Vessel filtering by decade // Region 4

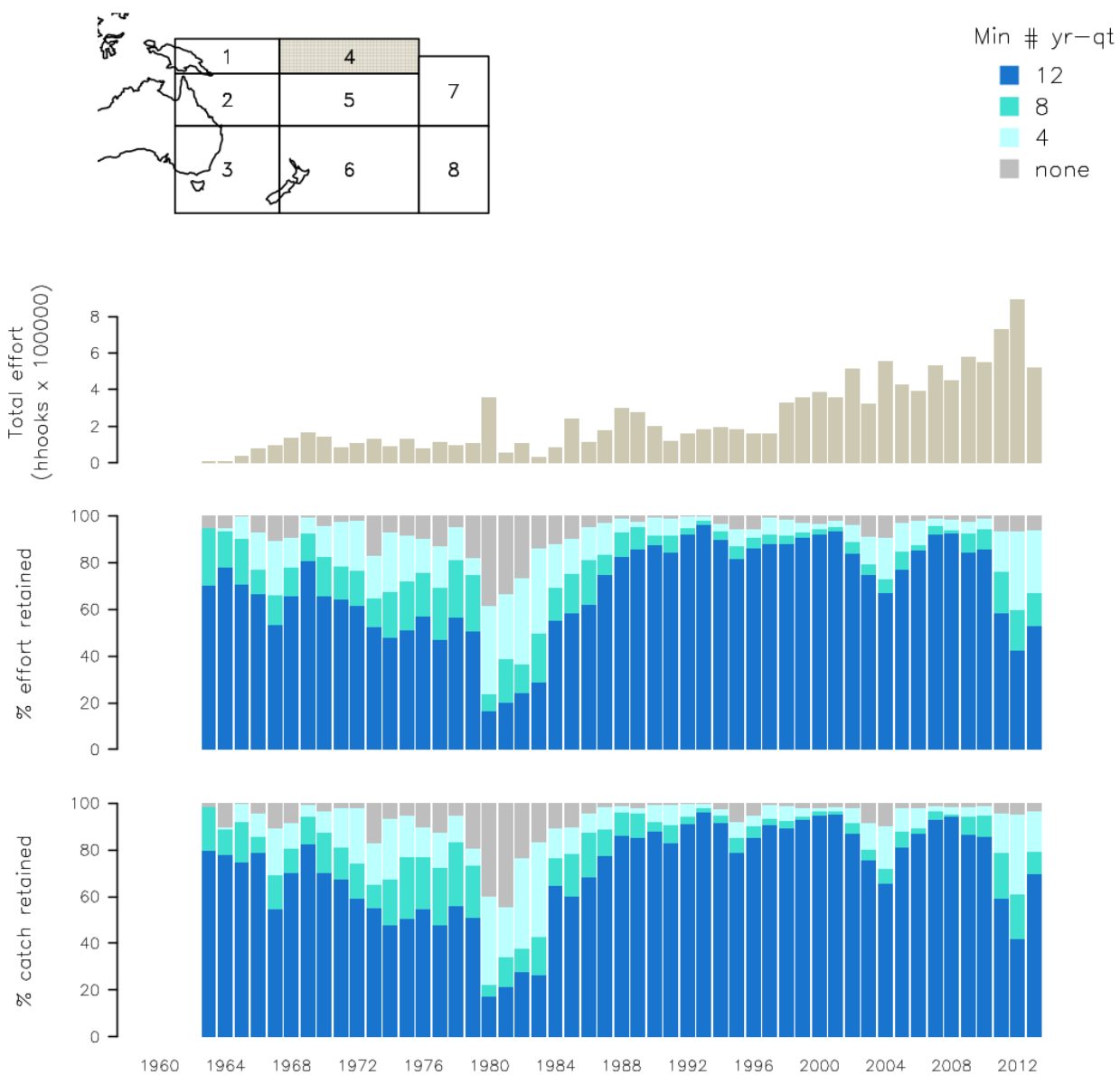


Figure 9: Effect of thresholds of minimal year-quarter presence for core fleet membership on the temporal trends in catch and effort retained for the CPUE analysis.

Vessel filtering // Region 4

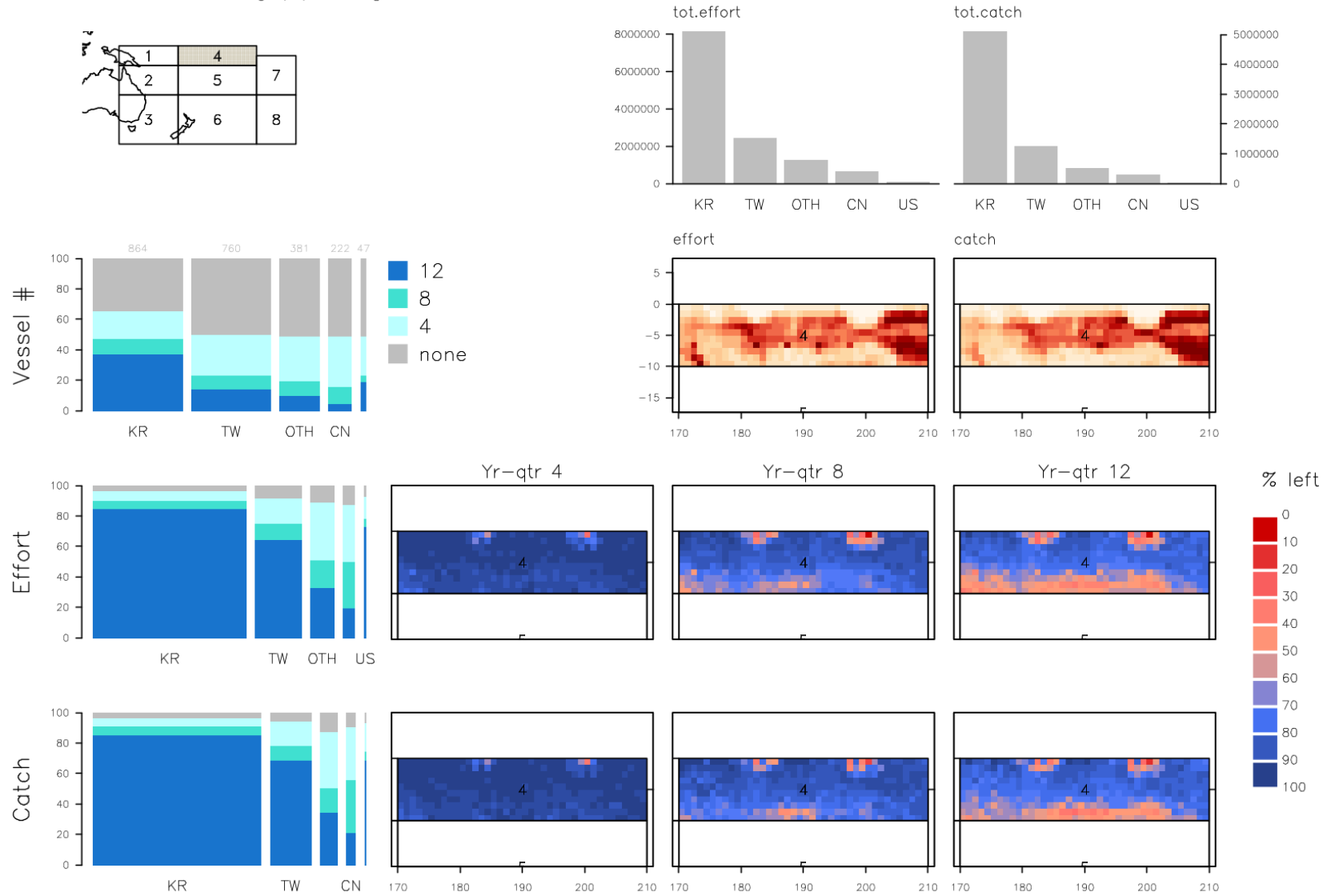


Figure 10: Effect of thresholds of minimal year-quarter presence for core fleet membership on the proportion of vessels remaining by fleet, and the spatial distribution of retained effort and catch.

Vessel filtering by decade // Region 5

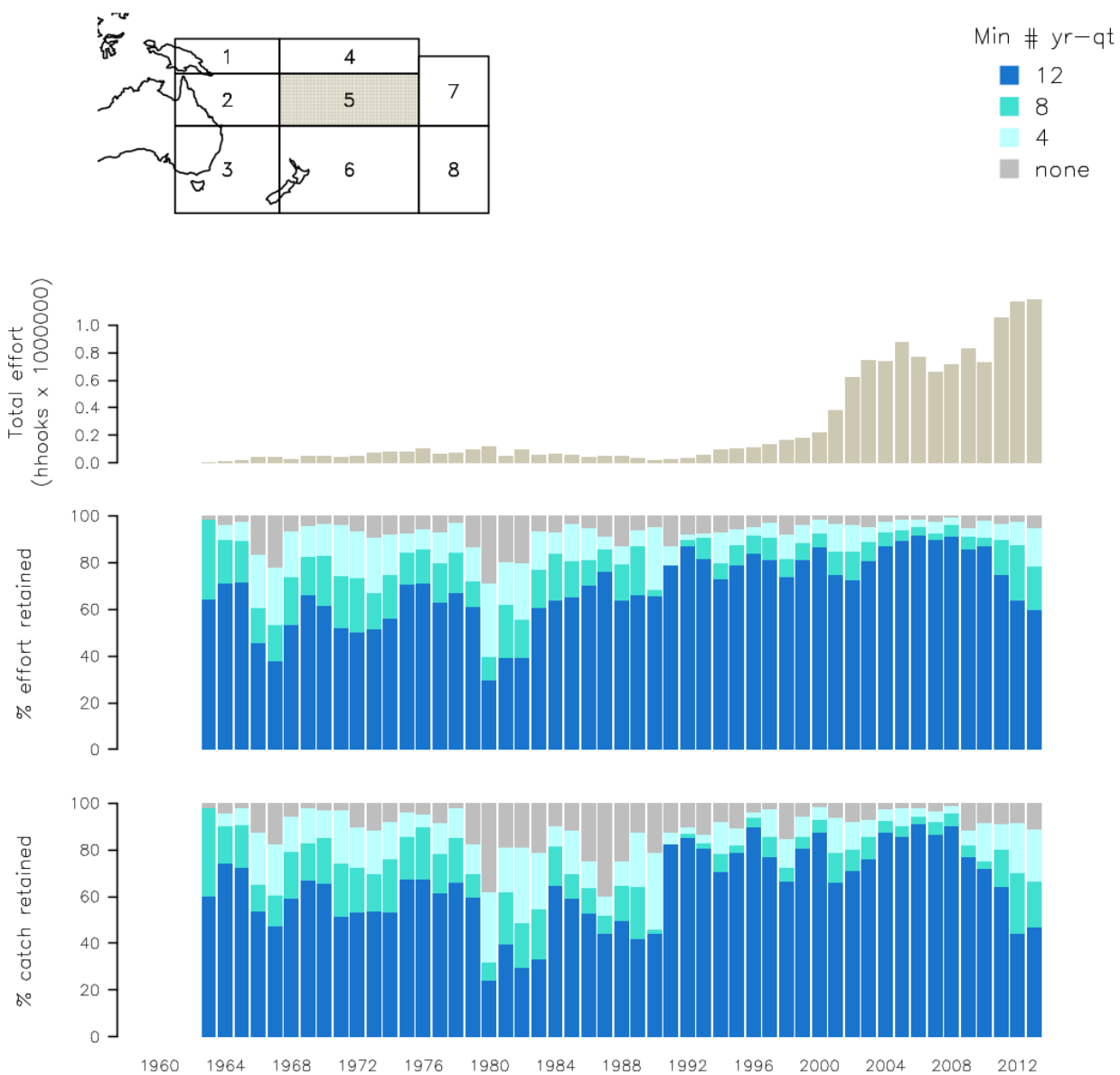


Figure 11: Effect of thresholds of minimal year-quarter presence for core fleet membership on the temporal trends in catch and effort retained for the CPUE analysis.

Vessel filtering // Region 5

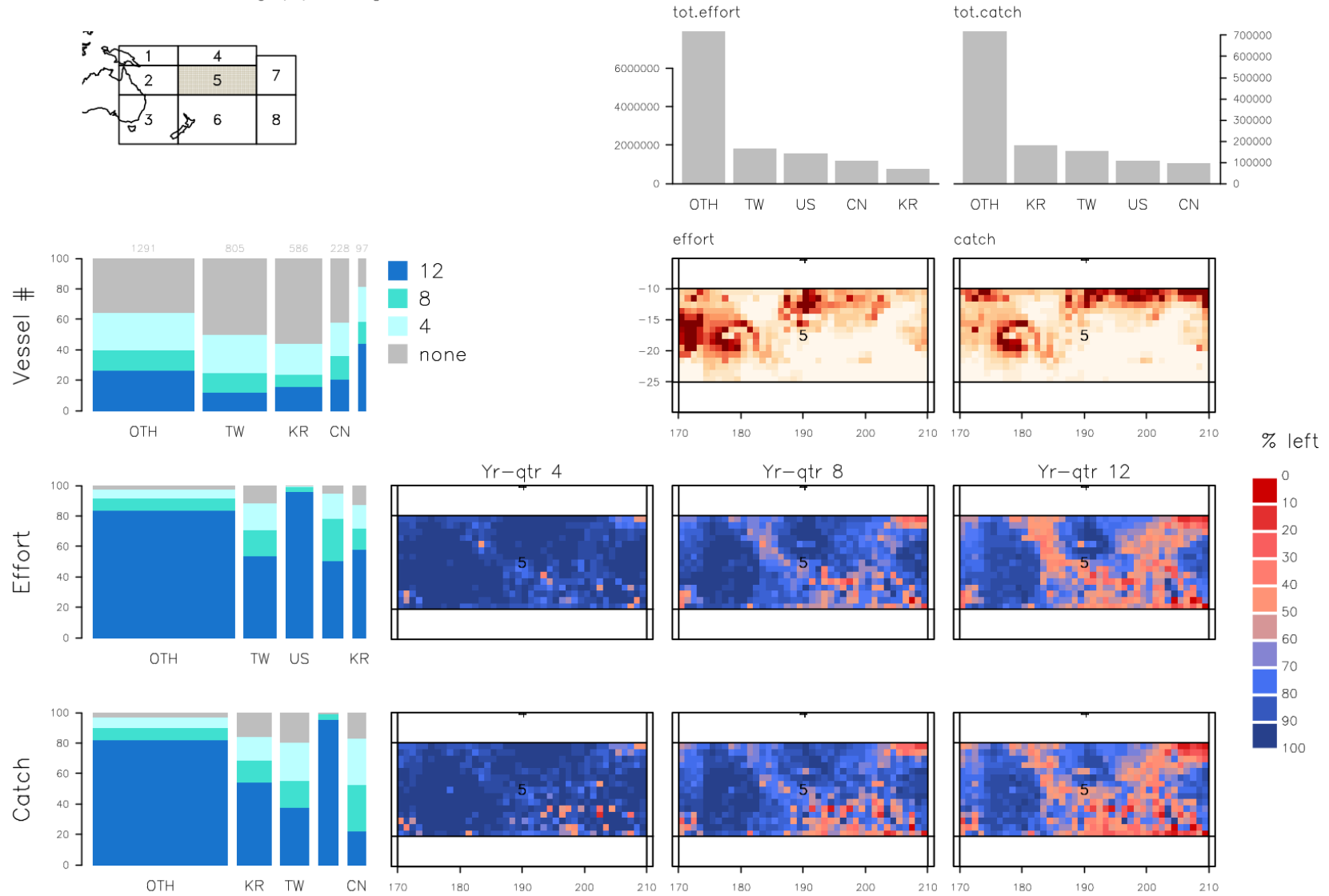


Figure 12: Effect of thresholds of minimal year-quarter presence for core fleet membership on the proportion of vessels remaining by fleet, and the spatial distribution of retained effort and catch.

Vessel filtering by decade // Region 6

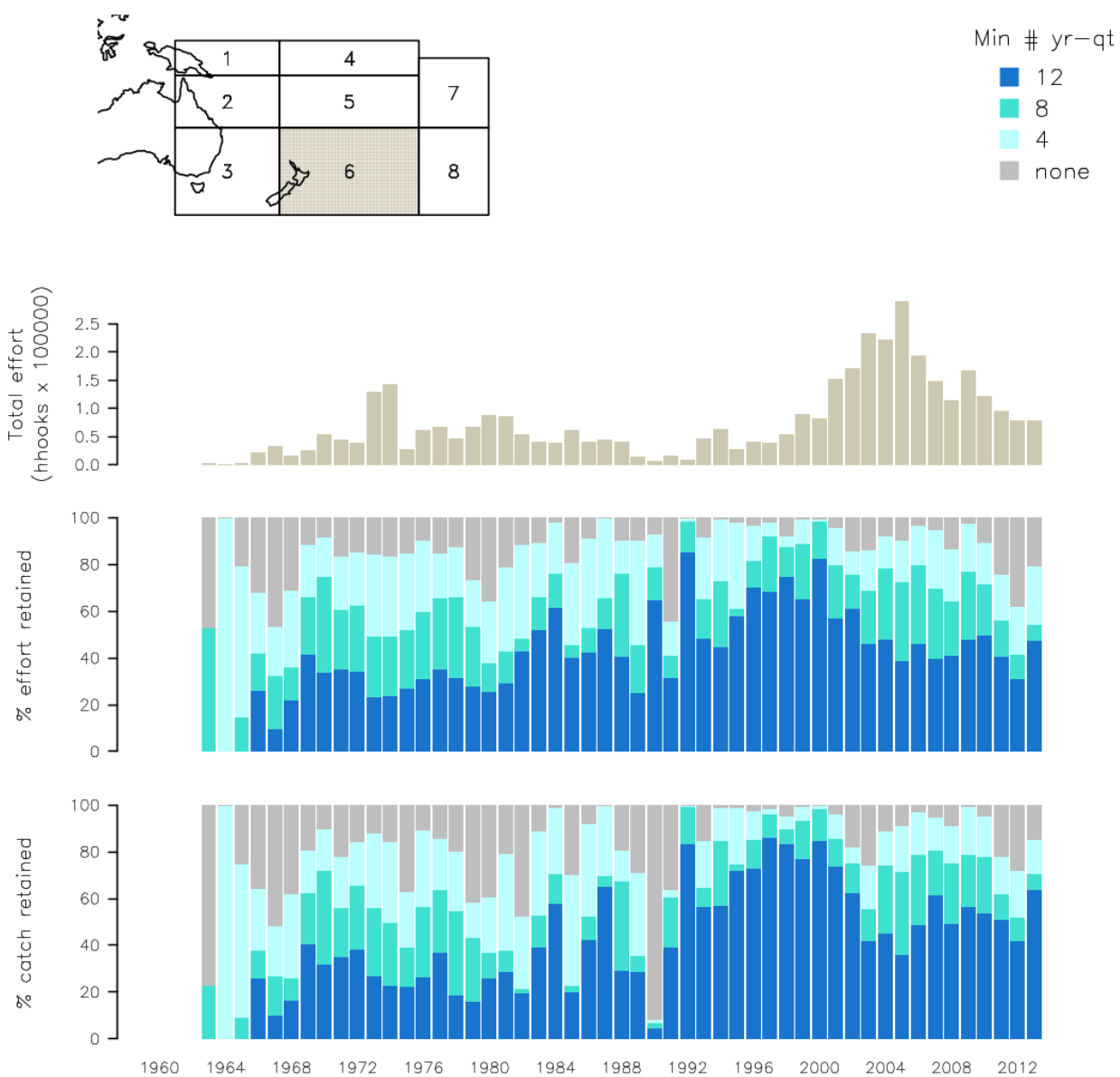


Figure 13: Effect of thresholds of minimal year-quarter presence for core fleet membership on the temporal trends in catch and effort retained for the CPUE analysis.

Vessel filtering // Region 6

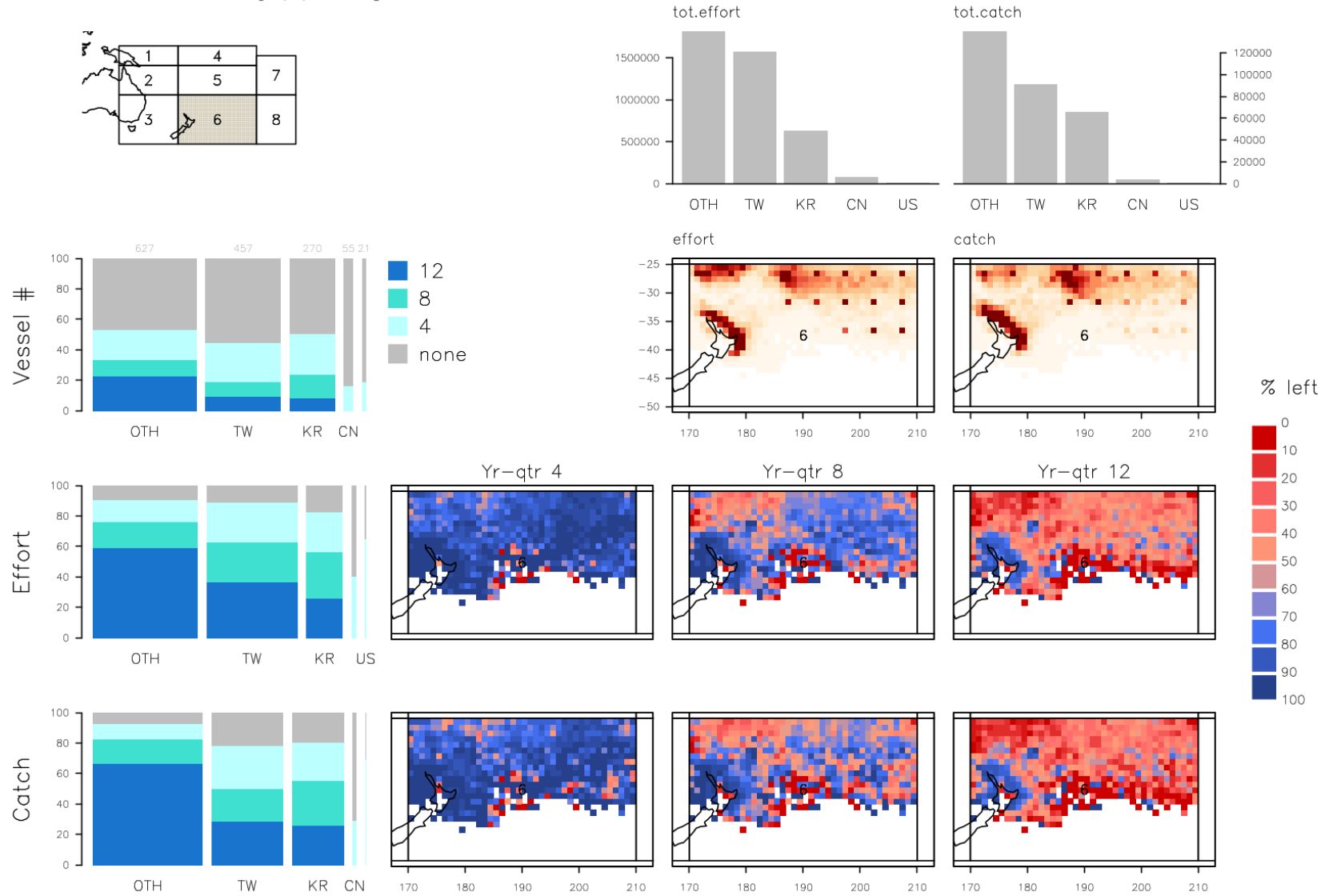


Figure 14: Effect of thresholds of minimal year-quarter presence for core fleet membership on the proportion of vessels remaining by fleet, and the spatial distribution of retained effort and catch.

Vessel filtering by decade // Region 7

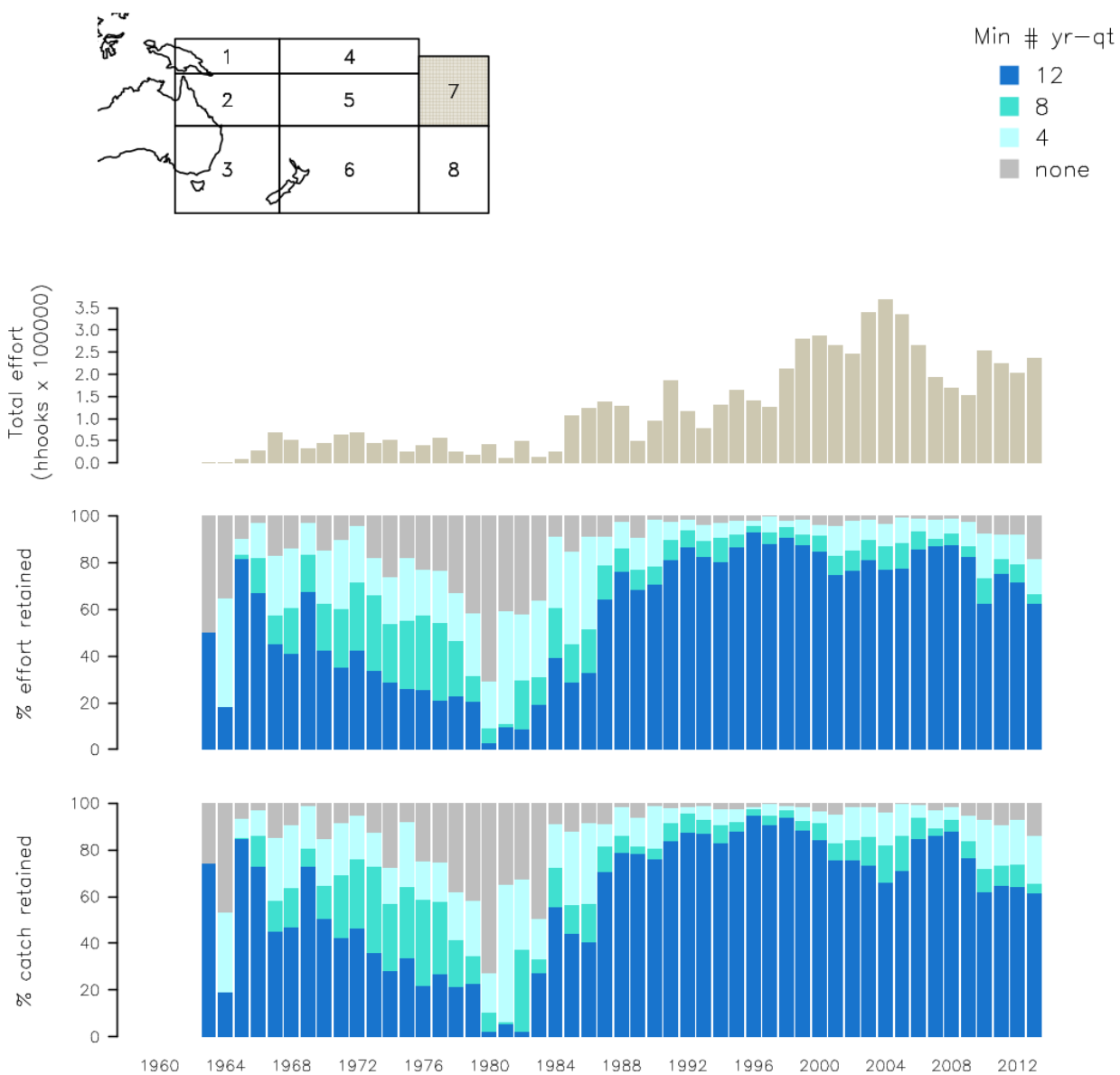


Figure 15: Effect of thresholds of minimal year-quarter presence for core fleet membership on the temporal trends in catch and effort retained for the CPUE analysis.

Vessel filtering // Region 7

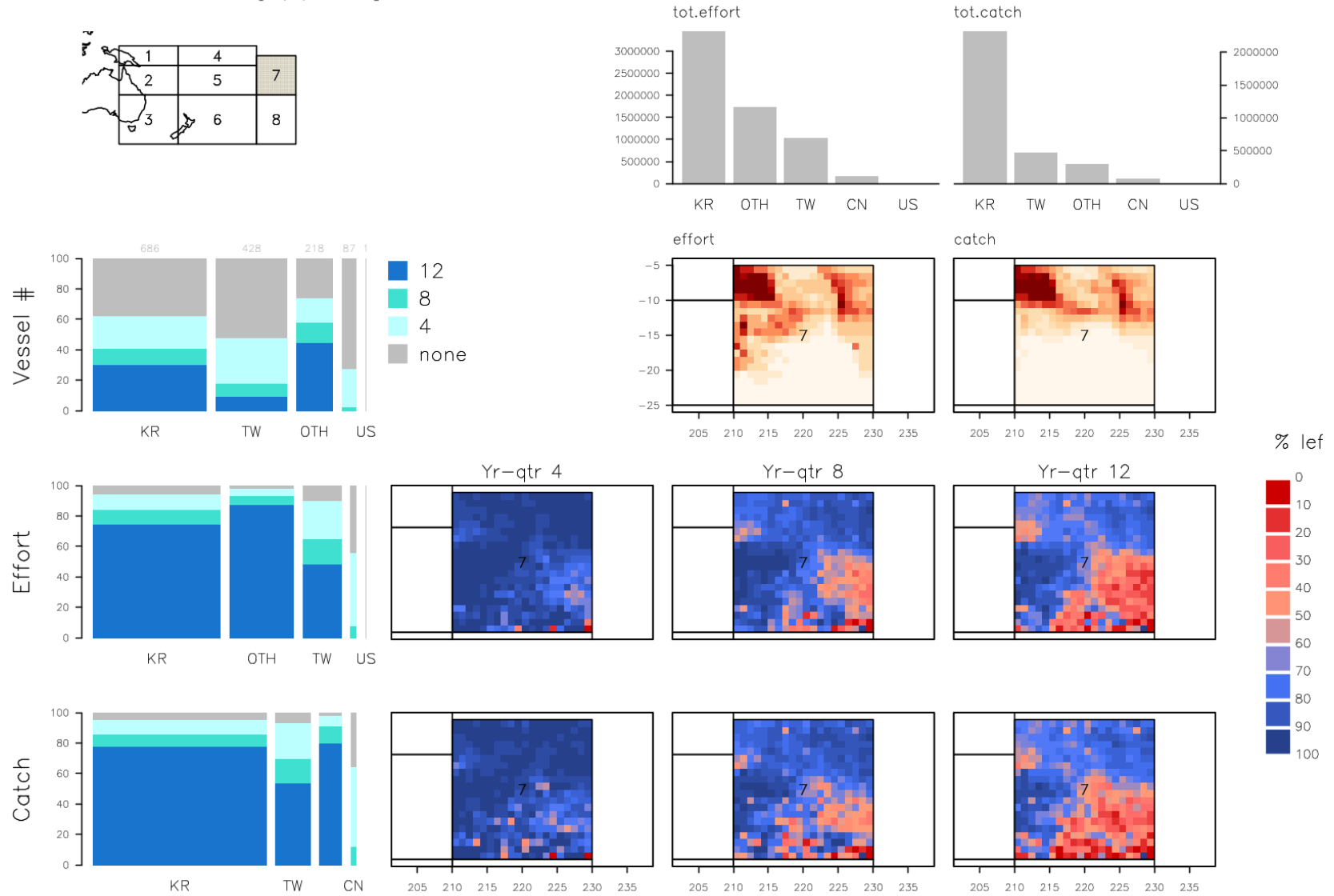


Figure 16: Effect of thresholds of minimal year-quarter presence for core fleet membership on the proportion of vessels remaining by fleet, and the spatial distribution of retained effort and catch.

Vessel filtering by decade // Region 8

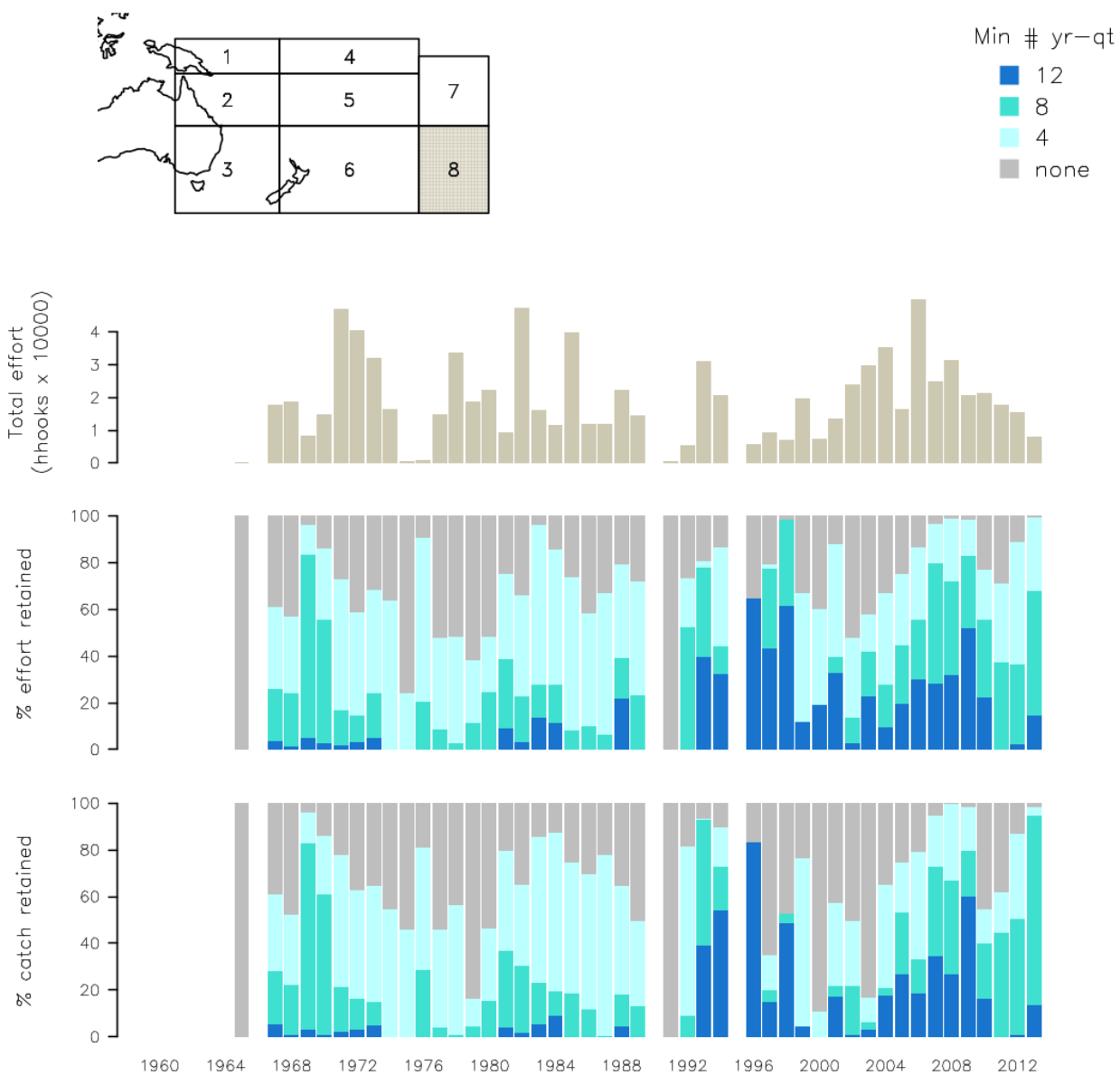


Figure 17: Effect of thresholds of minimal year-quarter presence for core fleet membership on the temporal trends in catch and effort retained for the CPUE analysis.

Vessel filtering // Region 8

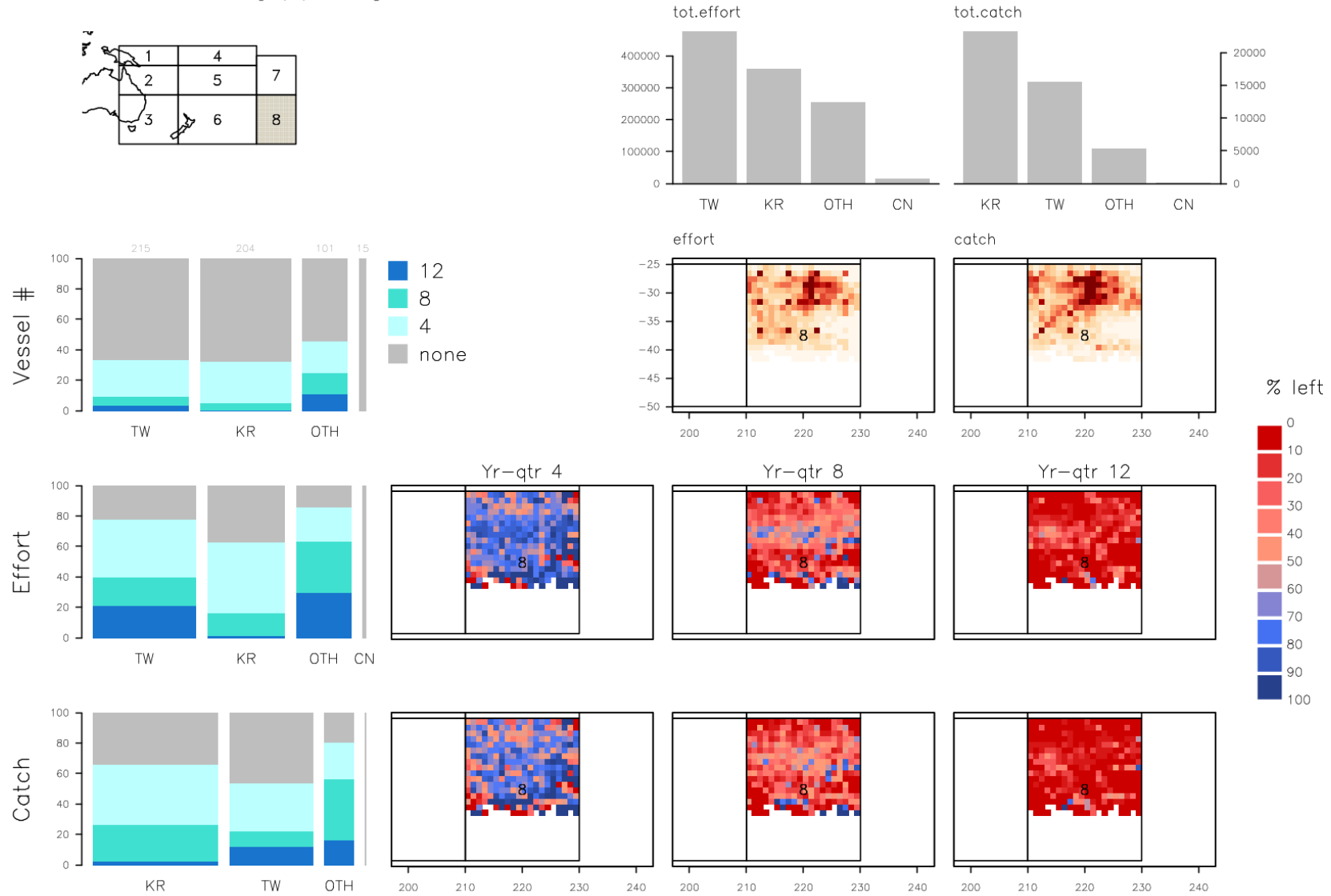


Figure 18: Effect of thresholds of minimal year-quarter presence for core fleet membership on the proportion of vessels remaining by fleet, and the spatial distribution of retained effort and catch.

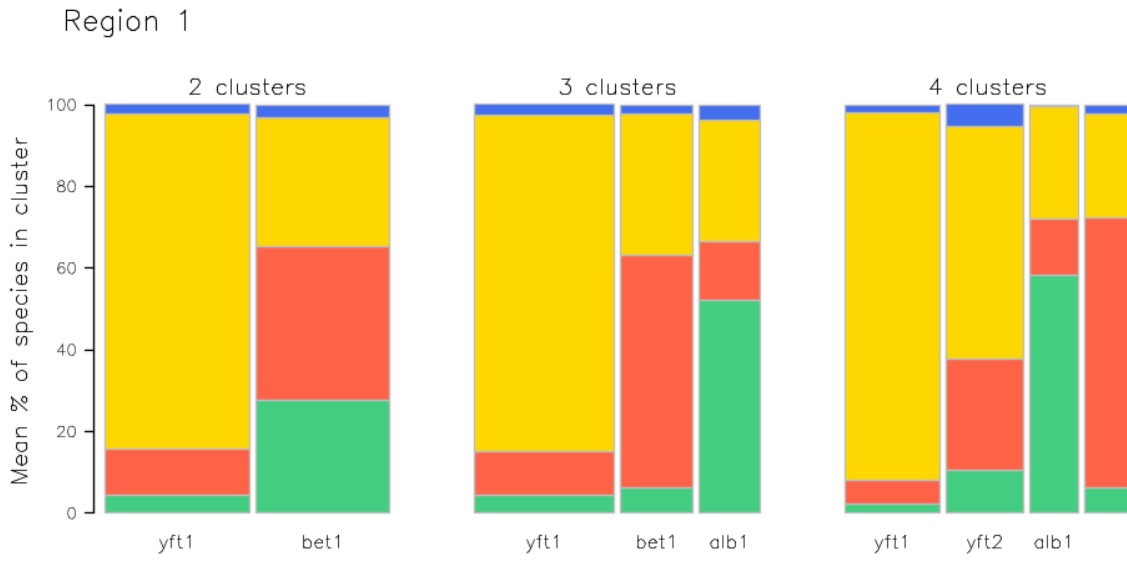


Figure 19: Mean proportion of species in the catch of targeting clusters in region 1, shown for 2, 3, and 4 cluster models. The width of the bar is proportional to the number of records in the cluster.

Region 1

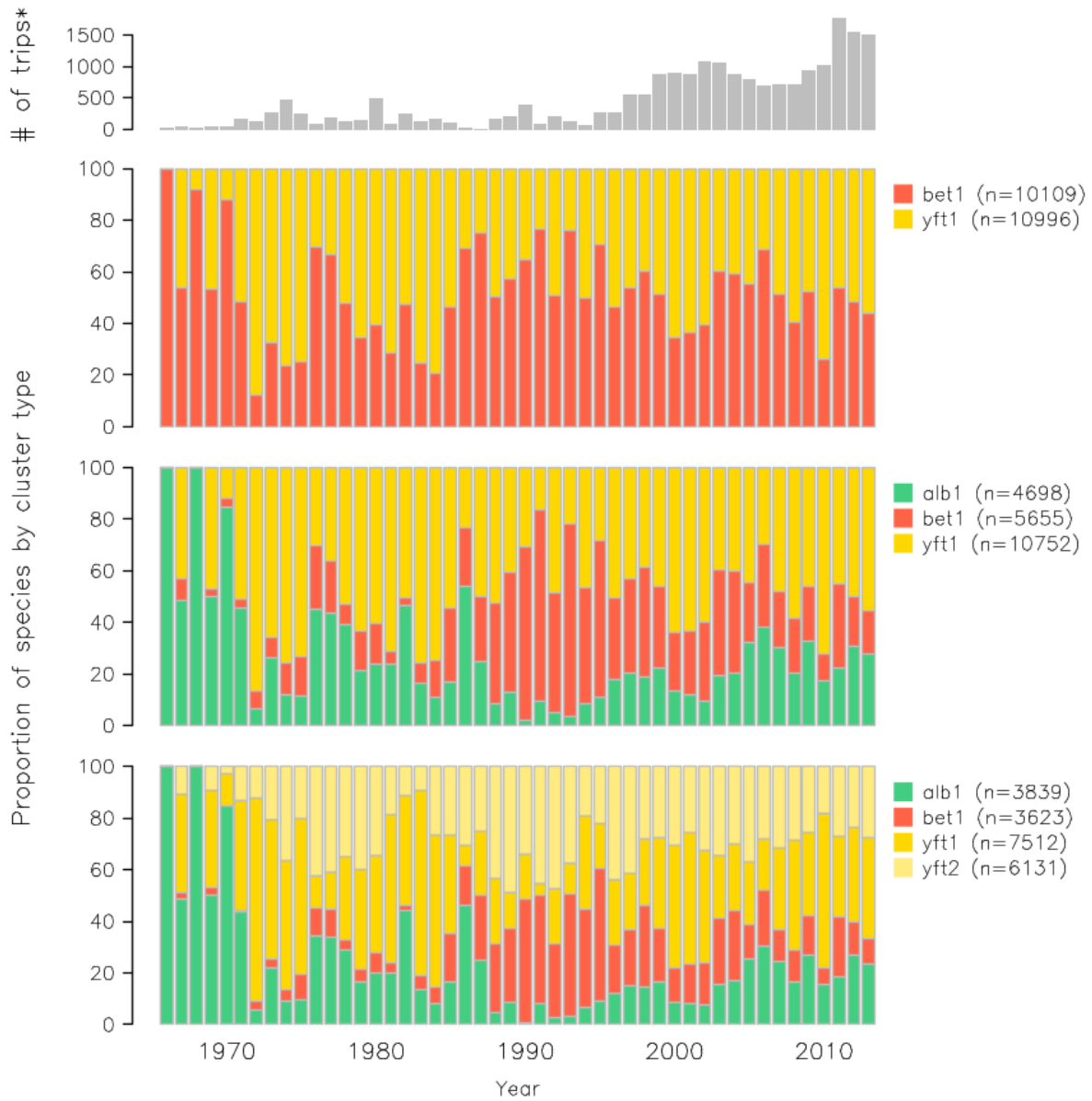


Figure 20: Time series of cluster membership for the 2, 3, and 4 cluster models, with the colour matching the dominant species in the cluster and the top panel indicating the number of records over time.

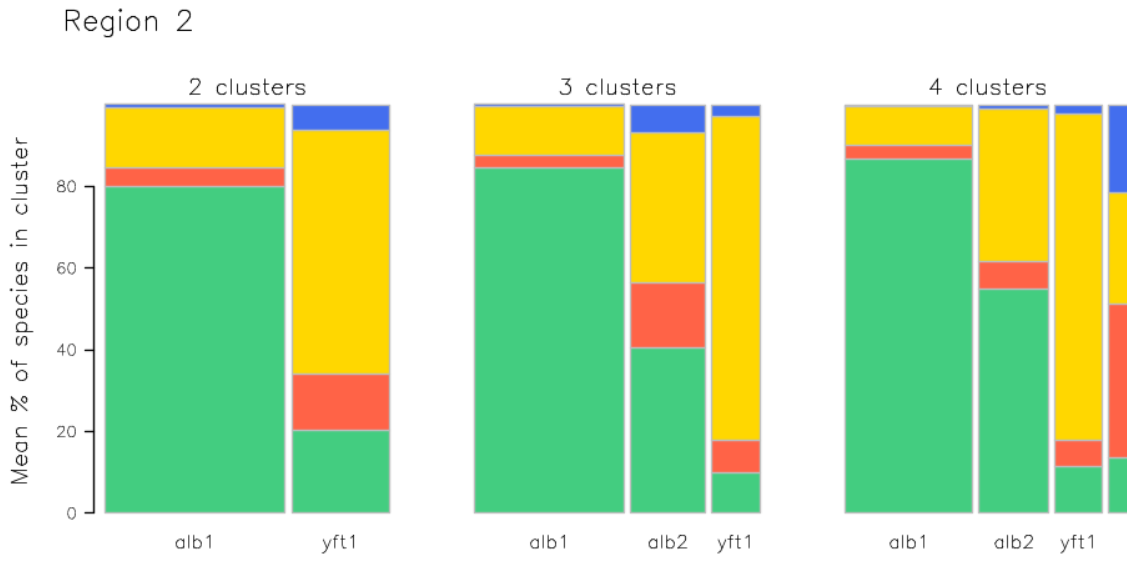


Figure 21: Mean proportion of species in the catch of targeting clusters in region 2, shown for 2, 3, and 4 cluster models. The width of the bar is proportional to the number of records in the cluster.

Region 2

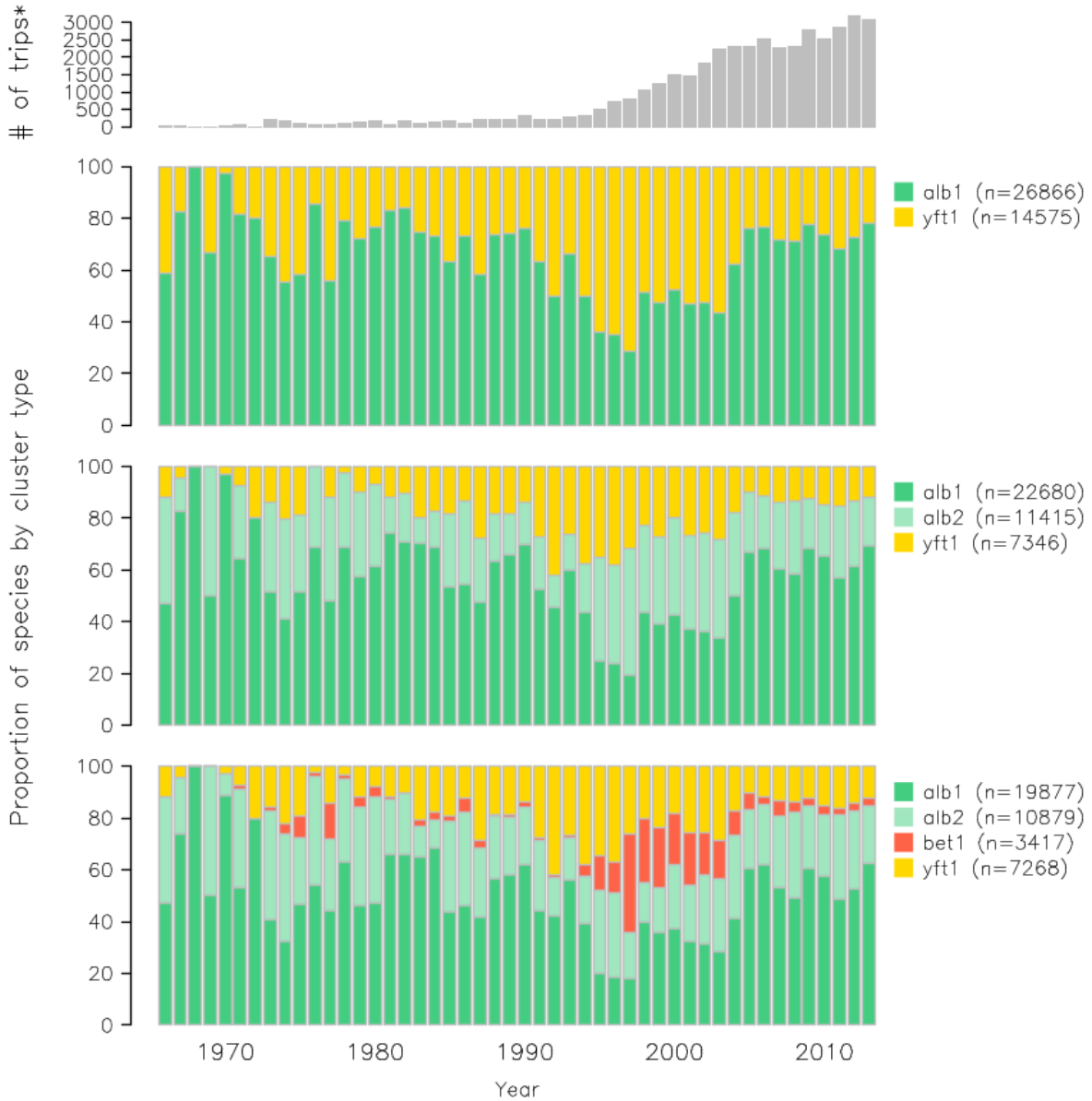


Figure 22: Time series of cluster membership for the 2, 3, and 4 cluster models, with the colour matching the dominant species in the cluster and the top panel indicating the number of records over time.

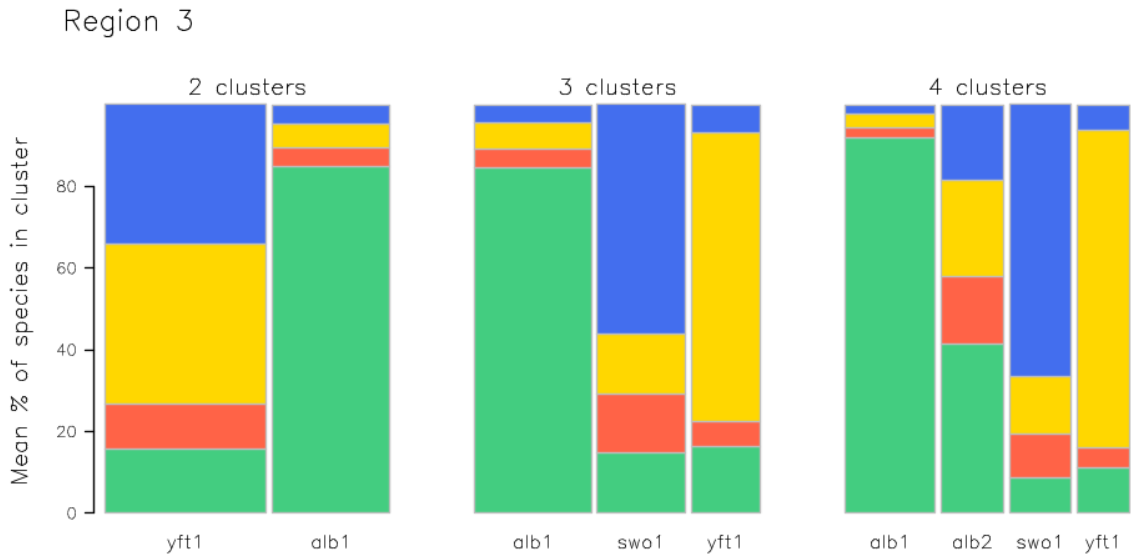


Figure 23: Mean proportion of species in the catch of targeting clusters in region 3, shown for 2, 3, and 4 cluster models. The width of the bar is proportional to the number of records in the cluster.

Region 3

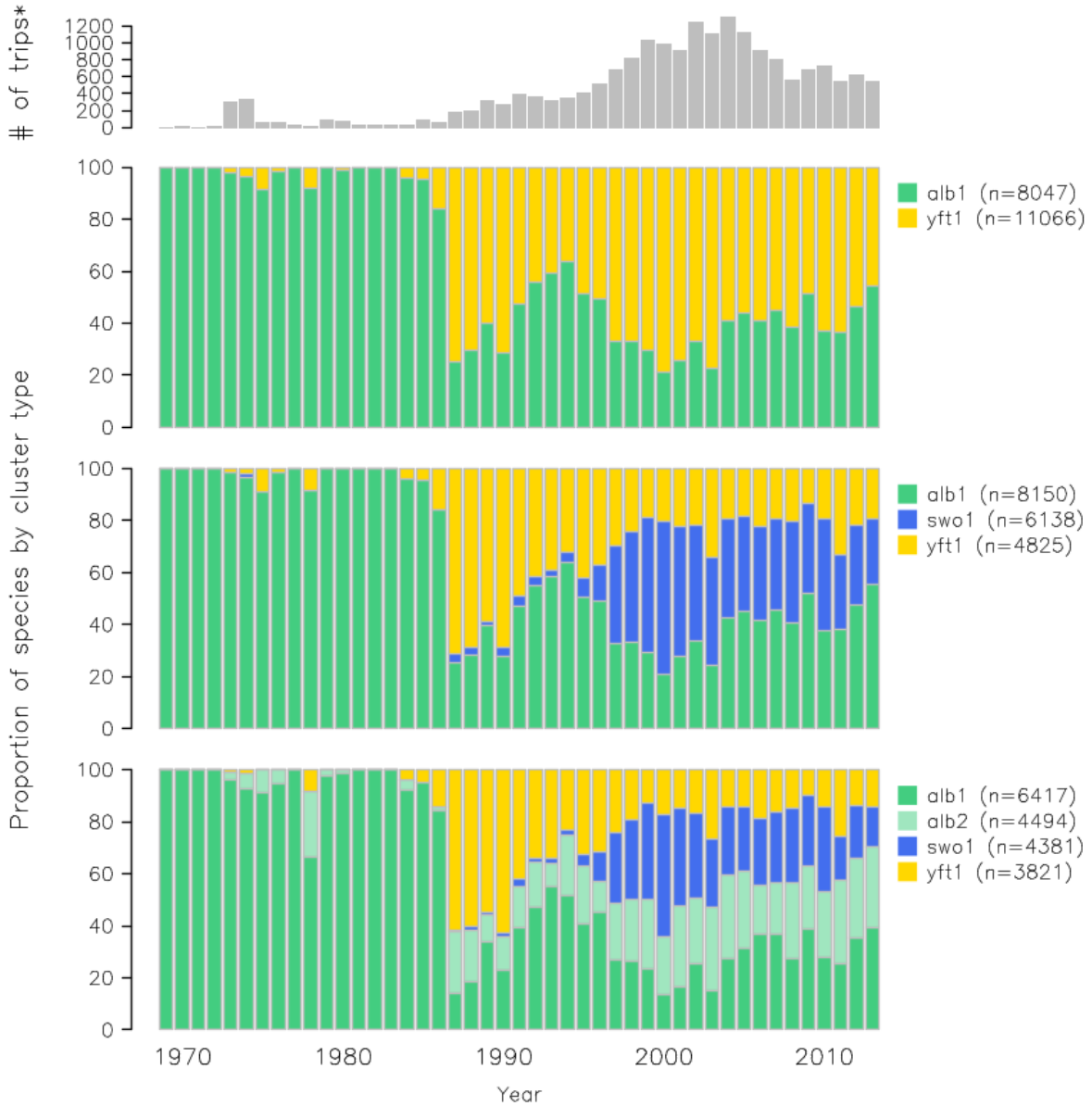


Figure 24: Time series of cluster membership for the 2, 3, and 4 cluster models, with the colour matching the dominant species in the cluster and the top panel indicating the number of records over time.

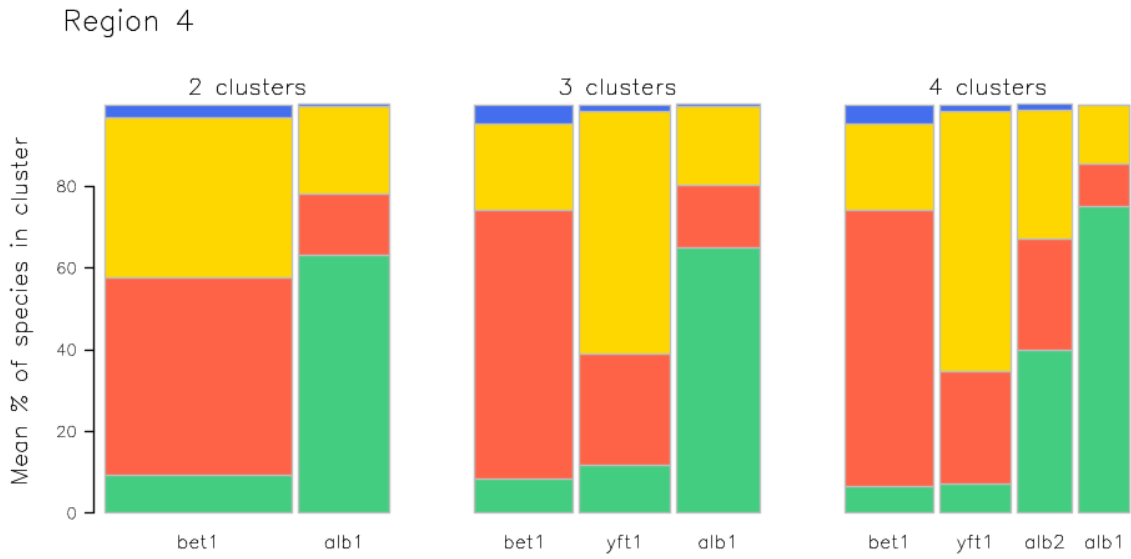


Figure 25: Mean proportion of species in the catch of targeting clusters in region 4, shown for 2, 3, and 4 cluster models. The width of the bar is proportional to the number of records in the cluster.

Region 4

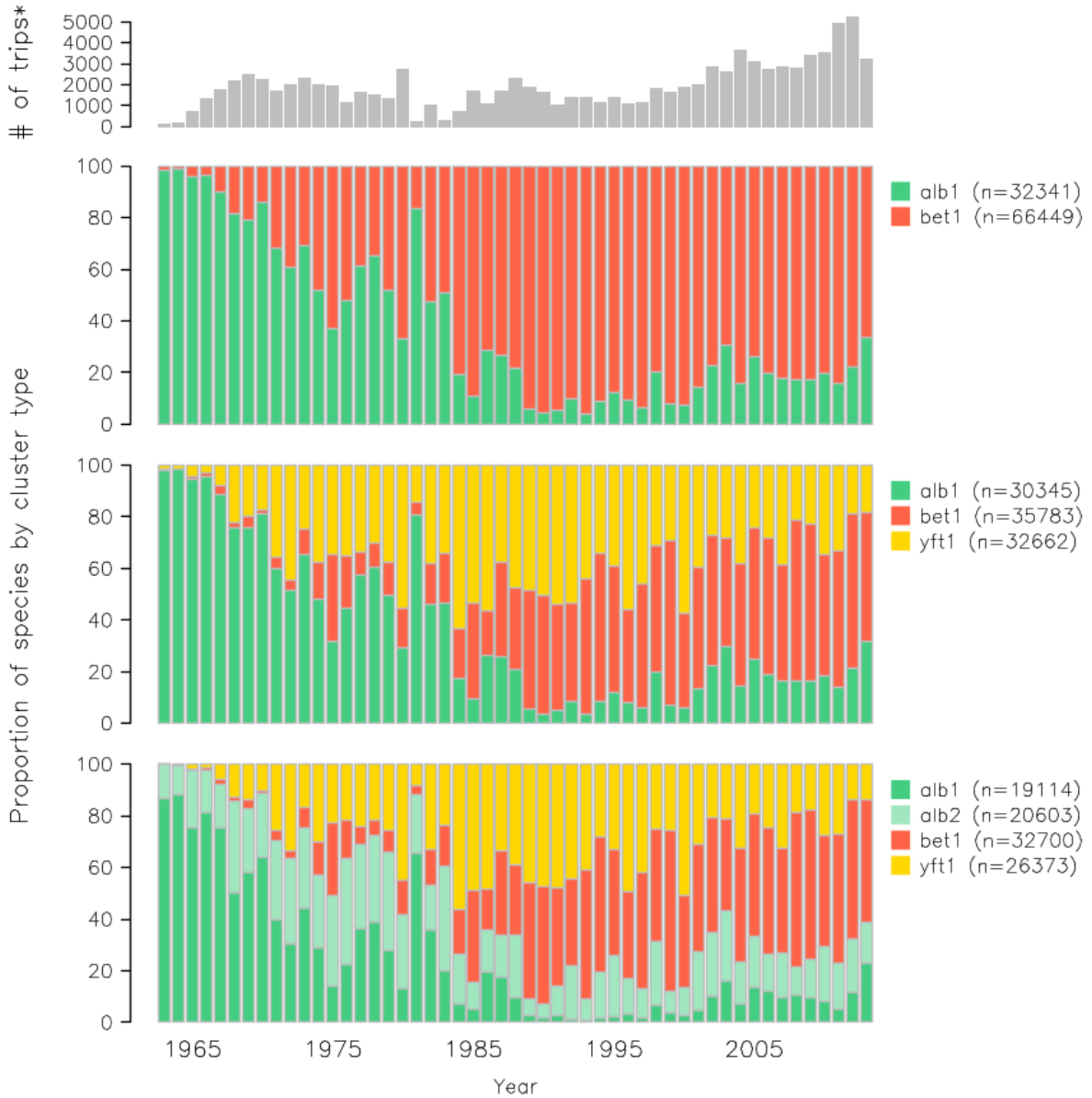


Figure 26: Time series of cluster membership for the 2, 3, and 4 cluster models, with the colour matching the dominant species in the cluster and the top panel indicating the number of records over time.



Figure 27: Mean proportion of species in the catch of targeting clusters in region 5, shown for 2, 3, and 4 cluster models. The width of the bar is proportional to the number of records in the cluster.

Region 5

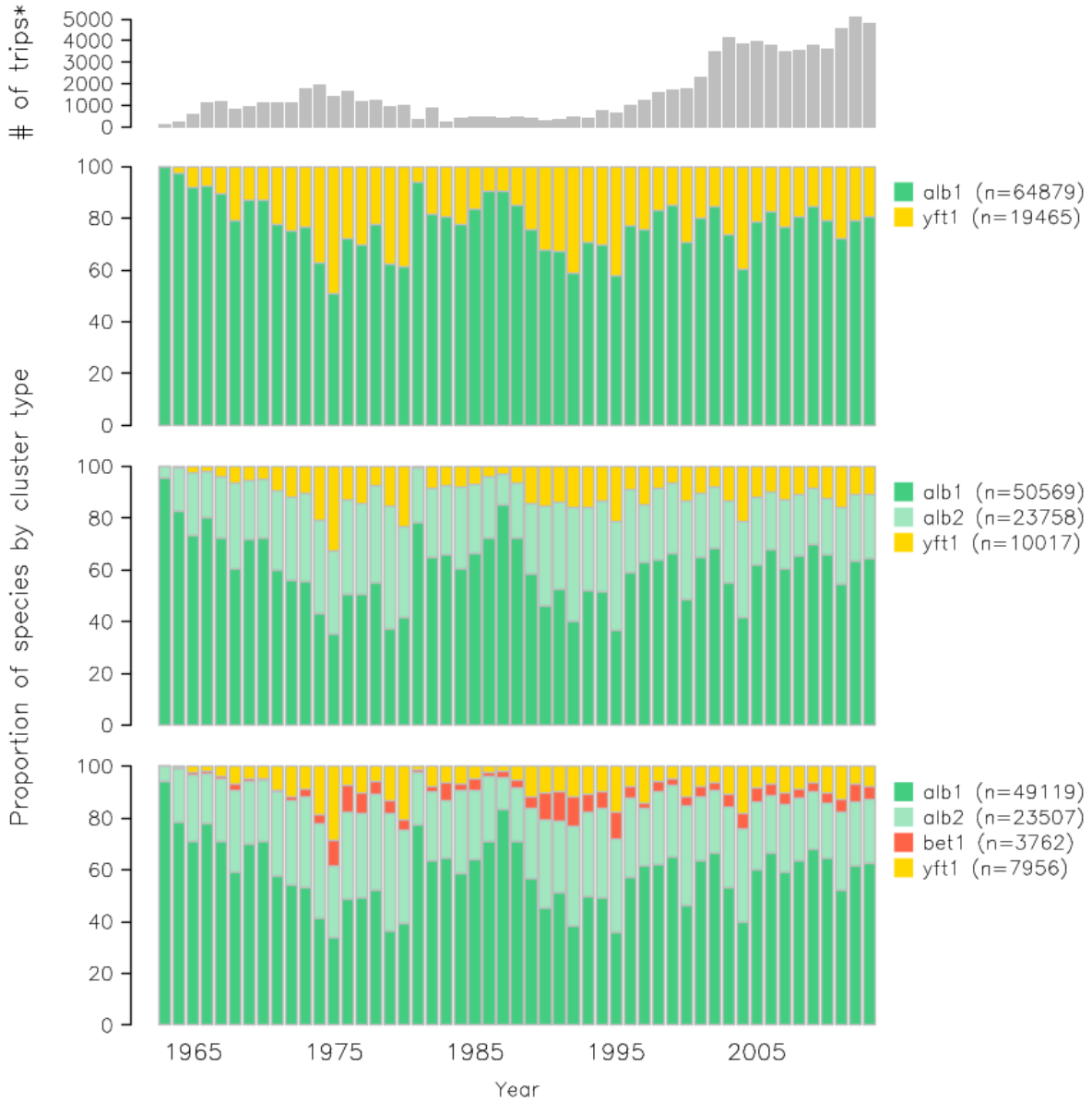


Figure 28: Time series of cluster membership for the 2, 3, and 4 cluster models, with the colour matching the dominant species in the cluster and the top panel indicating the number of records over time.

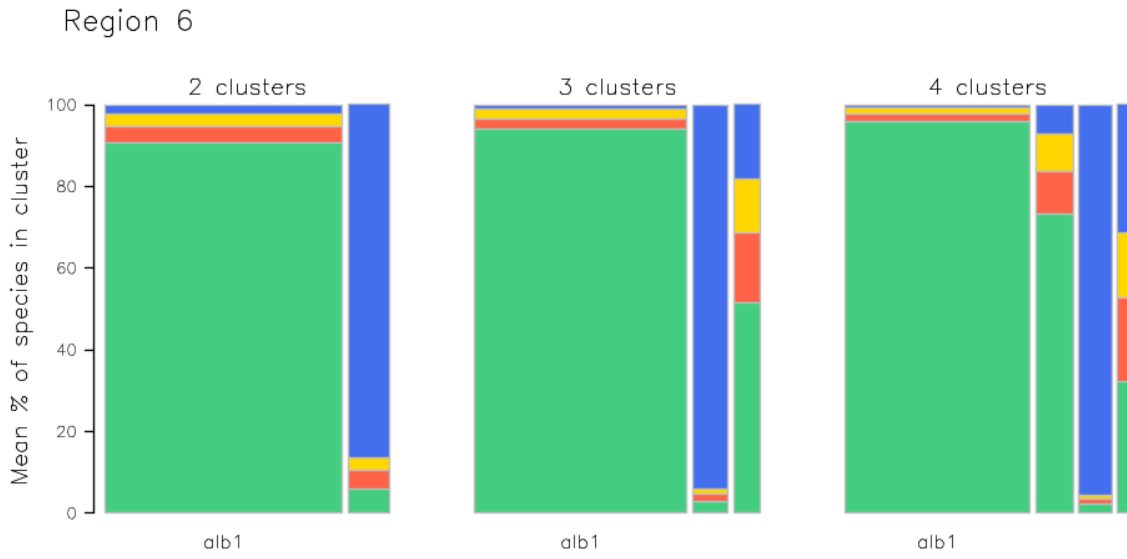


Figure 29: Mean proportion of species in the catch of targeting clusters in region 6, shown for 2, 3, and 4 cluster models. The width of the bar is proportional to the number of records in the cluster.

Region 6

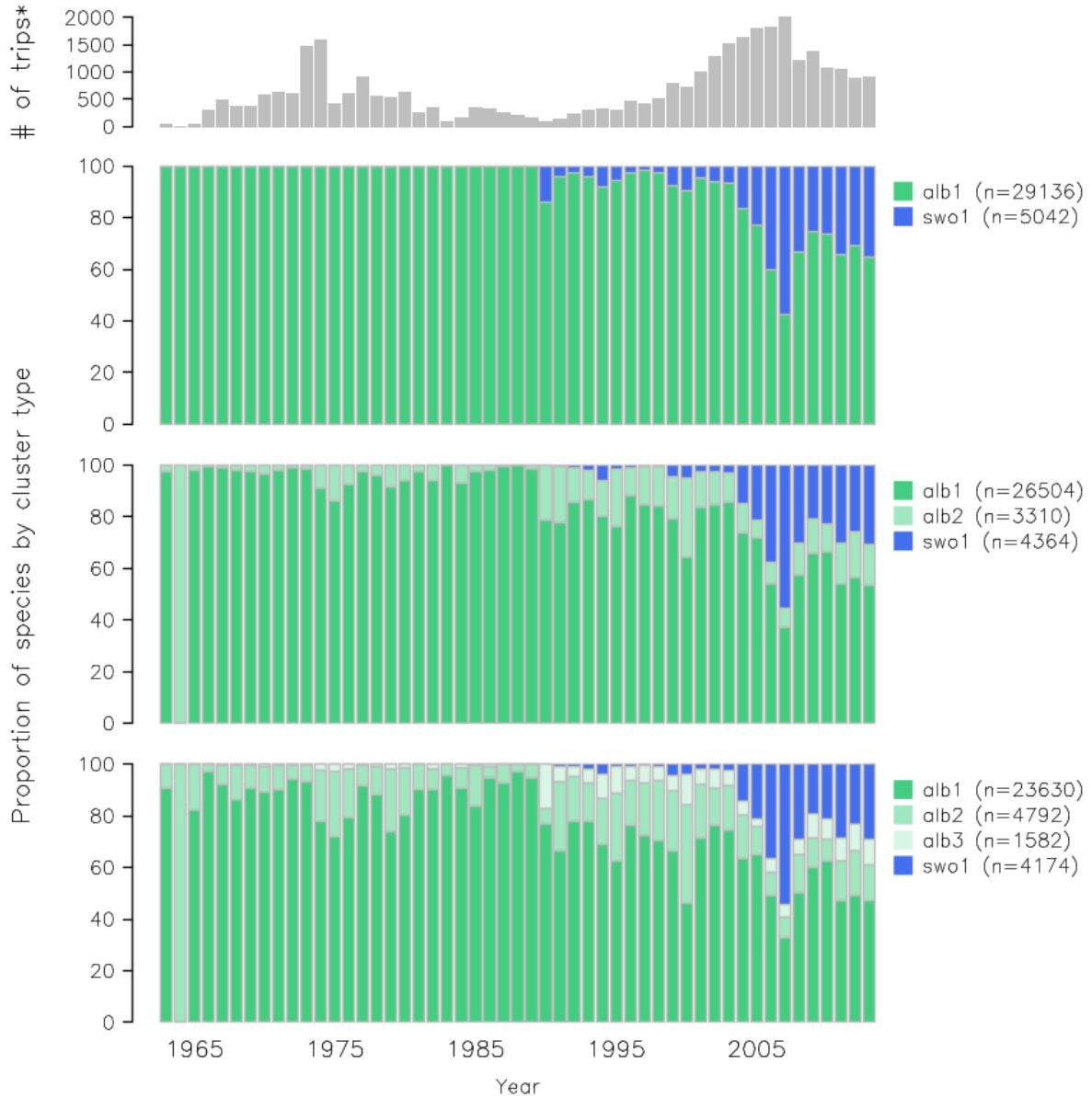


Figure 30: Time series of cluster membership for the 2, 3, and 4 cluster models, with the colour matching the dominant species in the cluster and the top panel indicating the number of records over time.

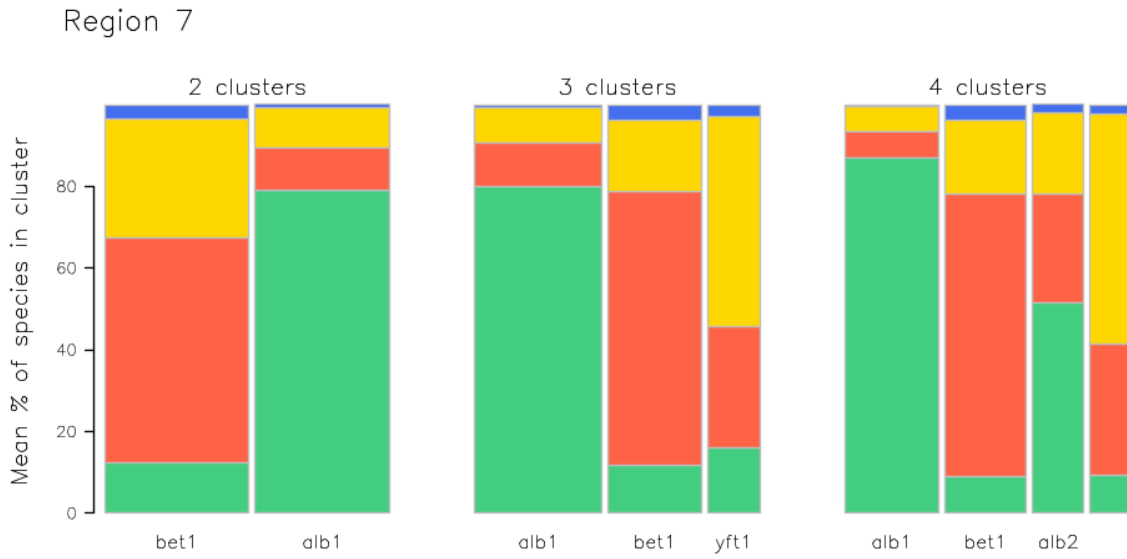


Figure 31: Mean proportion of species in the catch of targeting clusters in region 7, shown for 2, 3, and 4 cluster models. The width of the bar is proportional to the number of records in the cluster.

Region 7

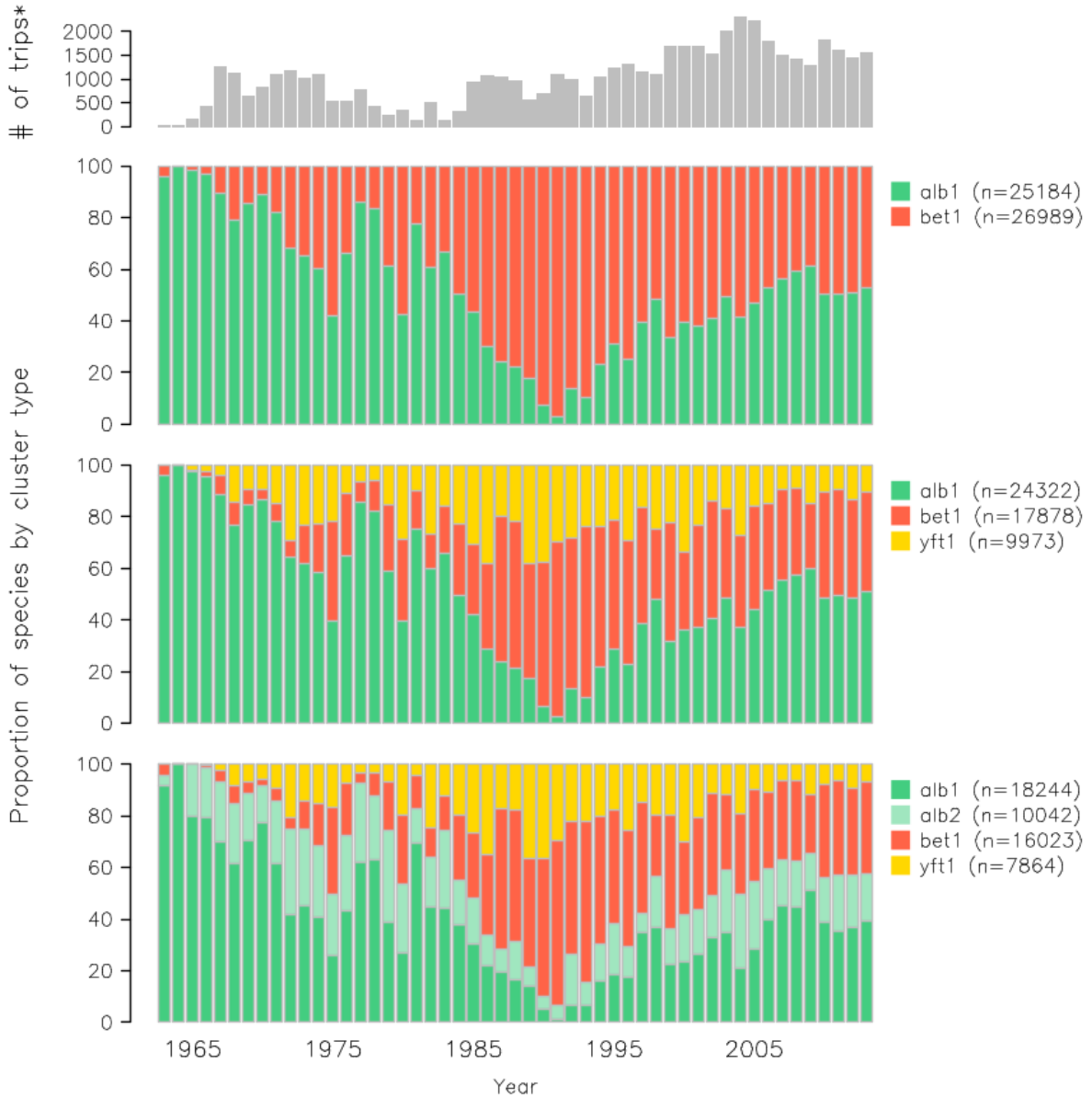


Figure 32: Time series of cluster membership for the 2, 3, and 4 cluster models, with the colour matching the dominant species in the cluster and the top panel indicating the number of records over time.

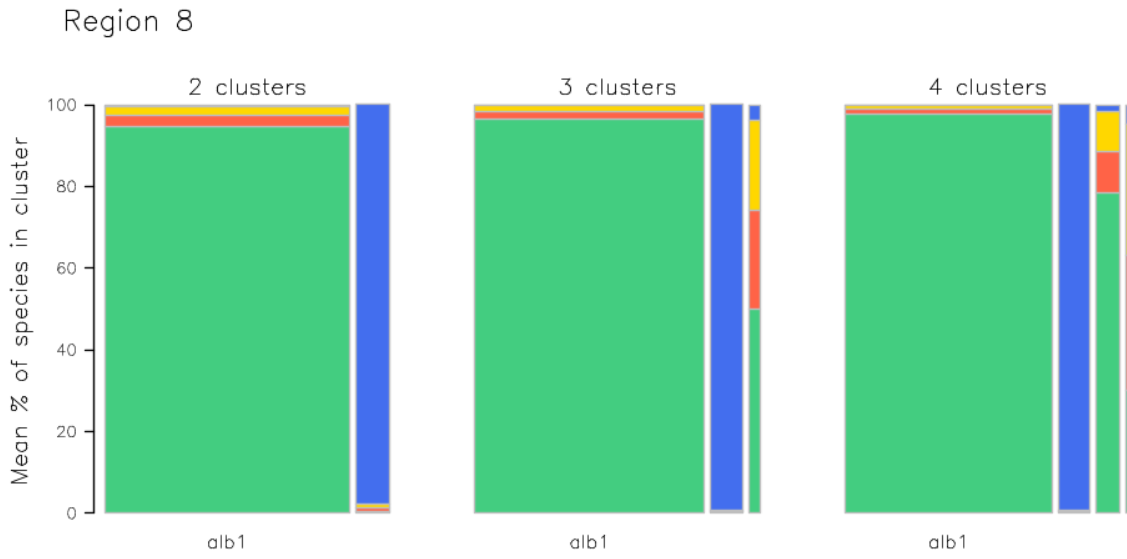


Figure 33: Mean proportion of species in the catch of targeting clusters in region 8, shown for 2, 3, and 4 cluster models. The width of the bar is proportional to the number of records in the cluster.

Region 8

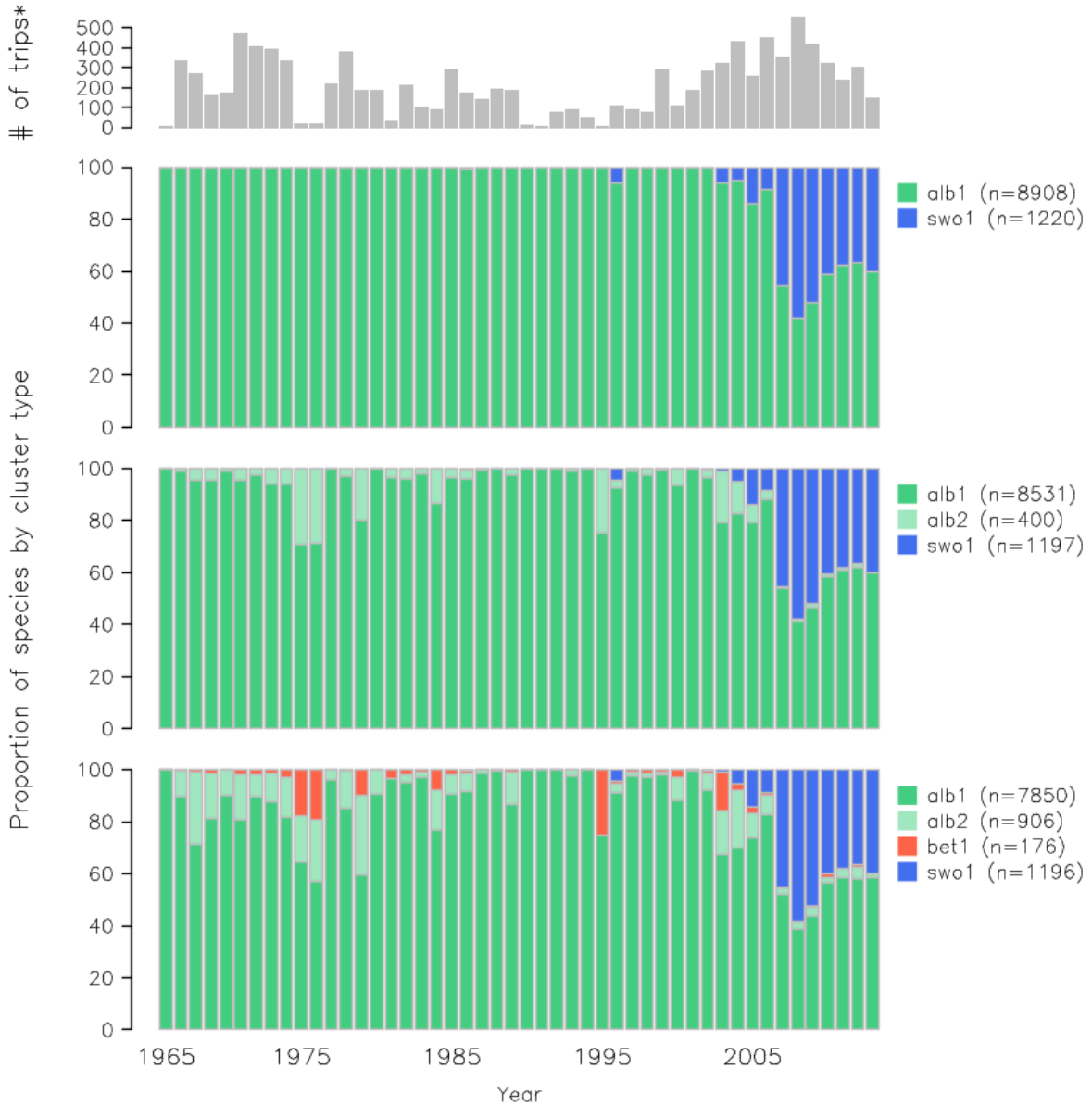


Figure 34: Time series of cluster membership for the 2, 3, and 4 cluster models, with the colour matching the dominant species in the cluster and the top panel indicating the number of records over time.

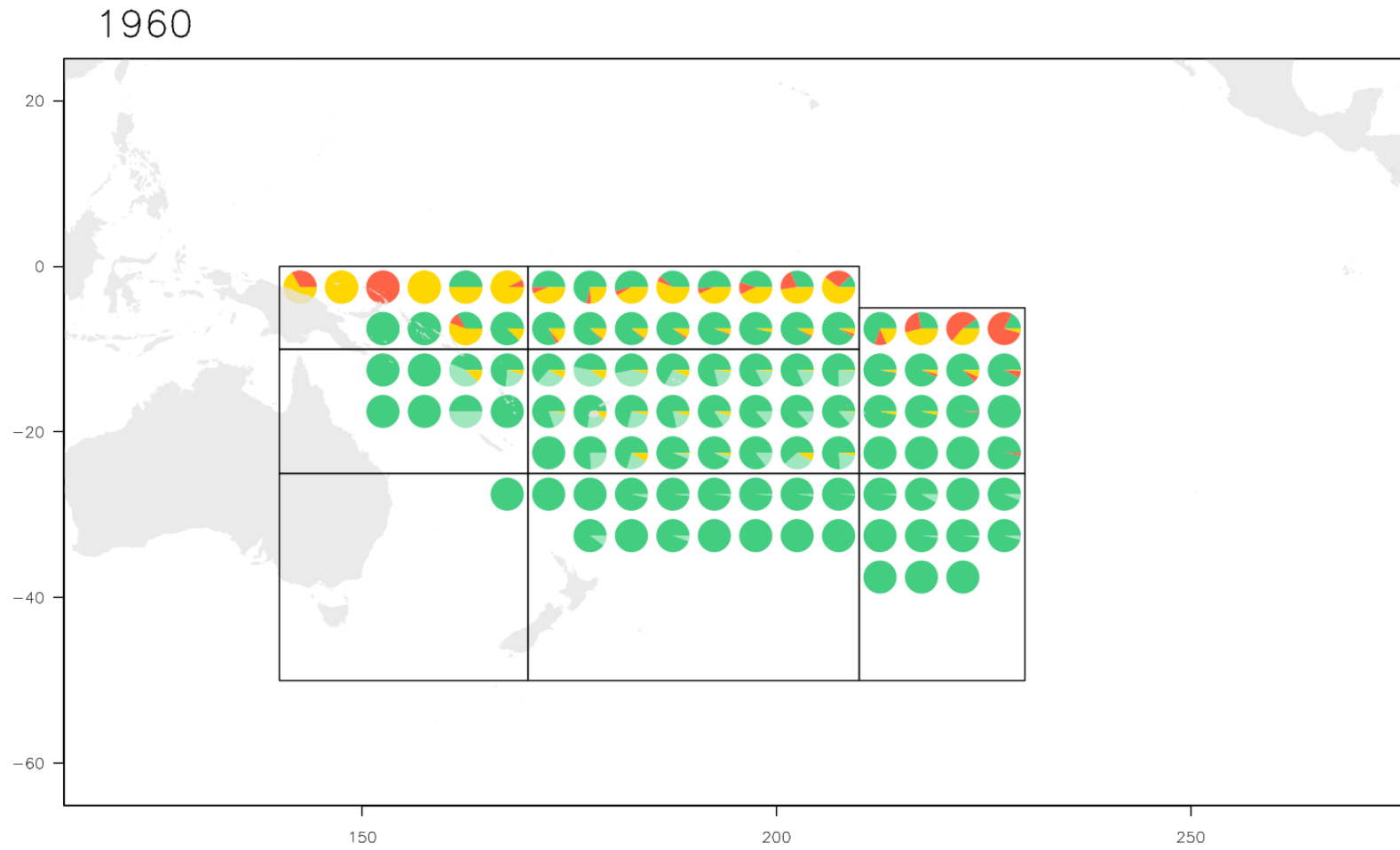


Figure 35: Map of cluster composition at the 5 degree scale, by decade, with region-specific cluster numbers as described in Table 2. ALB, BET, SWO and YFT are given by green, red, blue and yellow, respective

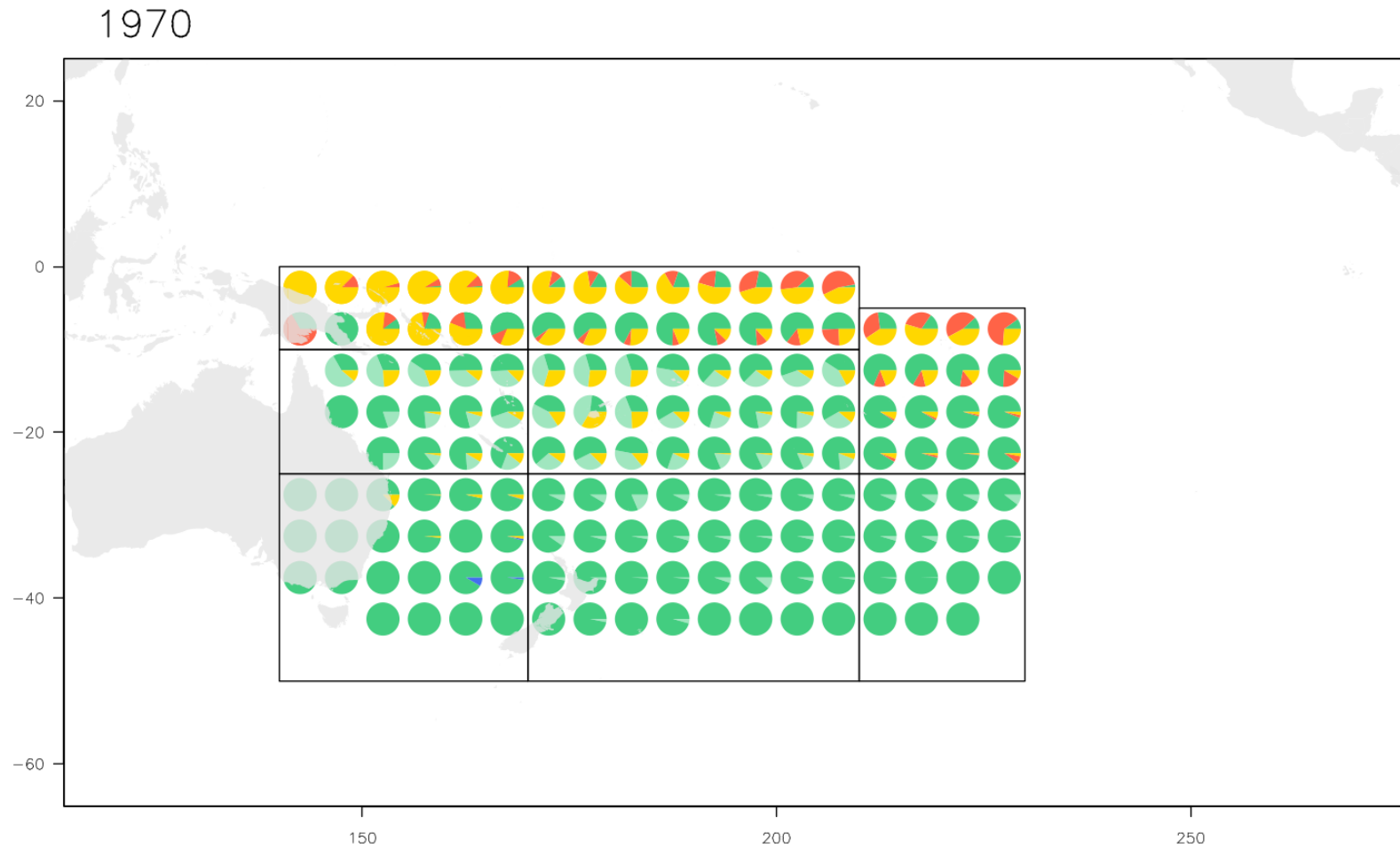


Figure 36: Map of cluster composition at the 5 degree scale, by decade, with region-specific cluster numbers as described in Table 2. ALB, BET, SWO and YFT are given by green, red, blue and yellow, respective

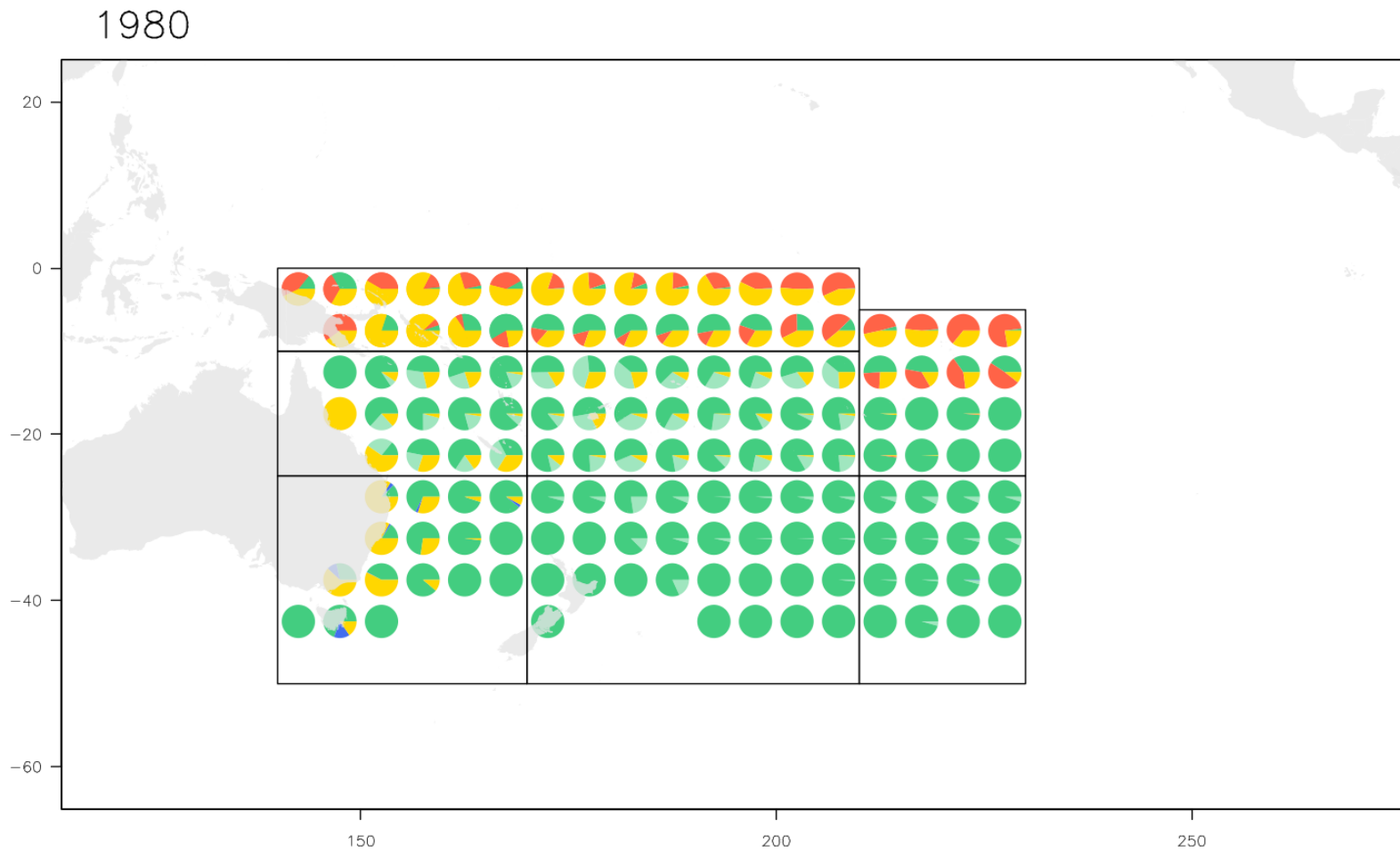


Figure 37: Map of cluster composition at the 5 degree scale, by decade, with region-specific cluster numbers as described in Table 2. ALB, BET, SWO and YFT are given by green, red, blue and yellow, respective

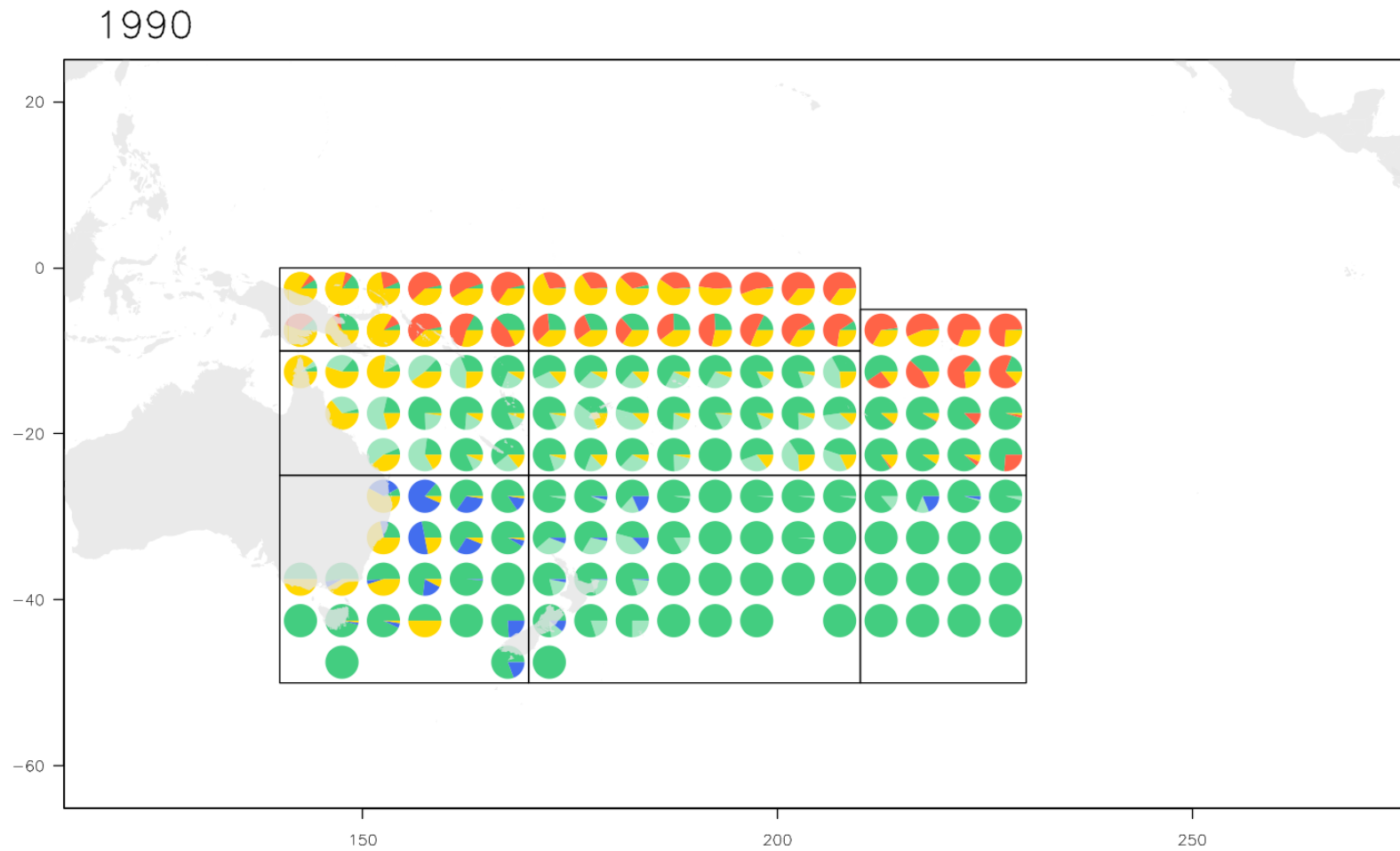


Figure 38: Map of cluster composition at the 5 degree scale, by decade, with region-specific cluster numbers as described in Table 2. ALB, BET, SWO and YFT are given by green, red, blue and yellow, respective

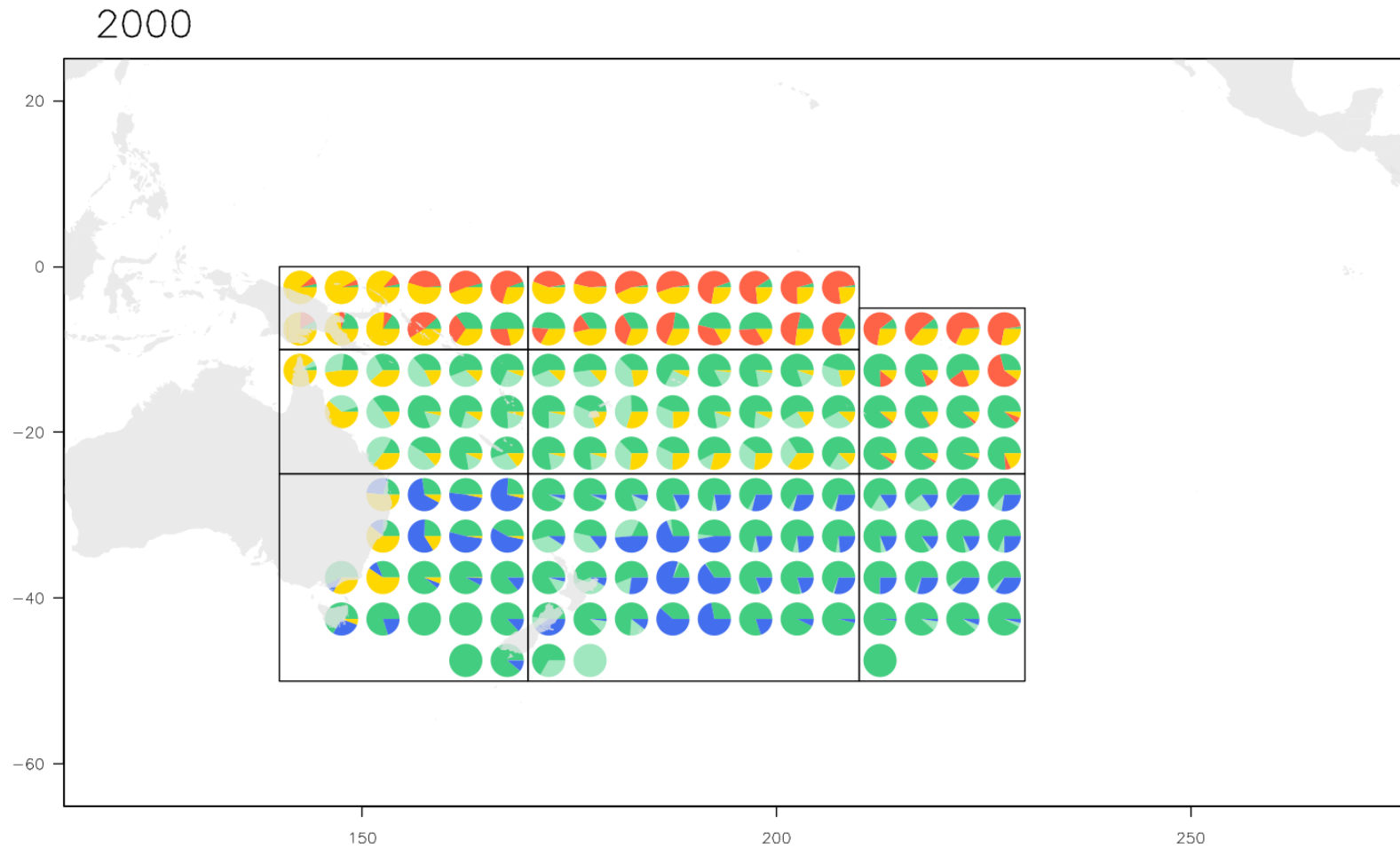


Figure 39: Map of cluster composition at the 5 degree scale, by decade, with region-specific cluster numbers as described in Table 2. ALB, BET, SWO and YFT are given by green, red, blue and yellow, respective

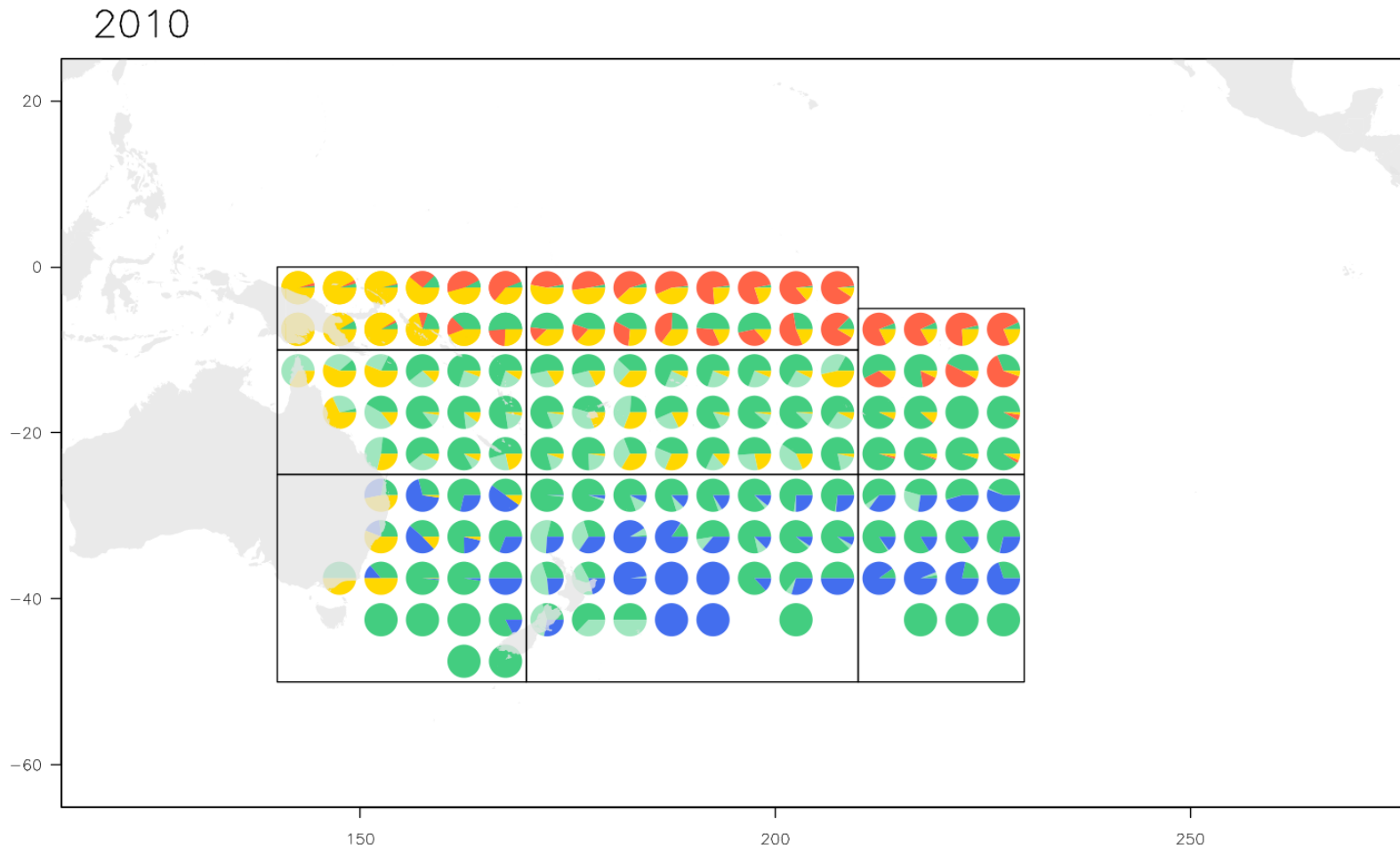


Figure 40: Map of cluster composition at the 5 degree scale, by decade, with region-specific cluster numbers as described in Table 2. ALB, BET, SWO and YFT are given by green, red, blue and yellow, respective

Region 1

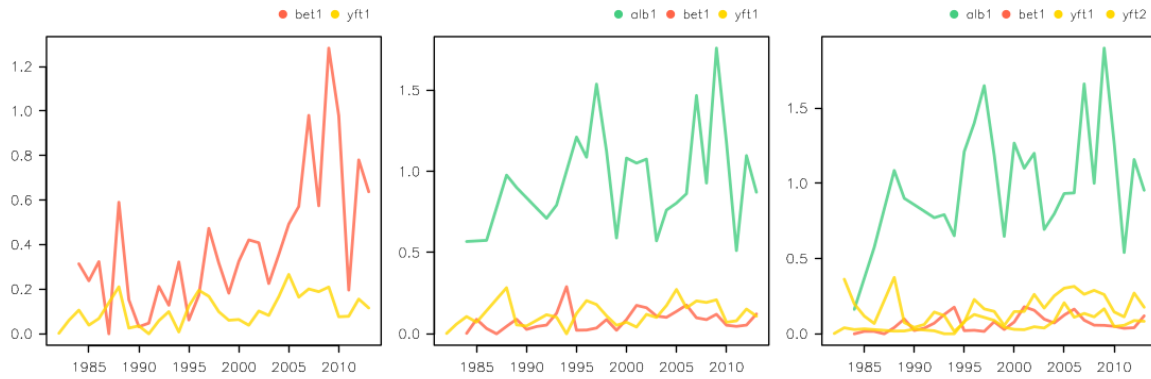


Figure 41: Nominal CPUE by main species targeting cluster for region 1, based on candidate number of targeting clusters 2 to 4.

Region 2

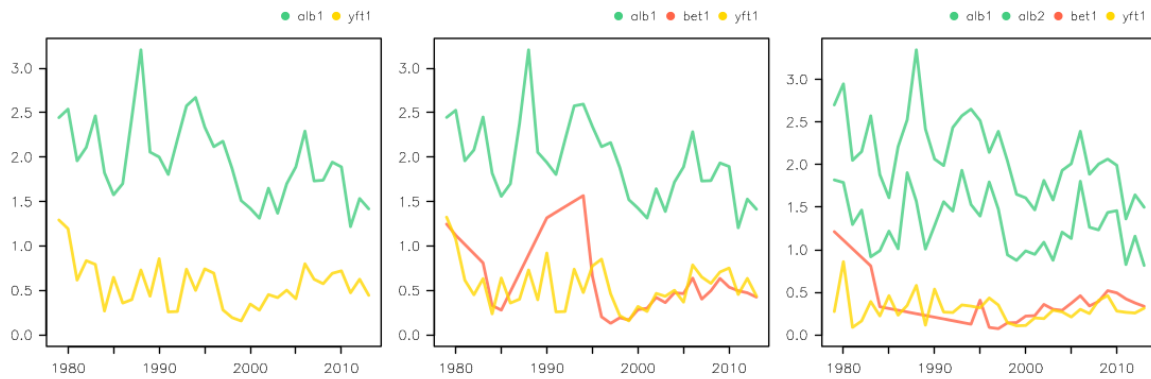


Figure 42: Nominal CPUE by main species targeting cluster for region 2, based on candidate number of targeting clusters 2 to 4.

Region 3

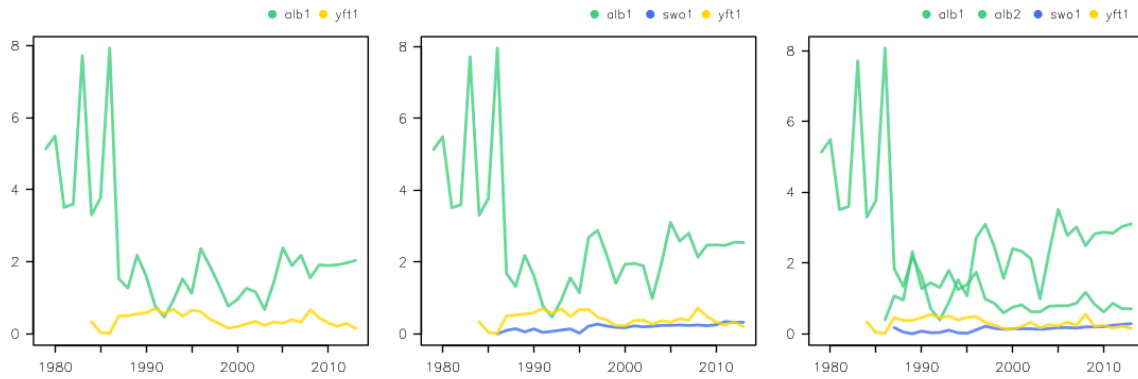


Figure 43: Nominal CPUE by main species targeting cluster for region 3, based on candidate number of targeting clusters 2 to 4.

Region 4

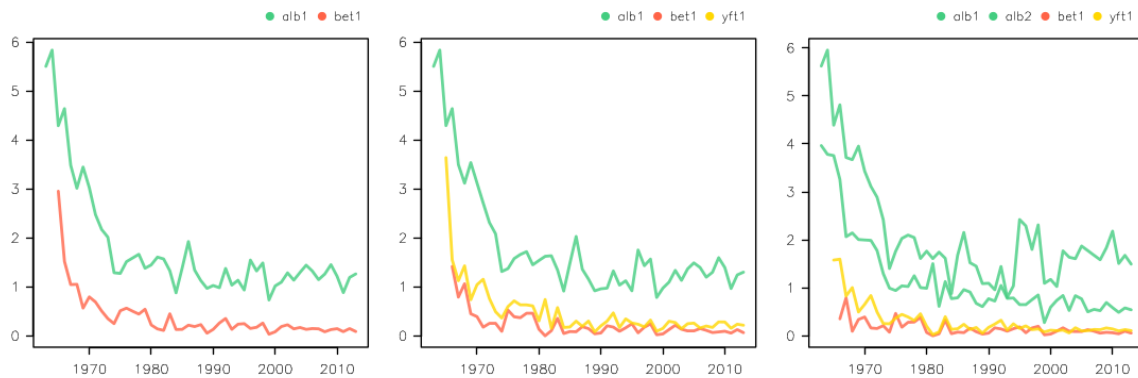


Figure 44: Nominal CPUE by main species targeting cluster for region 4, based on candidate number of targeting clusters 2 to 4.

Region 5

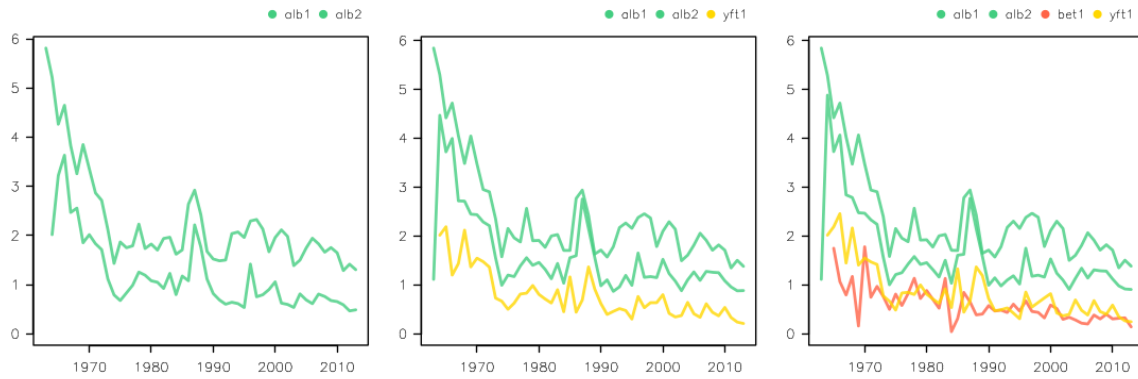


Figure 45: Nominal CPUE by main species targeting cluster for region 5, based on candidate number of targeting clusters 2 to 4.

Region 6

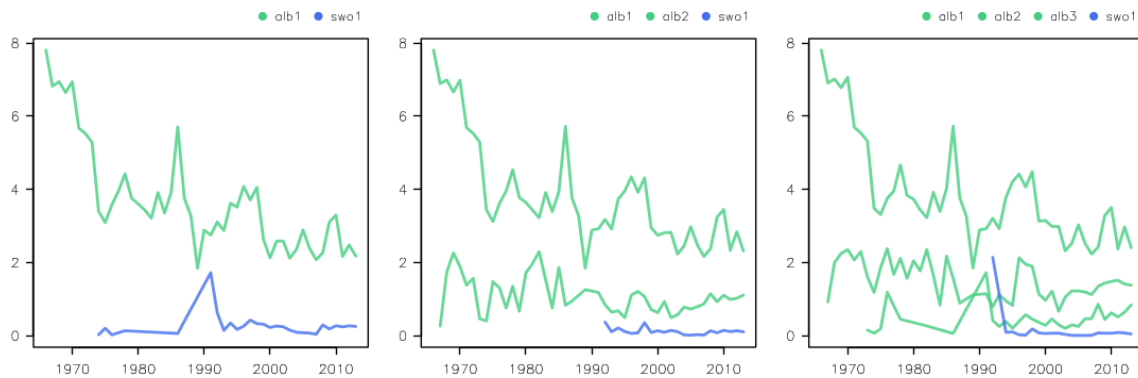


Figure 46: Nominal CPUE by main species targeting cluster for region 6, based on candidate number of targeting clusters 2 to 4.

Region 7

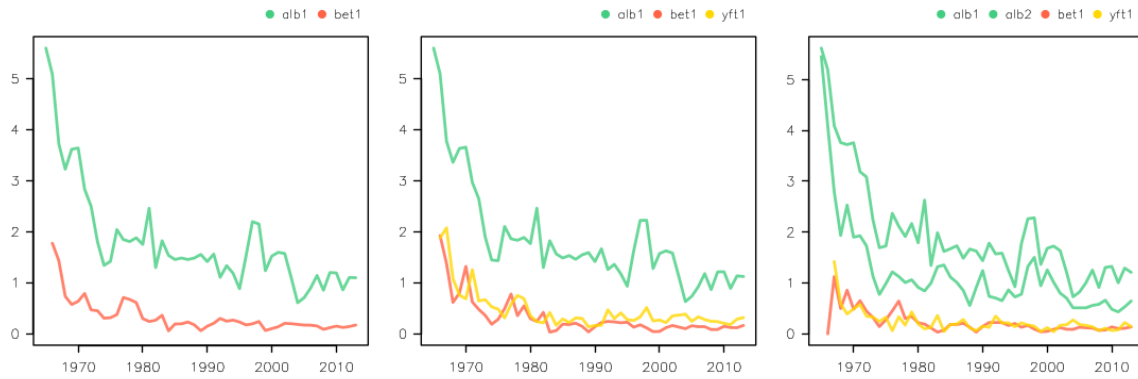


Figure 47: Nominal CPUE by main species targeting cluster for region 7, based on candidate number of targeting clusters 2 to 4.

Region 8

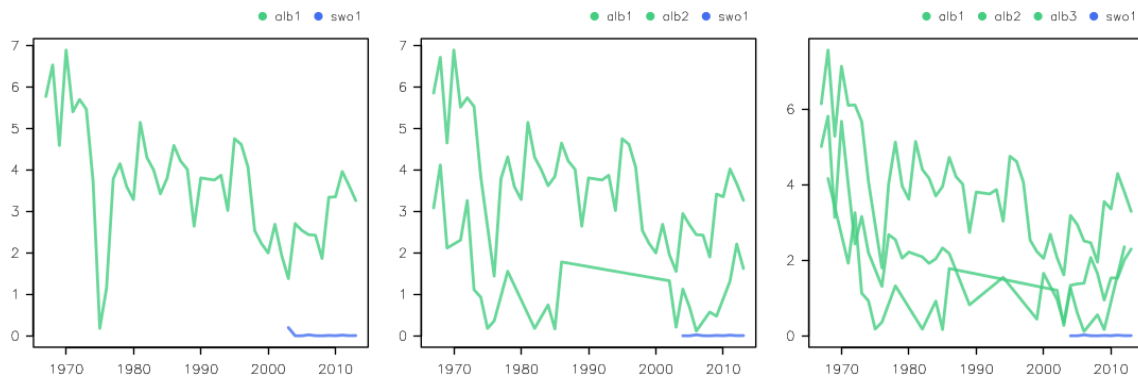


Figure 48: Nominal CPUE by main species targeting cluster for region 8, based on candidate number of targeting clusters 2 to 4.

Nominal CPUE (ind/hhooks) with cumulated levels of data filtering

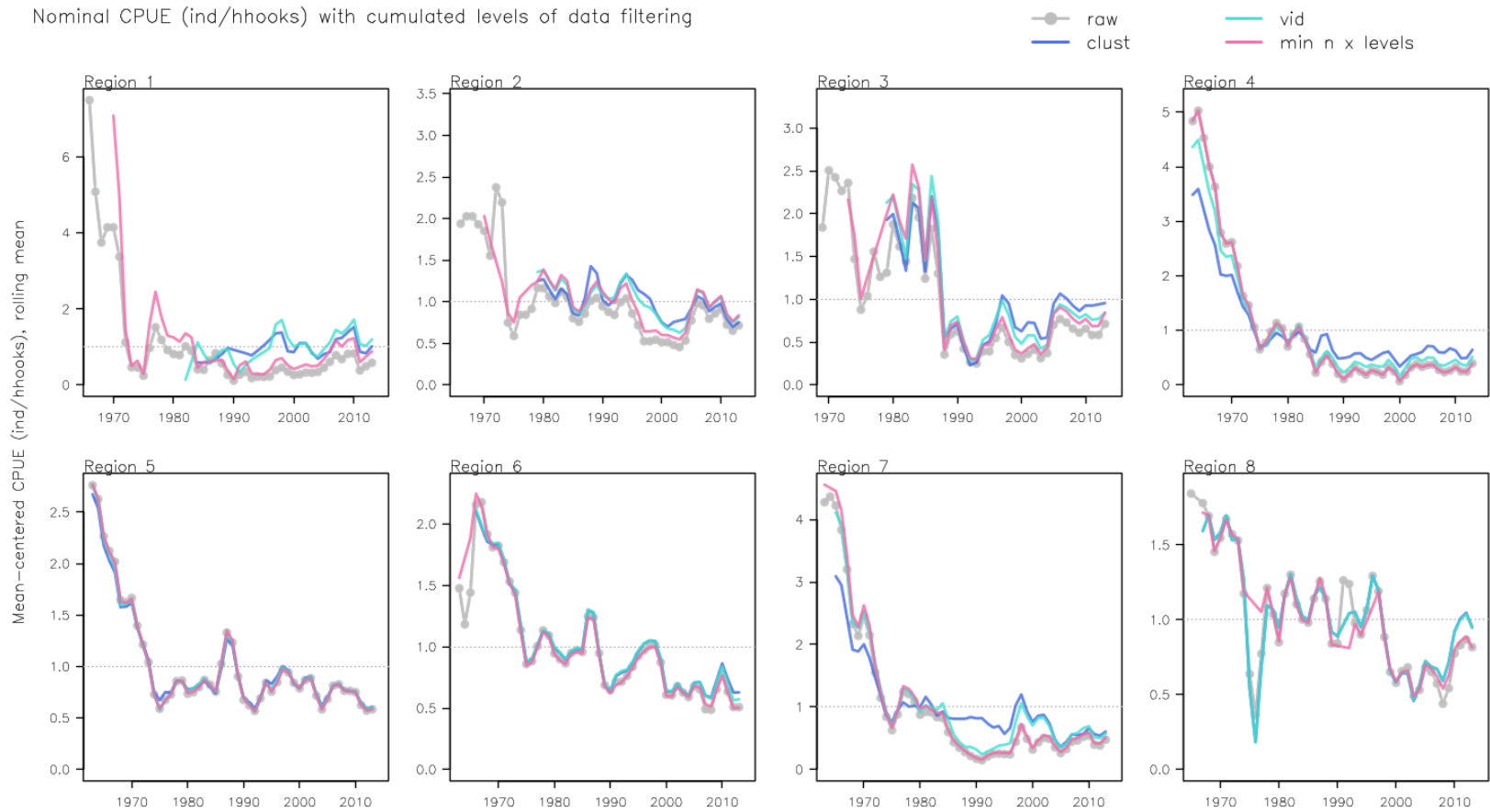


Figure 49: Effect of filter applied individually on nominal CPUE (# individual/100 hooks).

Standardized CPUE (ind/hooks) for full and truncated data series

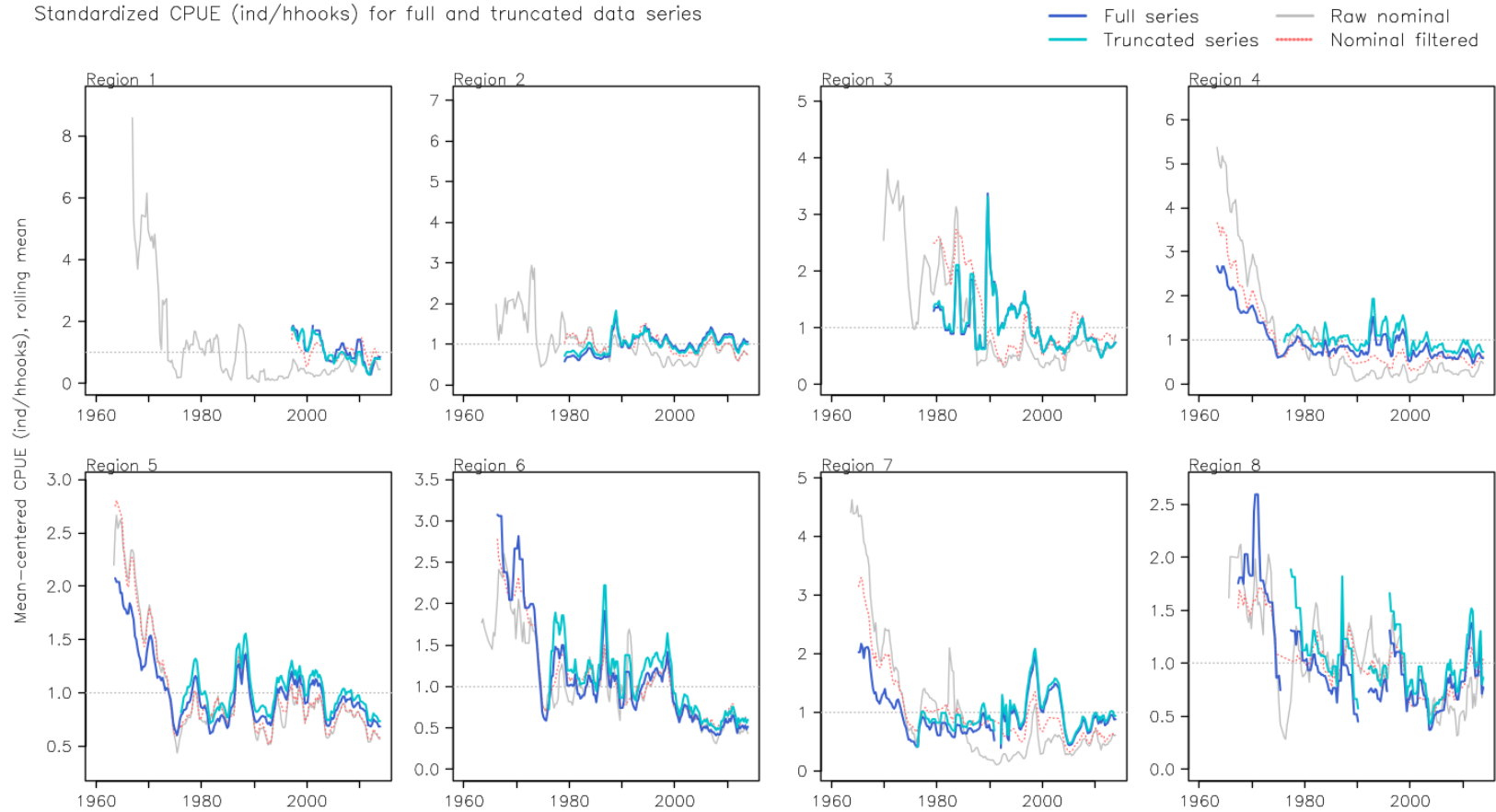


Figure 50: Comparison of final standardized CPUE indices for the full and truncated temporal span. Unfiltered and filtered standardized CPUEs are included for reference

Step plots: region 1

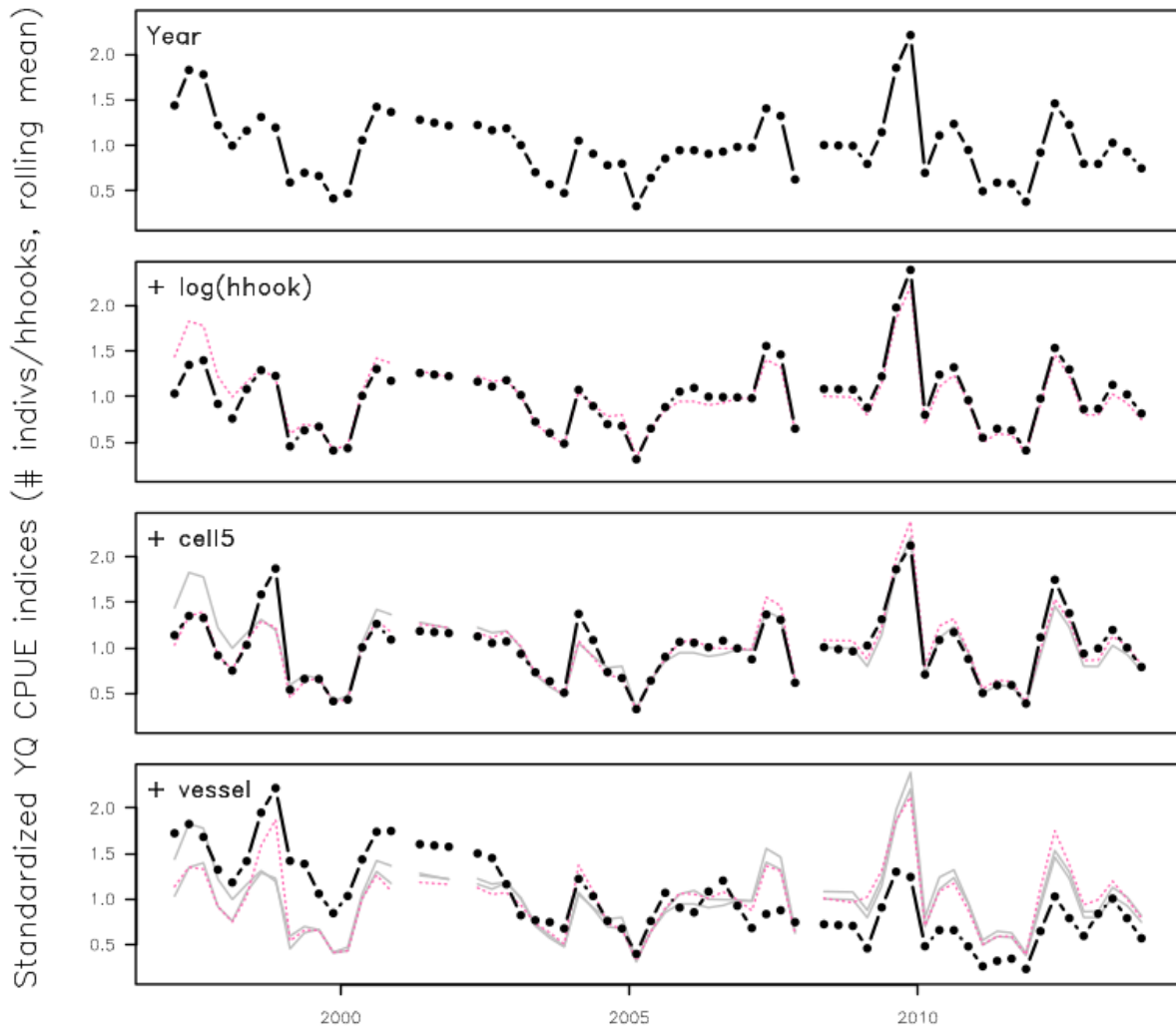


Figure 51: Step plots for region 1: cumulative impact on standardized year-quarter indices of adding, from top to bottom, log hook continuous predictor, 5 degree cell and vessel ID. The focal model is in black-bold, the previous model is in pink-dash, and models before that, when applicable, are in grey.

Step plots: region 2

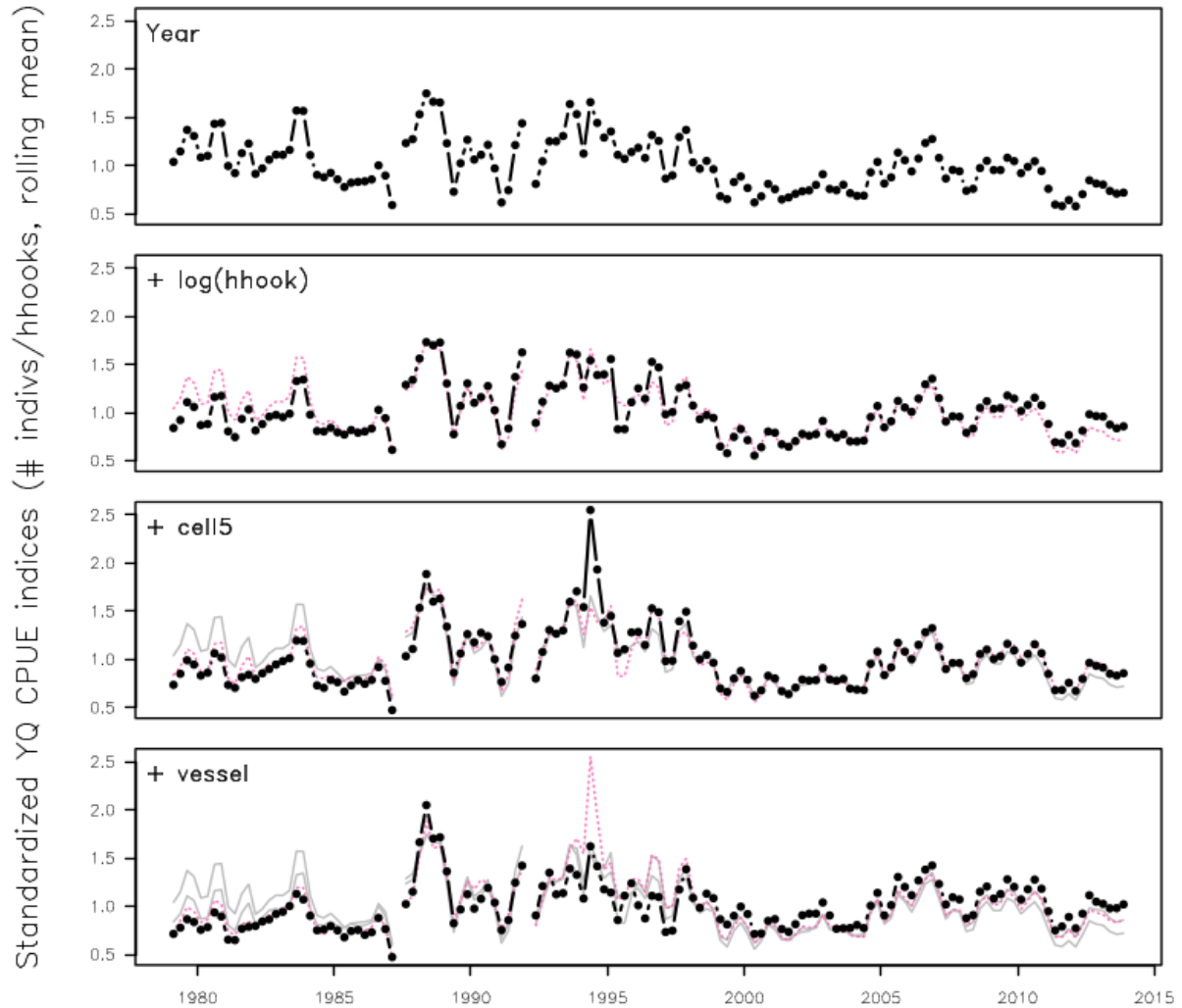


Figure 52: Step plots for region 2: cumulative impact on standardized year-quarter indices of adding, from top to bottom, log hook continuous predictor, 5 degree cell and vessel ID. The focal model is in black-bold, the previous model is in pink-dash, and models before that, when applicable, are in grey.

Step plots: region 3

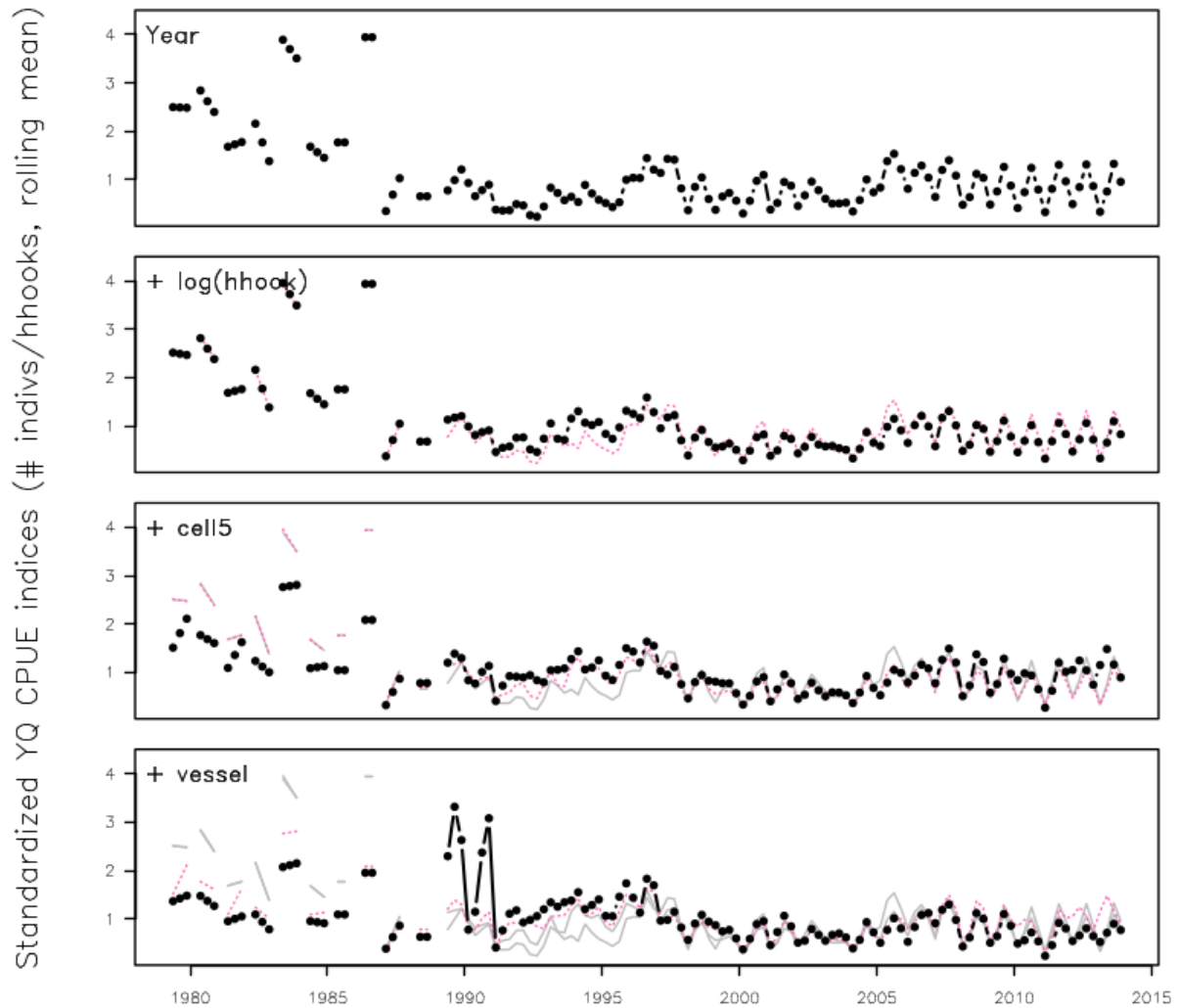


Figure 53: Step plots for region 3: cumulative impact on standardized year-quarter indices of adding, from top to bottom, log hook continuous predictor, 5 degree cell and vessel ID. The focal model is in black-bold, the previous model is in pink-dash, and models before that, when applicable, are in grey.

Step plots: region 4

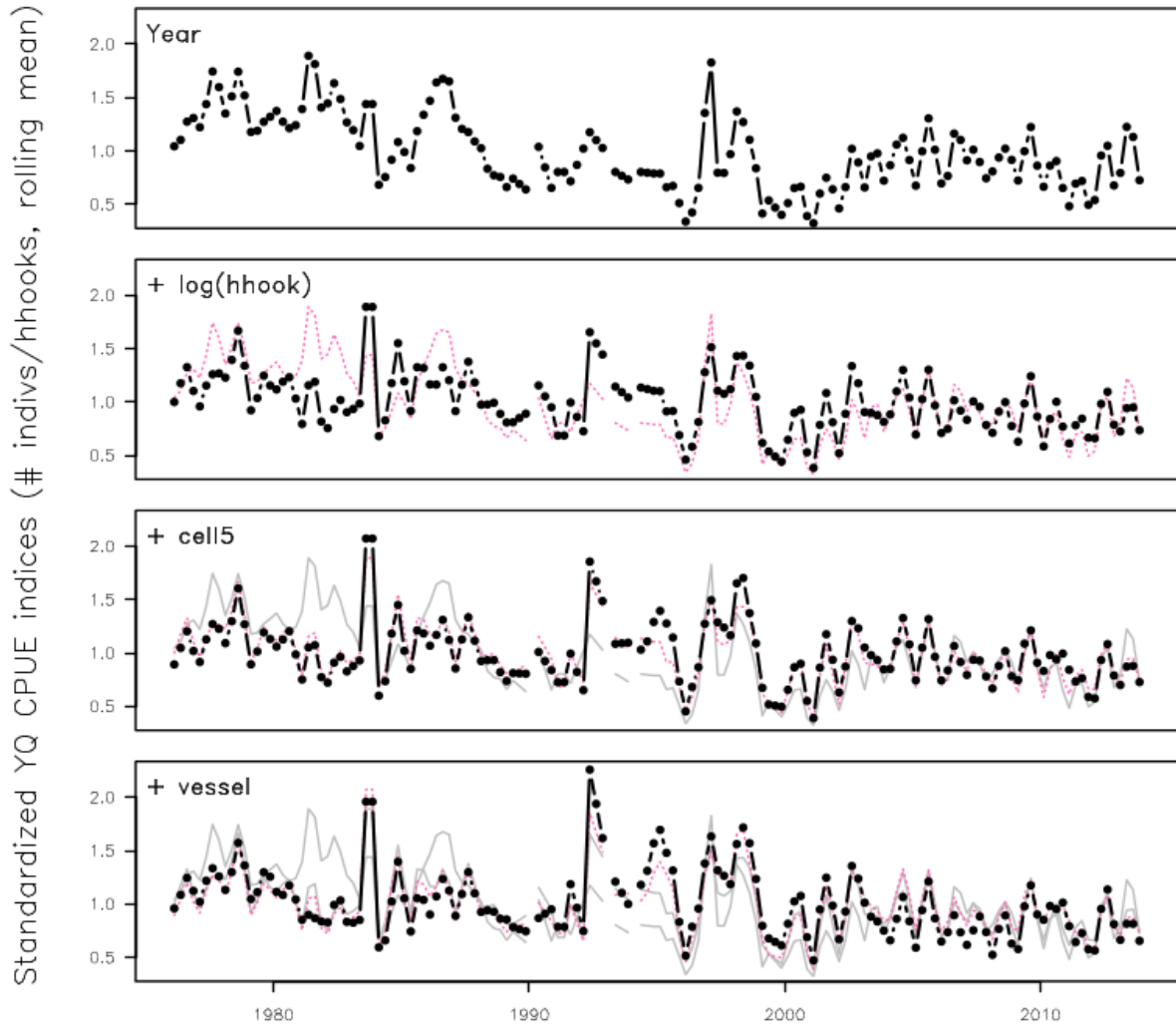


Figure 54: Step plots for region 4: cumulative impact on standardized year-quarter indices of adding, from top to bottom, log hook continuous predictor, 5 degree cell and vessel ID. The focal model is in black-bold, the previous model is in pink-dash, and models before that, when applicable, are in grey.

Step plots: region 5

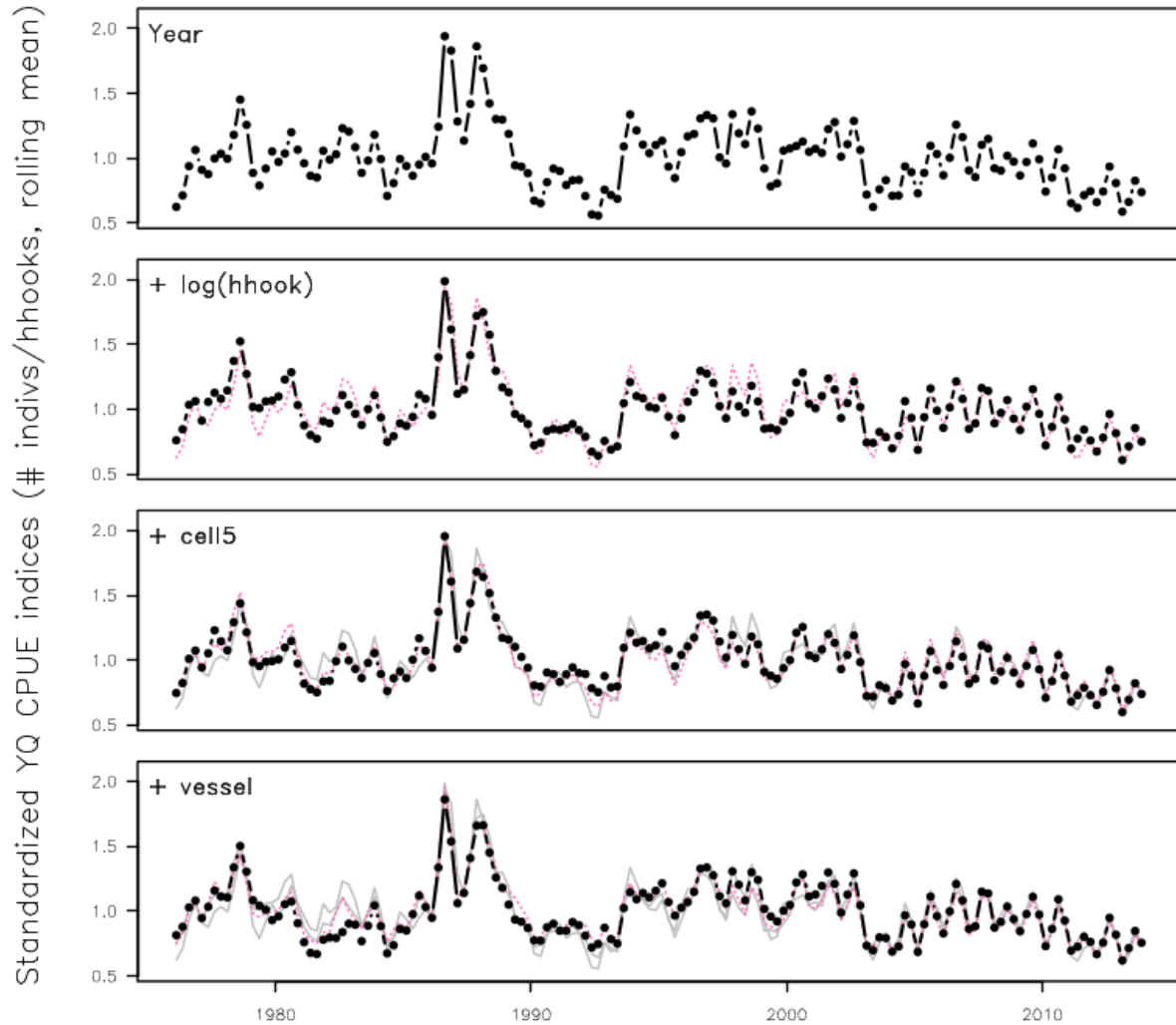


Figure 55: Step plots for region 5: cumulative impact on standardized year-quarter indices of adding, from top to bottom, log hook continuous predictor, 5 degree cell and vessel ID. The focal model is in black-bold, the previous model is in pink-dash, and models before that, when applicable, are in grey.

Step plots: region 6

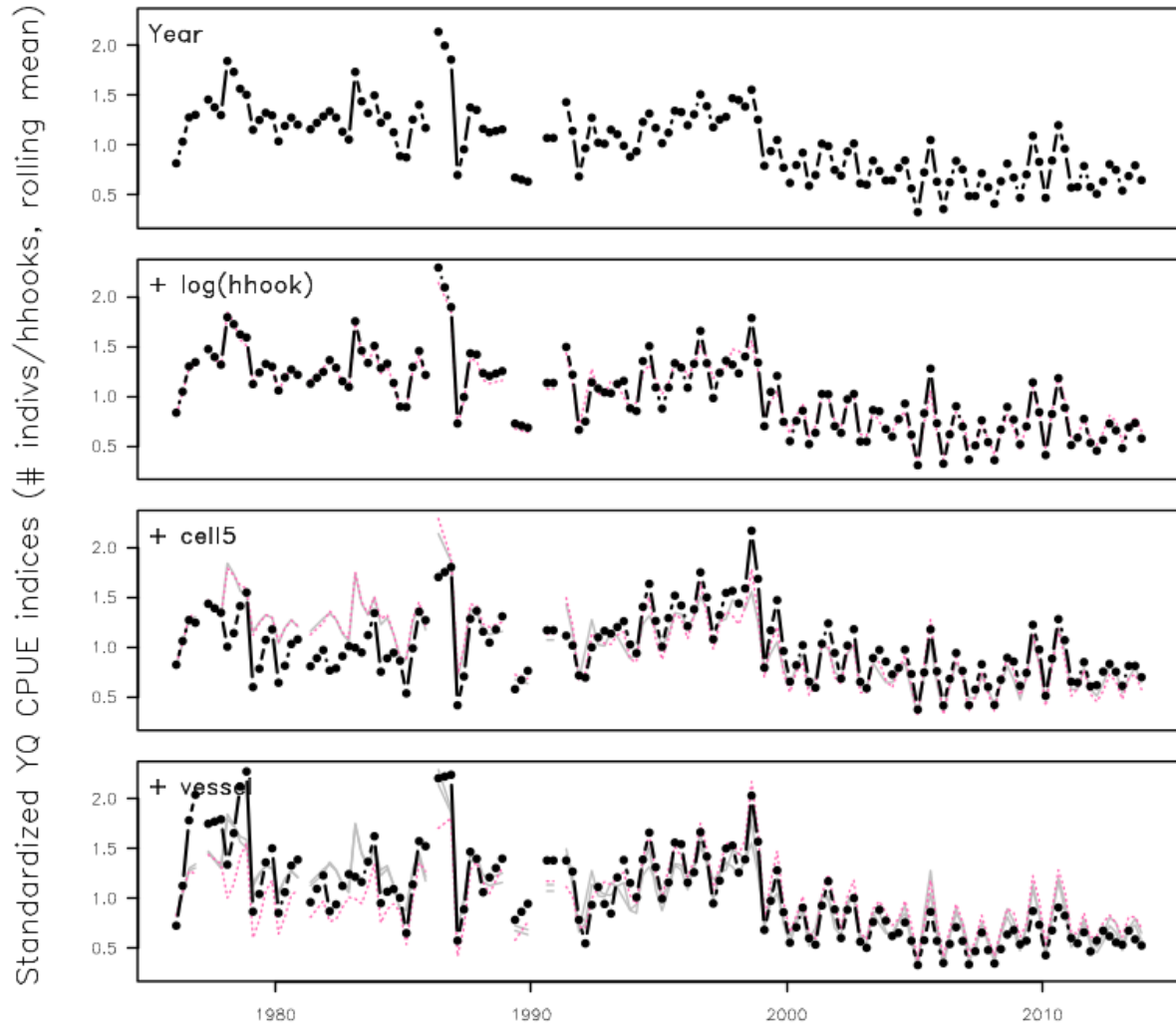


Figure 56: Step plots for region 6: cumulative impact on standardized year-quarter indices of adding, from top to bottom, log hook continuous predictor, 5 degree cell and vessel ID. The focal model is in black-bold, the previous model is in pink-dash, and models before that, when applicable, are in grey.

Step plots: region 7

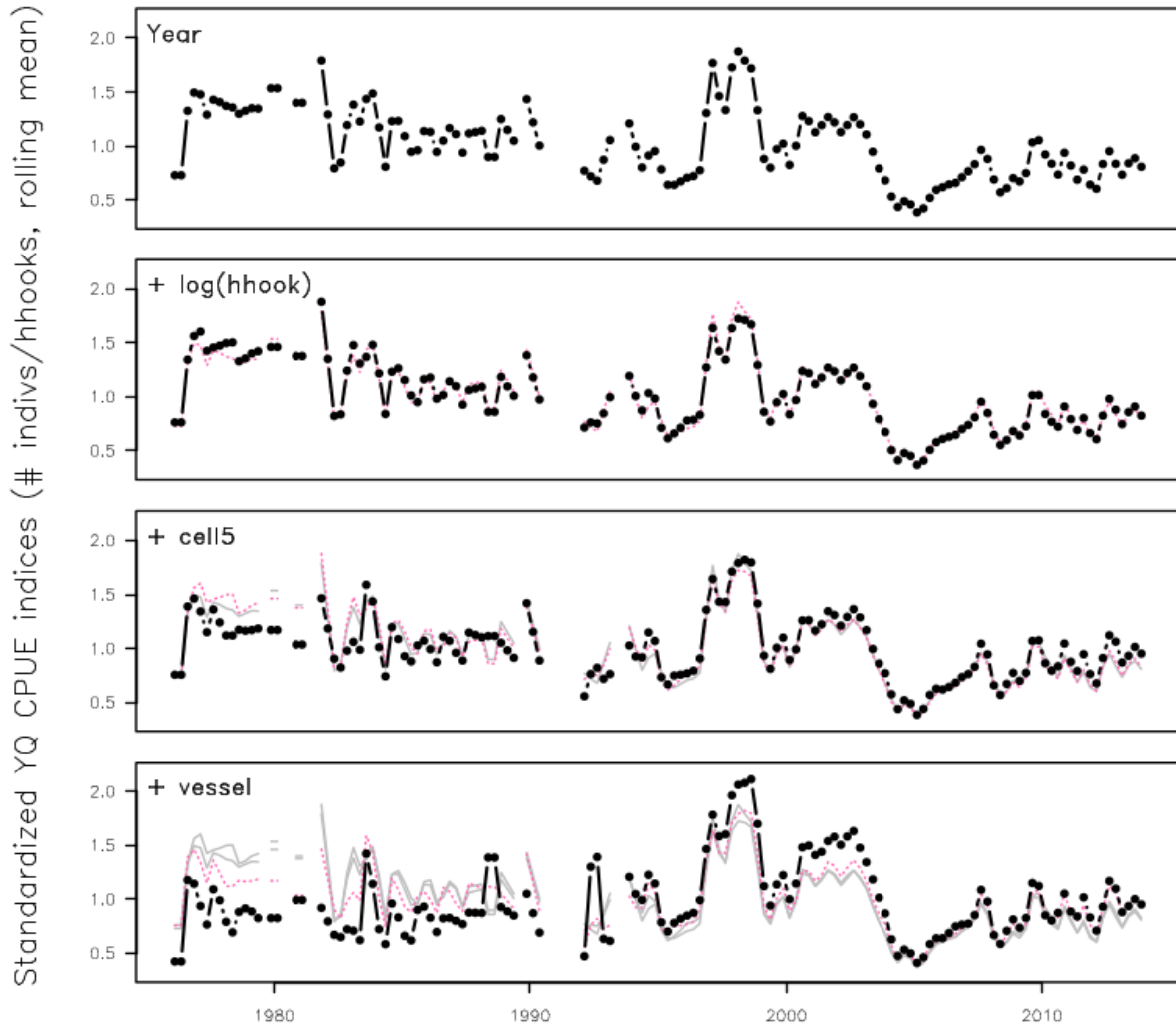


Figure 57: Step plots for region 7: cumulative impact on standardized year-quarter indices of adding, from top to bottom, log hook continuous predictor, 5 degree cell and vessel ID. The focal model is in black-bold, the previous model is in pink-dash, and models before that, when applicable, are in grey.

Step plots: region 8

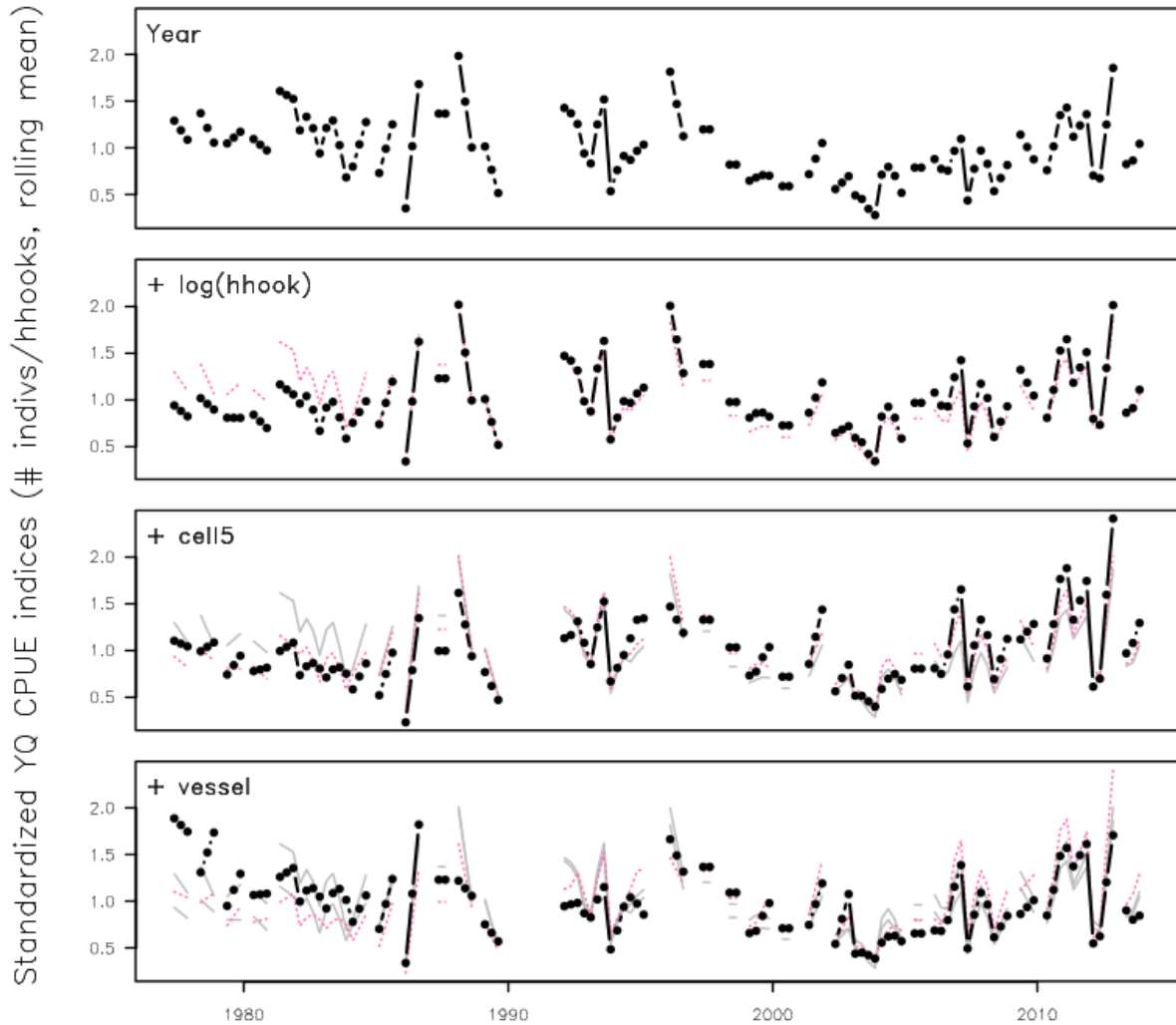


Figure 58: Step plots for region 8: cumulative impact on standardized year-quarter indices of adding, from top to bottom, log hook continuous predictor, 5 degree cell and vessel ID. The focal model is in black-bold, the previous model is in pink-dash, and models before that, when applicable, are in grey.

Diagnostic plots

The plots presented below display a range of diagnostics that describe the fit of the GLM models and the features of the model that affect the standardisation of the raw CPUE data. There are two figures for each model, a figure displaying the estimated coefficients for the main variables and their influence plot ('summary' plots) and a figure showing residuals and simulated data (diagnostic plots). The summary plots shown the influence plots on the left-hand side and the estimated coefficients on the right-hand side. Note that the vessel coefficients are ordered on the x-axis by the first year-quarter that they appeared in the dataset for the region, and cell coefficients are mapped according to their geographic location. Influence plots are color-coded by relative sample size, going from light-yellow (few) to reds (many). The residual figures plots the observed distribution of ALB counts and the distribution of data simulated from the fitted model (red lines, one for each simulated dataset). If applicable these are divided by cluster type (regions 4 and 5). The top right plot is a normal quantile-quantile of the observed quantile residuals. The left, second-row plot shows the same residuals against the model's fitted values. The remaining plots show box and whiskers of the residuals for the categorical variables in the model, color-coded by quarters or flag if applicable.

Region 1 (Negative binomial):

$\text{cnt} \sim \text{as.factor}(\text{yrqtr}) + \text{as.factor}(\text{cell5}) + \text{as.factor}(\text{vessel_id}) + \text{loghook}$

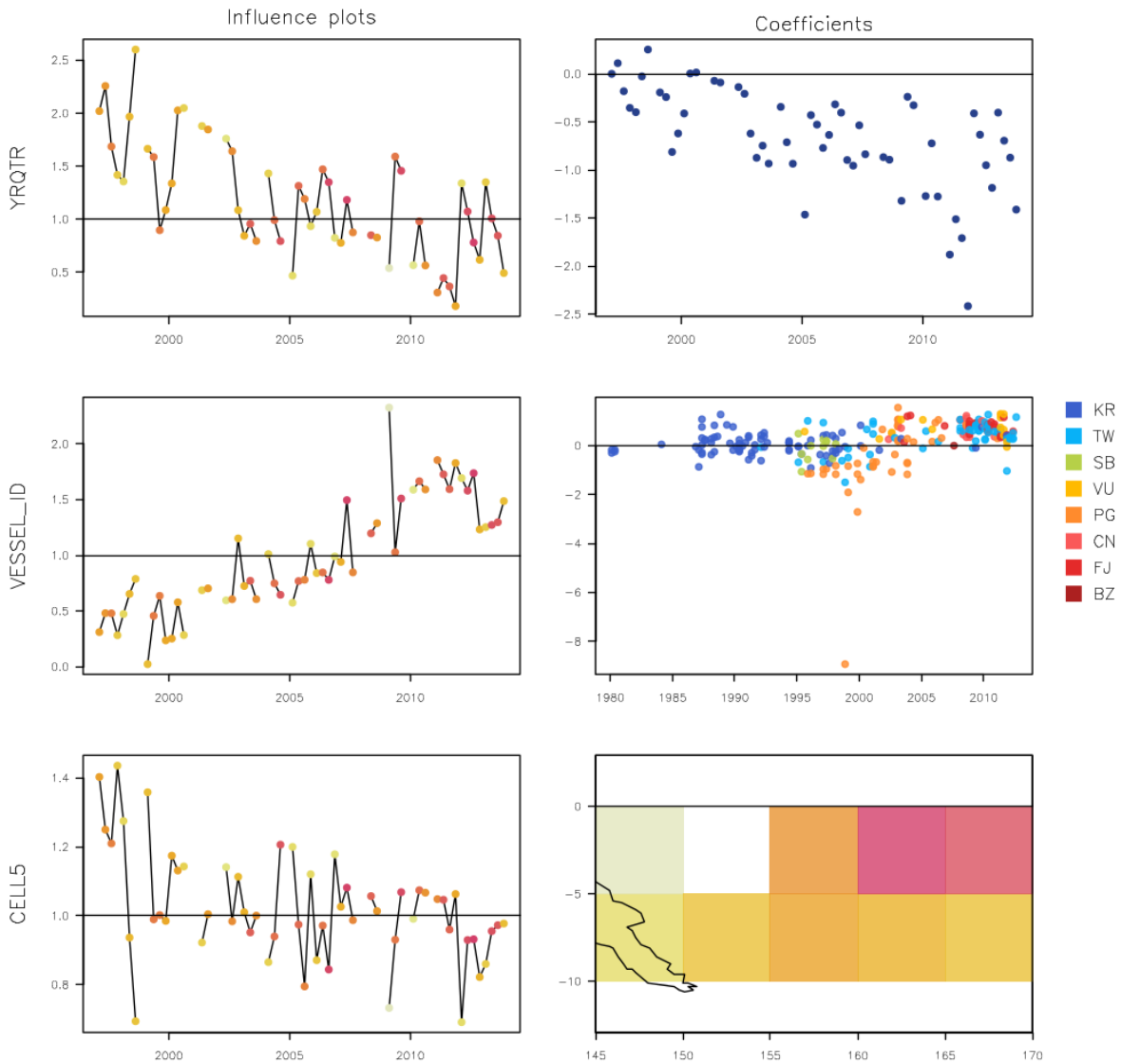


Figure 59: Summary plots of fitted GLM coefficients by variable for region 1: influence plots (left) over the time-span of the indices, colour-coded by relative sample size (yellows: low, reds: high), and model coefficients (right) for vessels ordered by first year of activity, and for cells arranged spatially.

Region 1 (Negative binomial): $\text{cnt} \sim \text{as.factor}(\text{yrqtr}) + \text{as.factor}(\text{cell5}) + \text{as.factor}(\text{vessel_id}) + \text{loghook}$

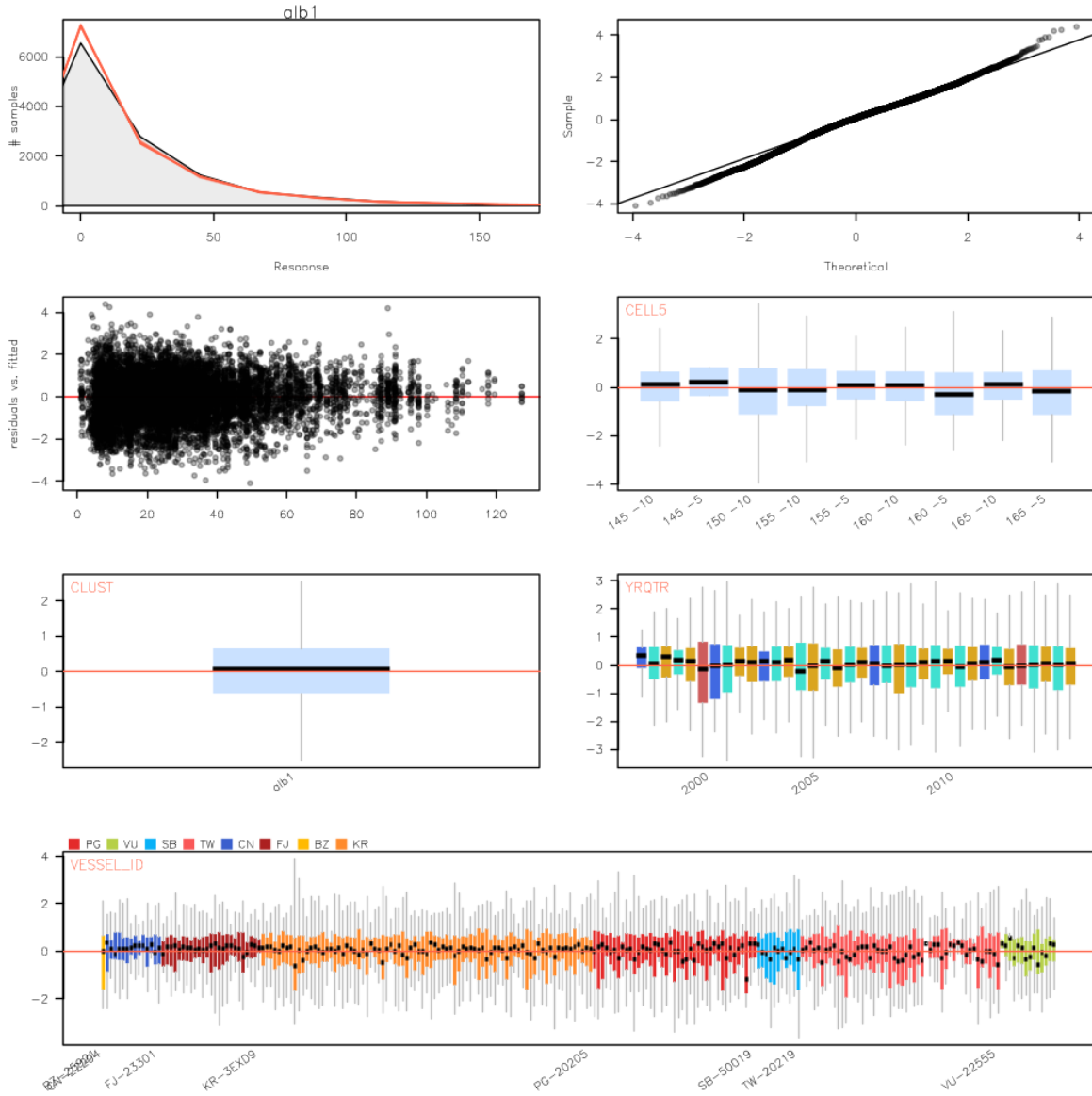


Figure 60: Diagnostic plots of fitted GLM models for region 1, step 1, showing characteristics of the model residuals and comparisons between observed and simulated data

Region 2 (Negative binomial):

$\text{cnt} \sim \text{as.factor}(\text{yrqtr}) + \text{as.factor}(\text{cell5}) + \text{as.factor}(\text{vessel_id}) + \text{loghook}$

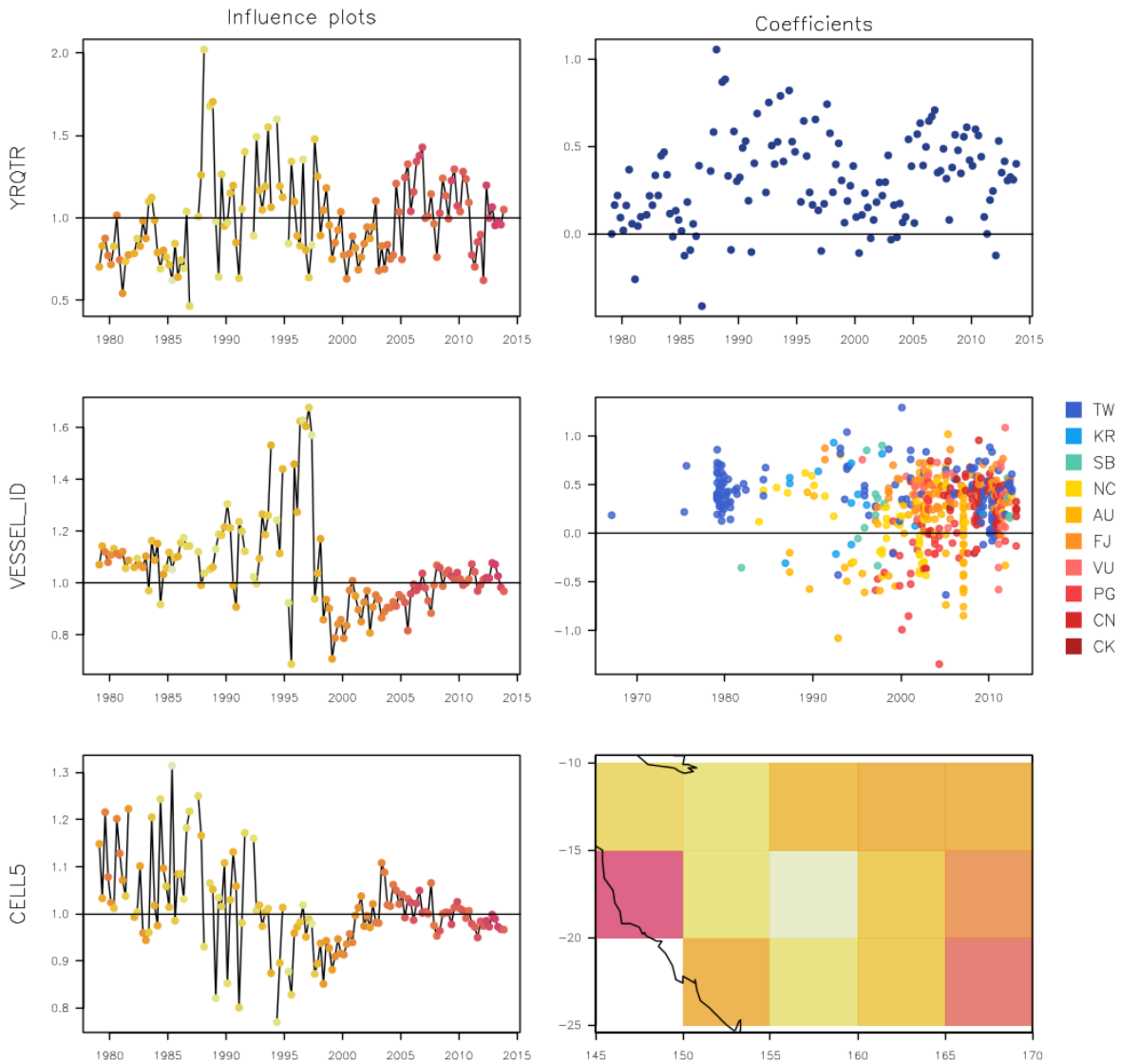


Figure 61: Summary plots of fitted GLM coefficients by variable for region 2: influence plots (left) over the time-span of the indices, colour-coded by relative sample size (yellows: low, reds: high), and model coefficients (right) for vessels ordered by first year of activity, and for cells arranged spatially.

Region 2 (Negative binomial): $\text{cnt} \sim \text{as.factor}(\text{yrqtr}) + \text{as.factor}(\text{cell5}) + \text{as.factor}(\text{vessel_id}) + \text{loghook}$

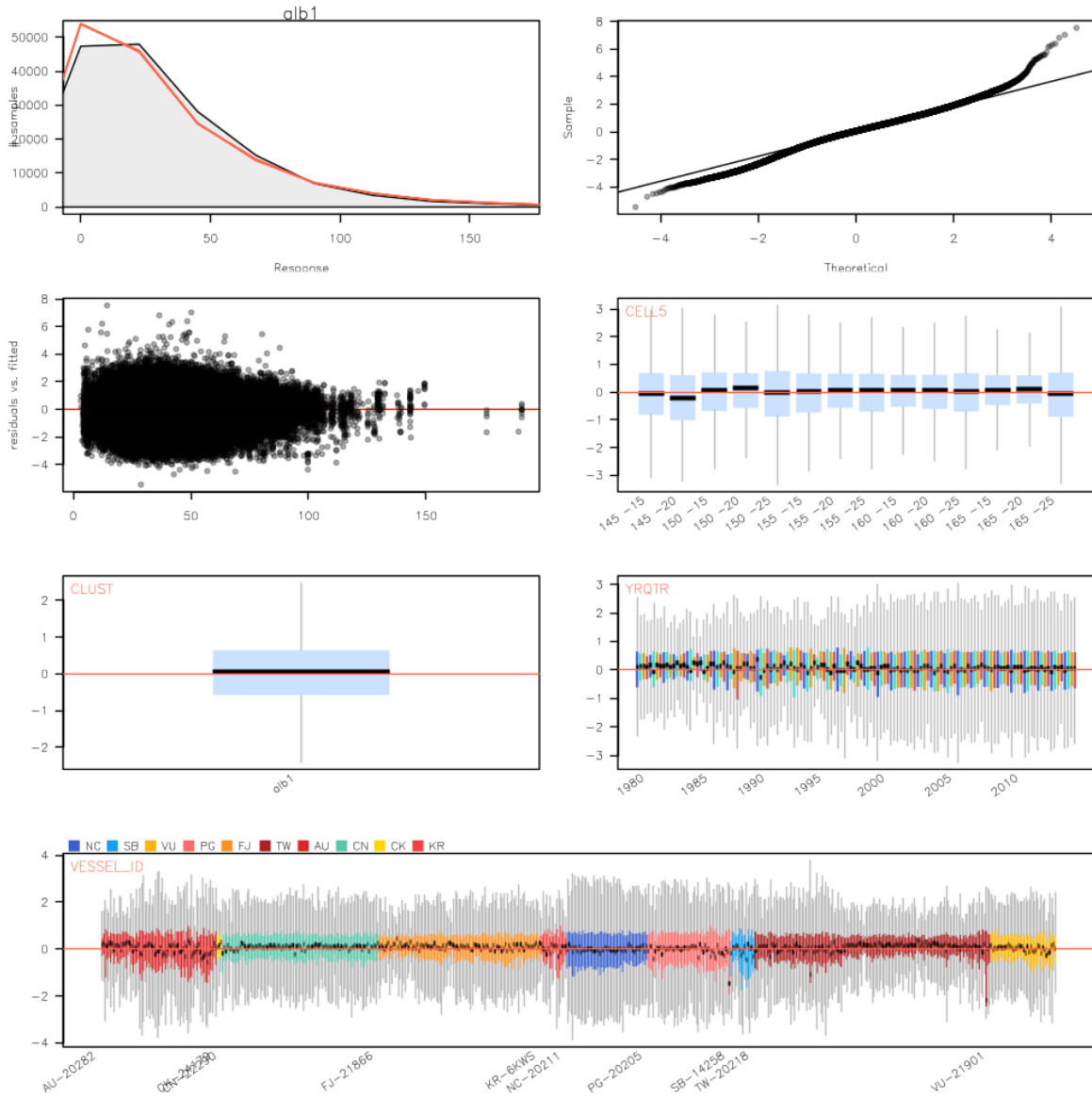


Figure 62: Diagnostic plots of fitted GLM models for region 2, step 1, showing characteristics of the model residuals and comparisons between observed and simulated data

Region 3 (Negative binomial):

$\text{cnt} \sim \text{as.factor}(\text{yrqtr}) + \text{as.factor}(\text{cell5}) + \text{as.factor}(\text{vessel_id}) + \text{loghook}$

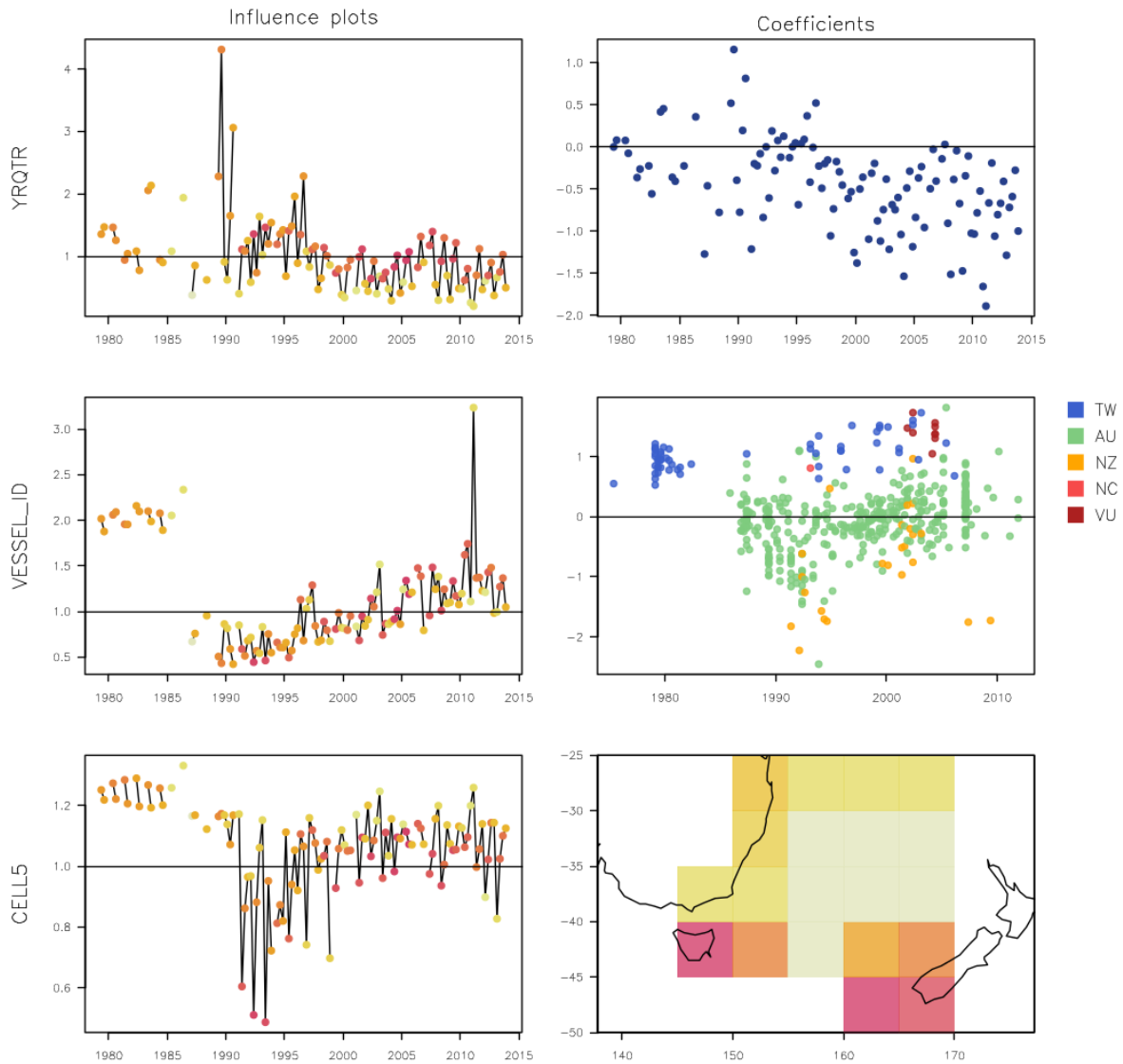


Figure 63: Summary plots of fitted GLM coefficients by variable for region 3: influence plots (left) over the time-span of the indices, colour-coded by relative sample size (yellows: low, reds: high), and model coefficients (right) for vessels ordered by first year of activity, and for cells arranged spatially.

Region 3 (Negative binomial): $\text{cnt} \sim \text{as.factor}(\text{yrqtr}) + \text{as.factor}(\text{cell5}) + \text{as.factor}(\text{vessel_id}) + \text{loghook}$

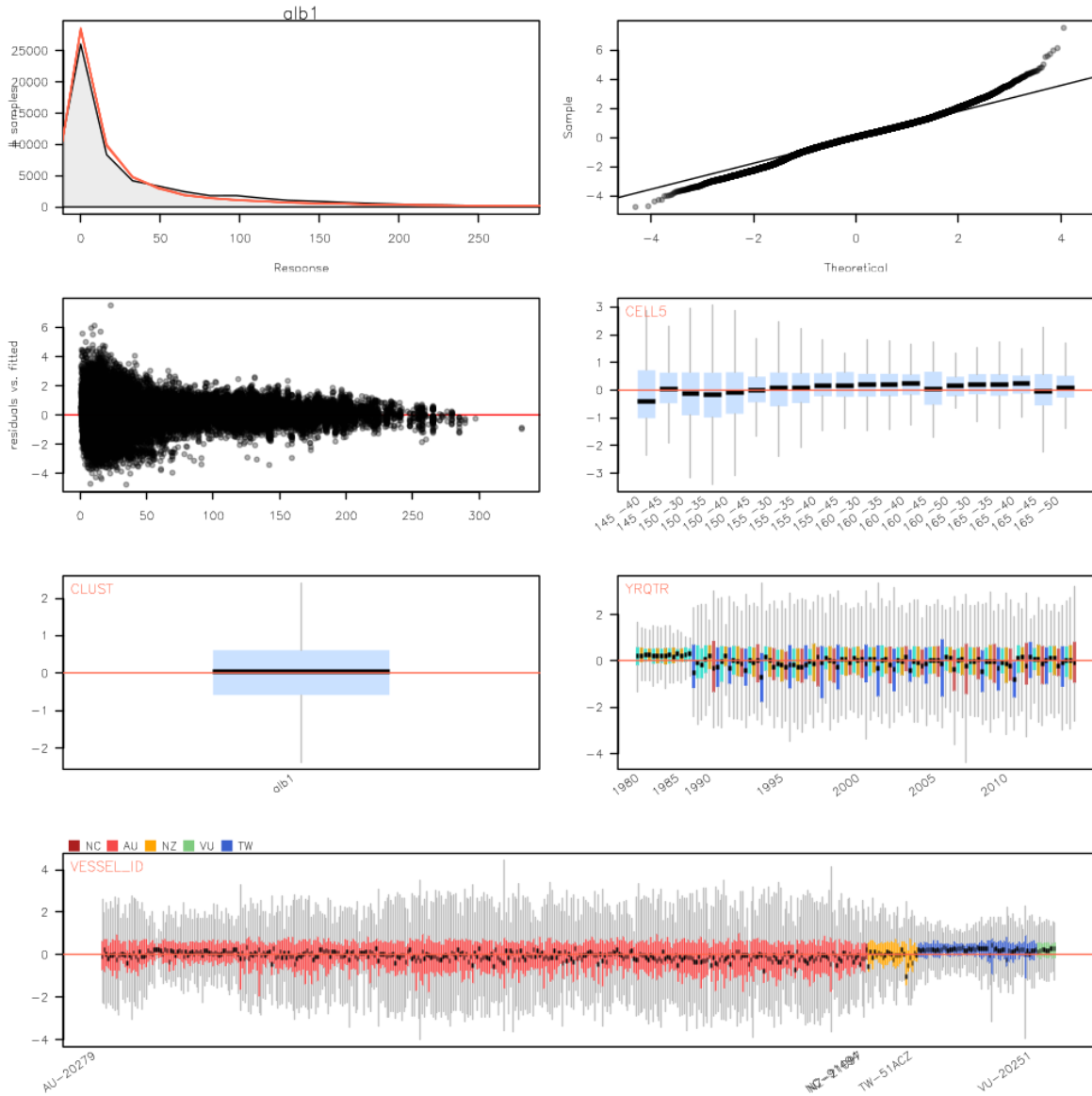


Figure 64: Diagnostic plots of fitted GLM models for region 3, step 1, showing characteristics of the model residuals and comparisons between observed and simulated data

Region 4 (Negative binomial):

$\text{cnt} \sim \text{as.factor}(\text{yrqtr}) + \text{as.factor}(\text{cell5}) + \text{as.factor}(\text{vessel_id}) + \text{as.factor}(\text{clust4.vessel.yq4}) + \text{loghook}$

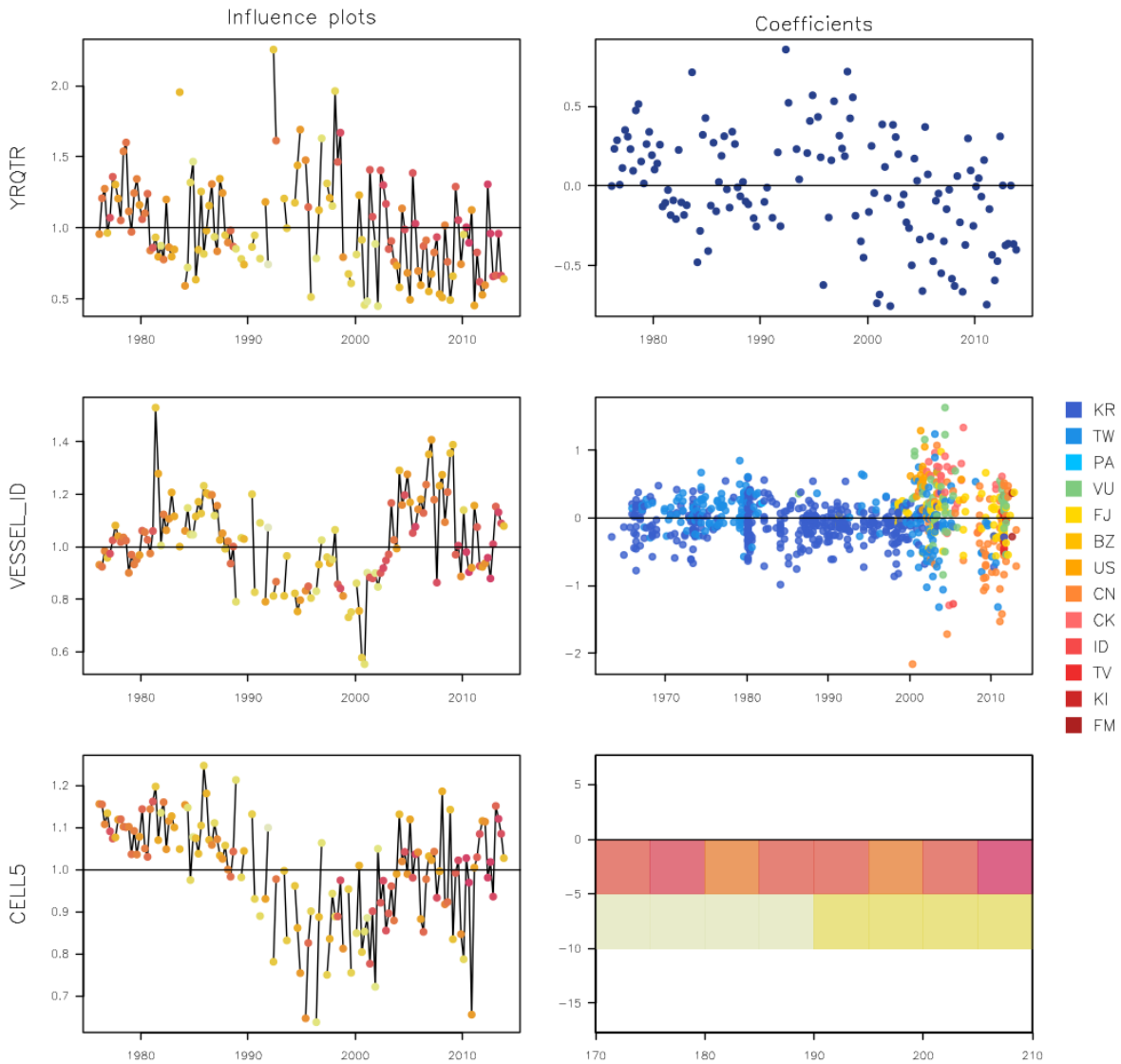


Figure 65: Summary plots of fitted GLM coefficients by variable for region 4: influence plots (left) over the time-span of the indices, colour-coded by relative sample size (yellows: low, reds: high), and model coefficients (right) for vessels ordered by first year of activity, and for cells arranged spatially.

Region 4 (Negative binomial): $\text{cnt} \sim \text{as.factor}(\text{yrqtr}) + \text{as.factor}(\text{cell5}) + \text{as.factor}(\text{vessel_id}) + \text{as.factor}(\text{clust4.vessel.yq4})$

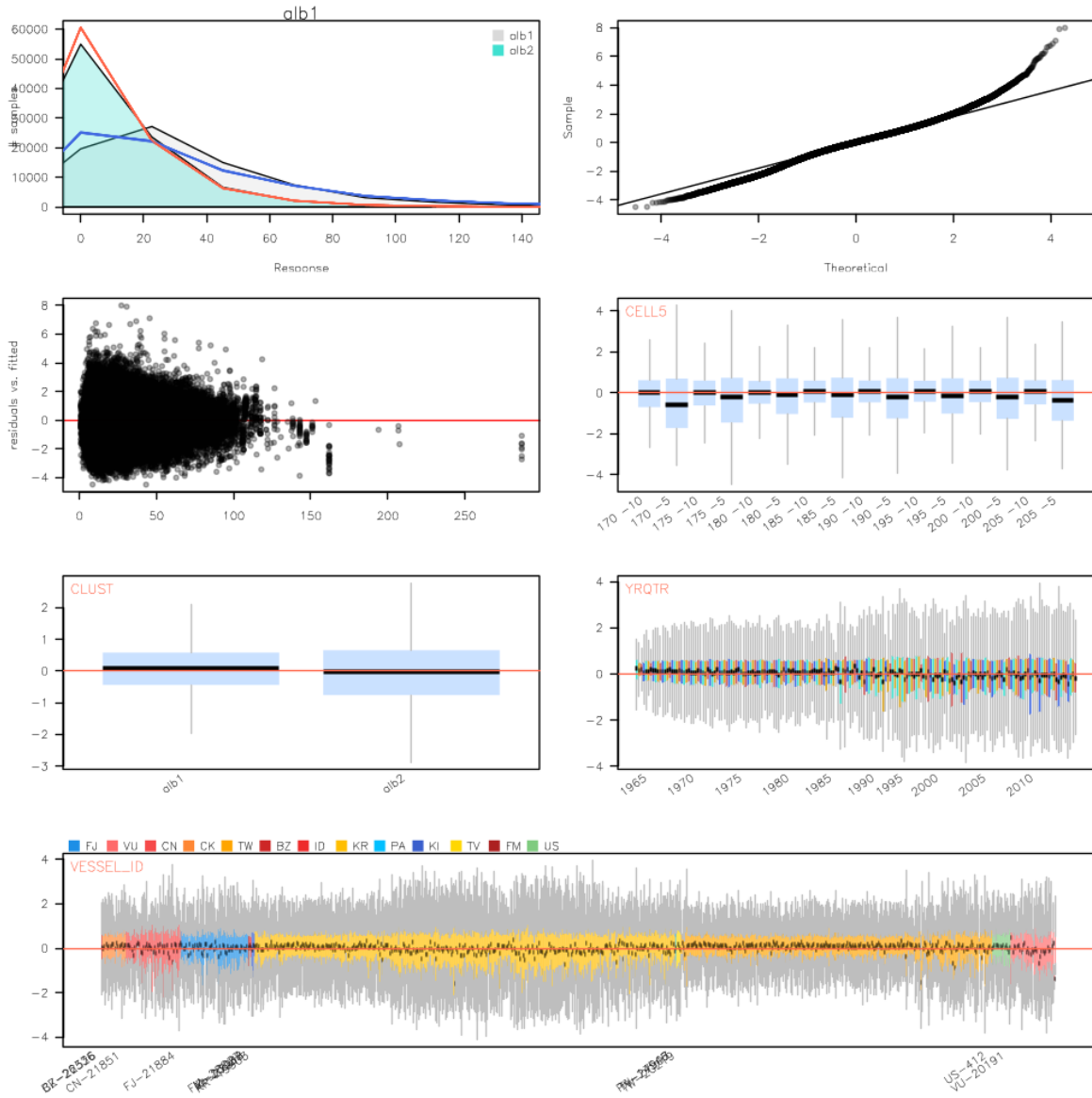


Figure 66: Diagnostic plots of fitted GLM models for region 4, step 1, showing characteristics of the model residuals and comparisons between observed and simulated data

Region 5 (Negative binomial):

$\text{cnt} \sim \text{as.factor}(\text{yrqtr}) + \text{as.factor}(\text{cell5}) + \text{as.factor}(\text{vessel_id}) + \text{as.factor}(\text{clust3.vessel.yq4}) + \text{loghook}$

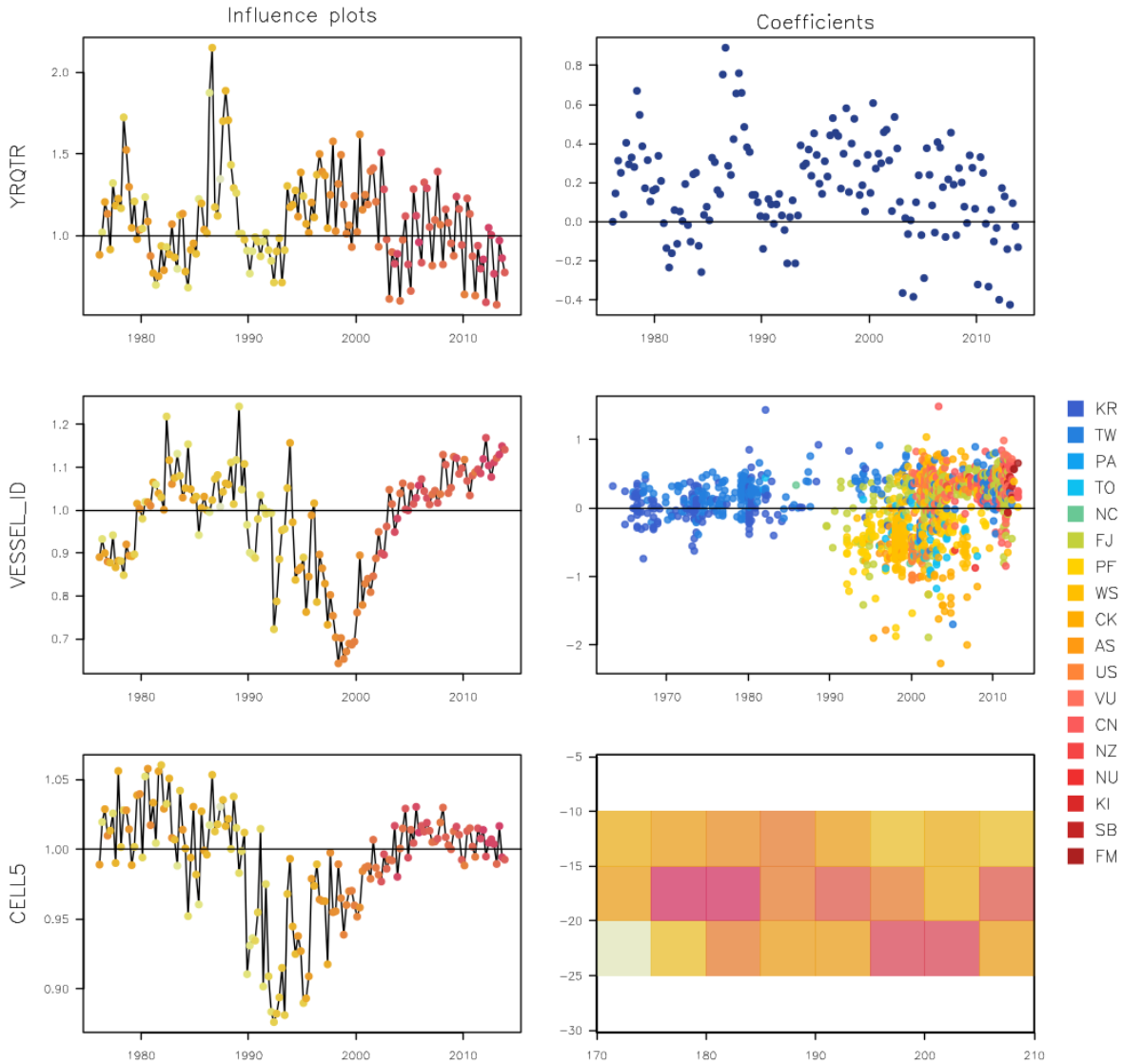


Figure 67: Summary plots of fitted GLM coefficients by variable for region 5: influence plots (left) over the time-span of the indices, colour-coded by relative sample size (yellows: low, reds: high), and model coefficients (right) for vessels ordered by first year of activity, and for cells arranged spatially.

Region 5 (Negative binomial): $\text{cnt} \sim \text{as.factor}(\text{yrqtr}) + \text{as.factor}(\text{cell5}) + \text{as.factor}(\text{vessel_id}) + \text{as.factor}(\text{clust3.vessel.yq4})$

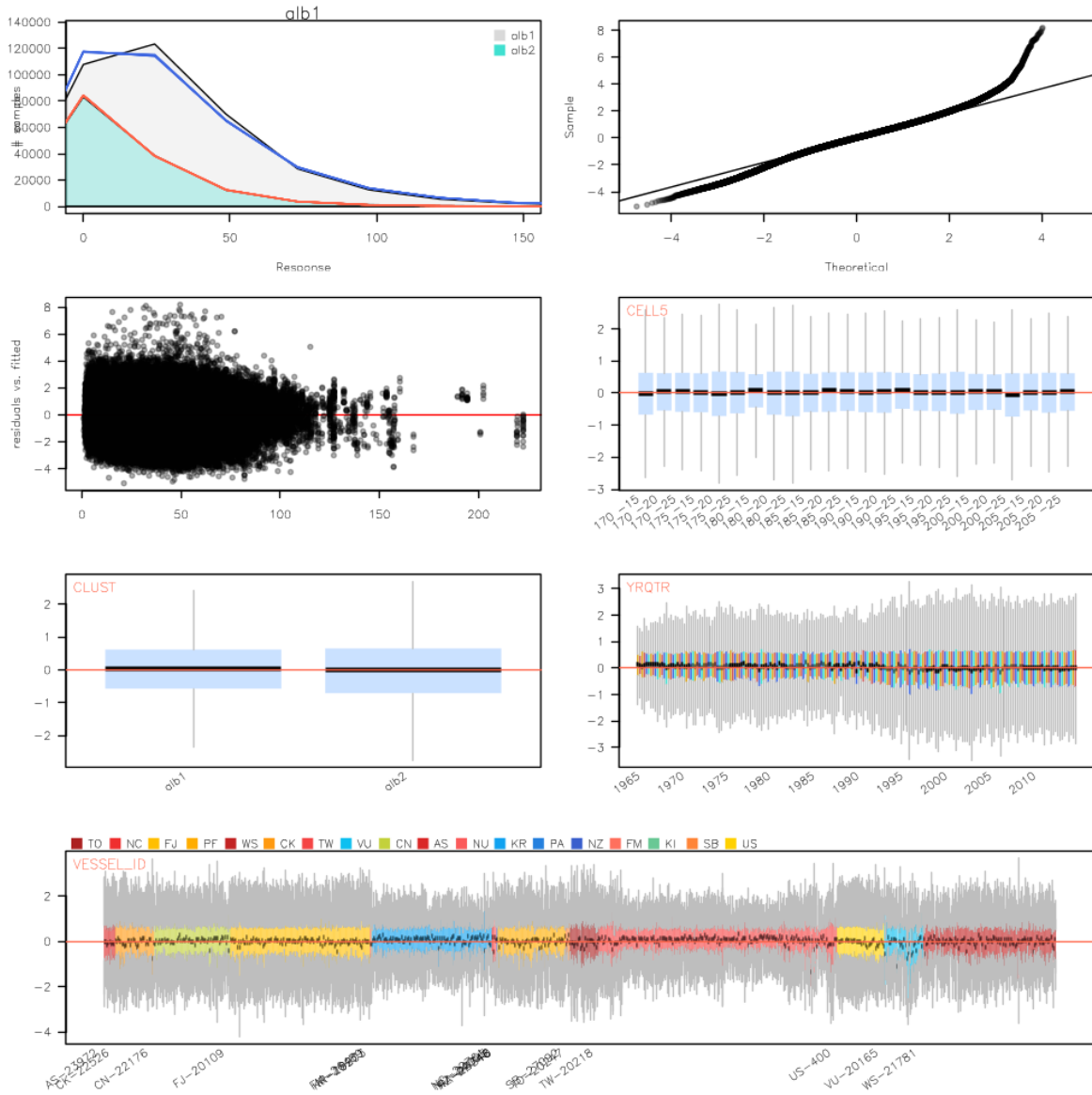


Figure 68: Diagnostic plots of fitted GLM models for region 5, step 1, showing characteristics of the model residuals and comparisons between observed and simulated data

Region 6 (Negative binomial):

$\text{cnt} \sim \text{as.factor}(\text{yrqtr}) + \text{as.factor}(\text{cell5}) + \text{as.factor}(\text{vessel_id}) + \text{loghook}$

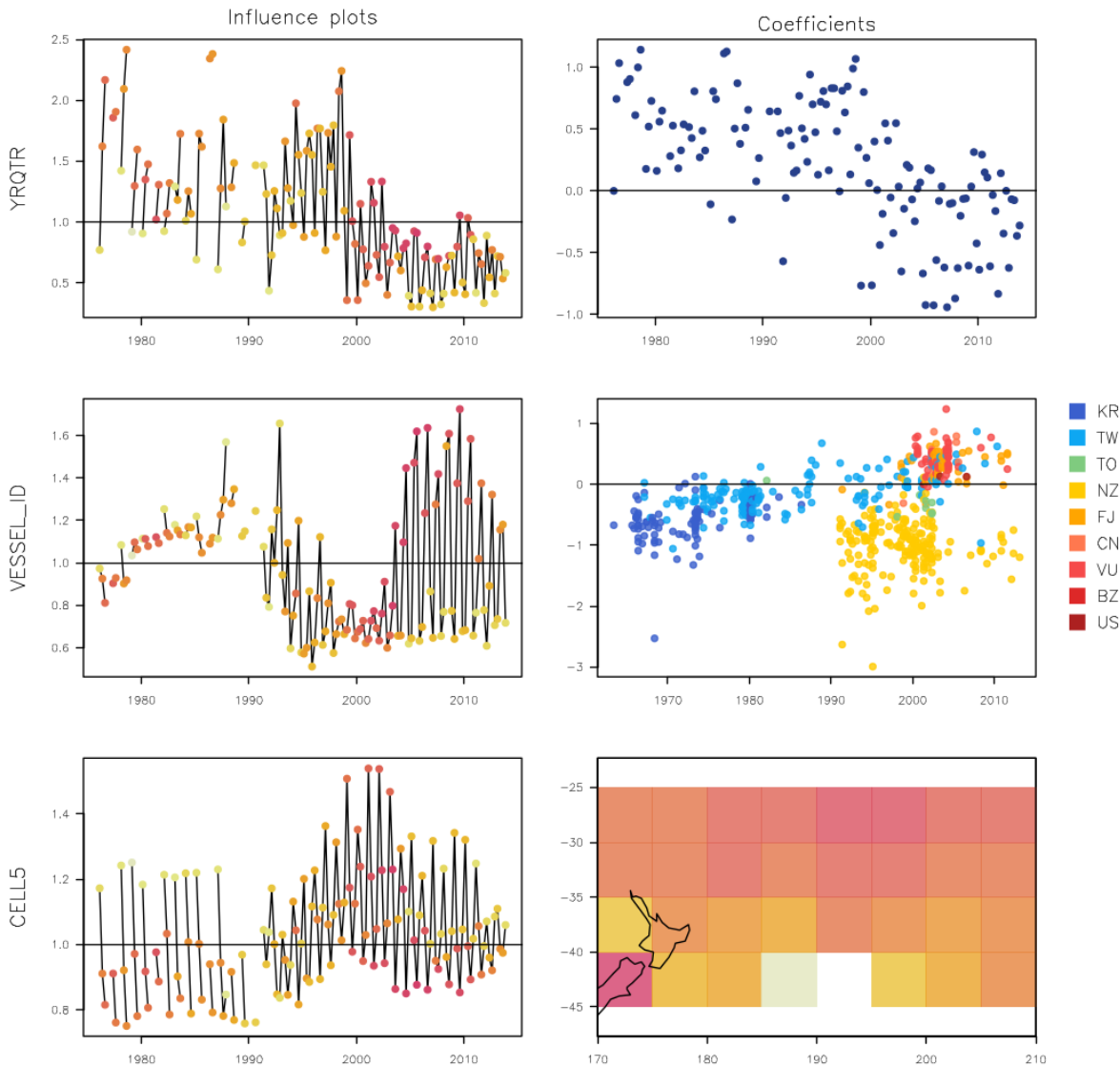


Figure 69: Summary plots of fitted GLM coefficients by variable for region 6: influence plots (left) over the time-span of the indices, colour-coded by relative sample size (yellows: low, reds: high), and model coefficients (right) for vessels ordered by first year of activity, and for cells arranged spatially.

Region 6 (Negative binomial): $\text{cnt} \sim \text{as.factor}(\text{yrqtr}) + \text{as.factor}(\text{cell5}) + \text{as.factor}(\text{vessel_id}) + \text{loghook}$

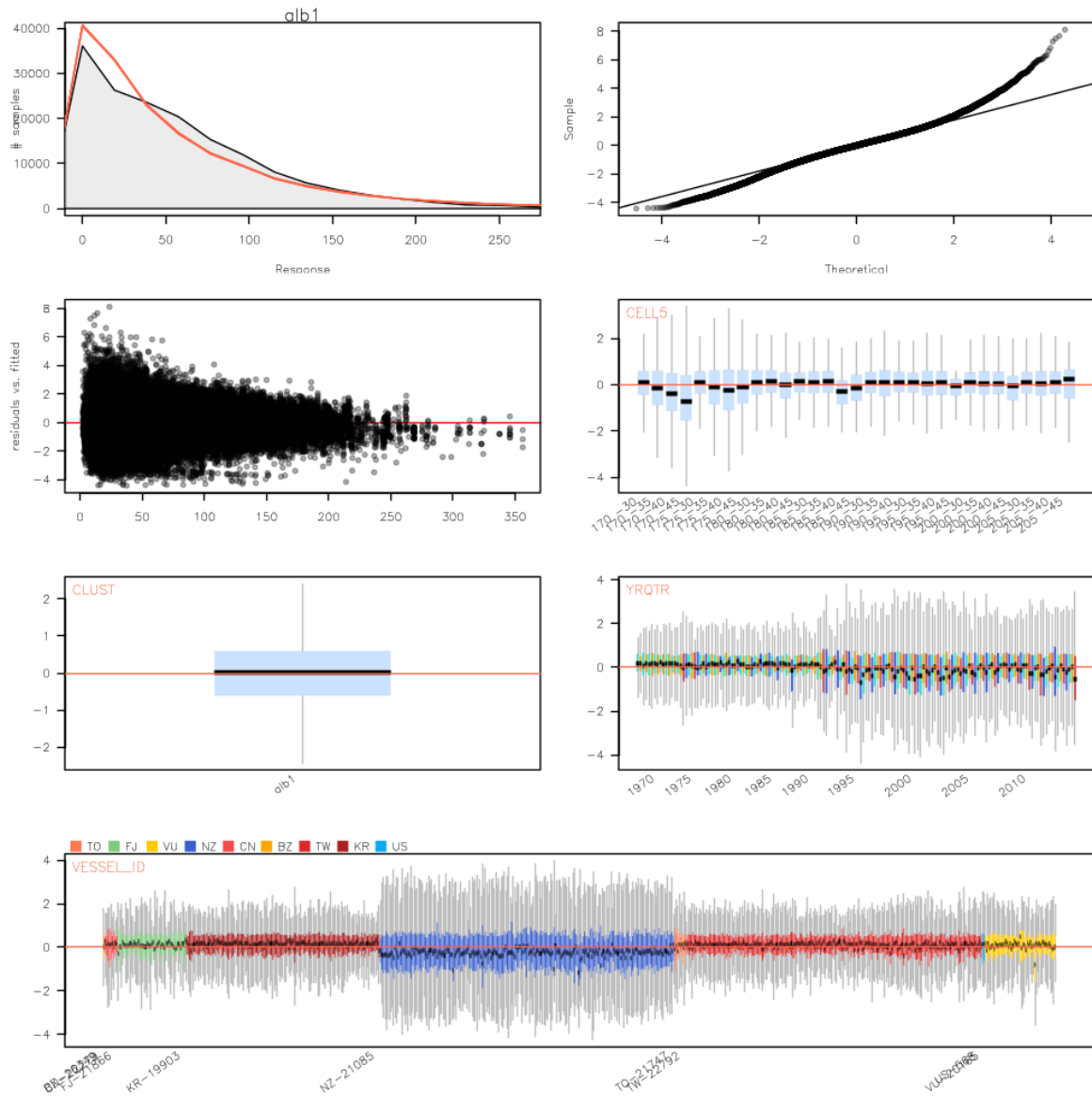


Figure 70: Diagnostic plots of fitted GLM models for region 6, step 1, showing characteristics of the model residuals and comparisons between observed and simulated data

Region 7 (Negative binomial):

$\text{cnt} \sim \text{as.factor}(\text{yrqtr}) + \text{as.factor}(\text{cell5}) + \text{as.factor}(\text{vessel_id}) + \text{loghook}$

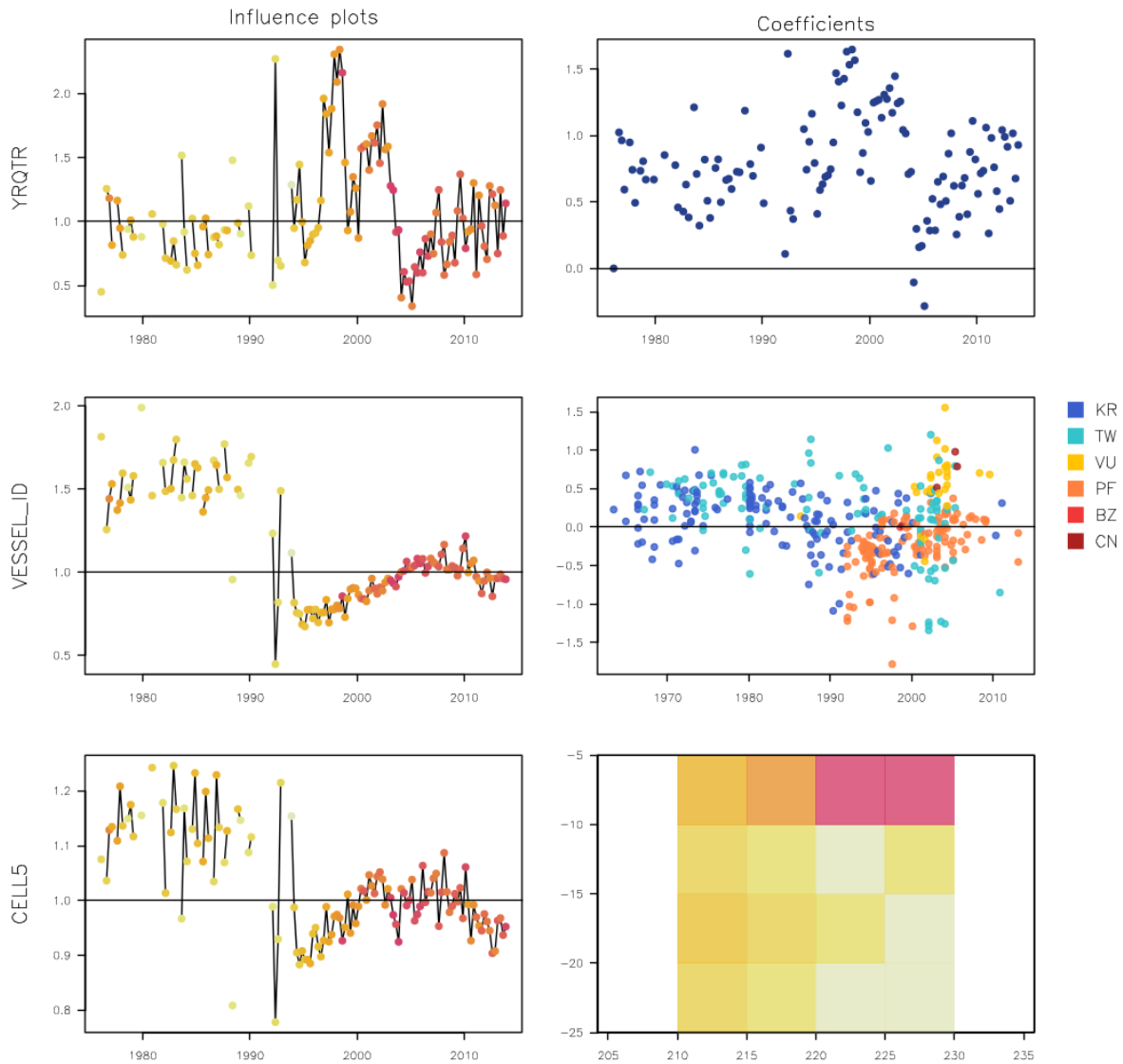


Figure 71: Summary plots of fitted GLM coefficients by variable for region 7: influence plots (left) over the time-span of the indices, colour-coded by relative sample size (yellows: low, reds: high), and model coefficients (right) for vessels ordered by first year of activity, and for cells arranged spatially.

Region 7 (Negative binomial): $\text{cnt} \sim \text{as.factor}(\text{yrqtr}) + \text{as.factor}(\text{cell5}) + \text{as.factor}(\text{vessel_id}) + \text{loghook}$

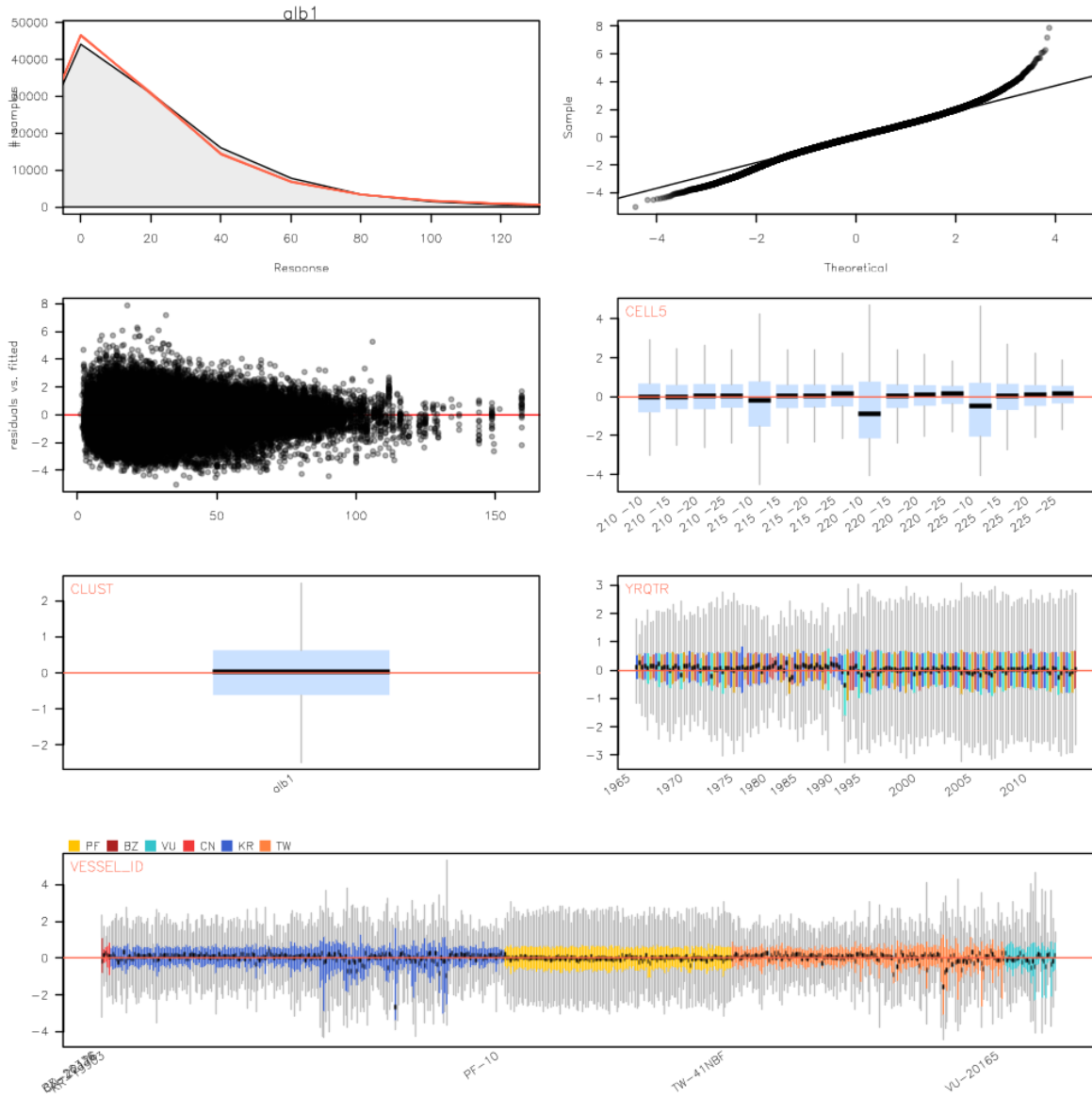


Figure 72: Diagnostic plots of fitted GLM models for region 7, step 1, showing characteristics of the model residuals and comparisons between observed and simulated data

Region 8 (Negative binomial):

$\text{cnt} \sim \text{as.factor}(\text{yrqtr}) + \text{as.factor}(\text{cell5}) + \text{as.factor}(\text{vessel_id}) + \text{loghook}$

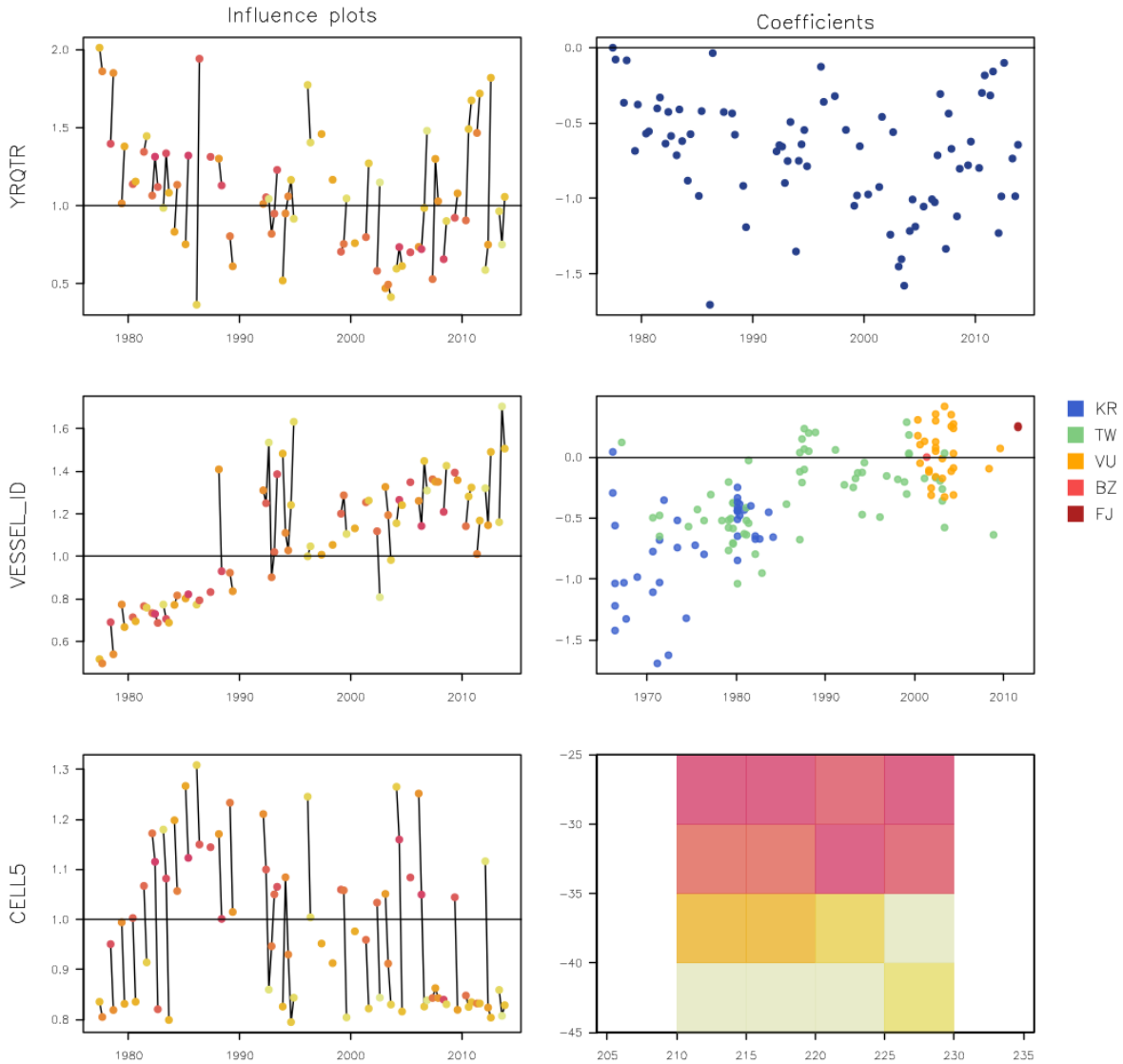


Figure 73: Summary plots of fitted GLM coefficients by variable for region 8: influence plots (left) over the time-span of the indices, colour-coded by relative sample size (yellows: low, reds: high), and model coefficients (right) for vessels ordered by first year of activity, and for cells arranged spatially.

Region 8 (Negative binomial): $\text{cnt} \sim \text{as.factor}(\text{yrqtr}) + \text{as.factor}(\text{cell5}) + \text{as.factor}(\text{vessel_id}) + \text{loghook}$

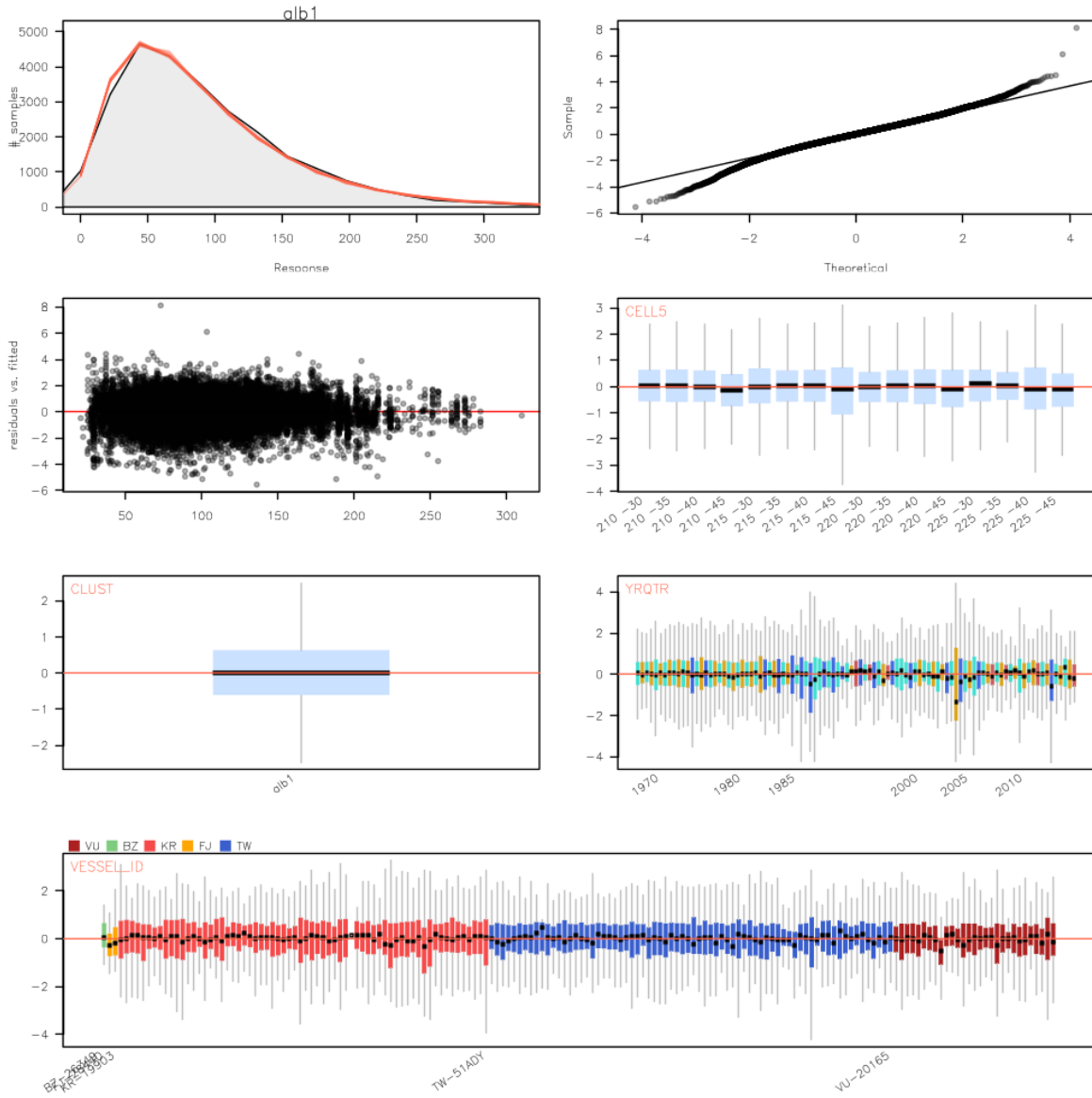


Figure 74: Diagnostic plots of fitted GLM models for region 8, step 1, showing characteristics of the model residuals and comparisons between observed and simulated data

A Appendix

Weighted standardized CPUE indices

The current region-wise CPUE indices assume that abundance trends in unfished cells are well represented by those observed for fished cells in the same region. This is a very strong assumption early in the time-series, where fished cells tend to represent only a small proportion of the cells available for fishing in the region. Another scenario, explored here, would be to assume that unfished cells show no decline in abundance until they are fished for the first time. In other words, as soon as cells have been fished at least once, they have been “discovered” by the fishery and we assume that their abundance trends match those of other fished cells in the region (i.e. go back to the initial assumption). Even this scenario is conservative as, presumably, once all cells have been discovered (see plateau in bottom panel of figures 75 to 82), unfished cells should have lower productivity than fished cells.

In order to extract CPUE indices for this alternative scenario, we first extracted GLM-based standardized CPUE indices (we will call those the “region indices”) and normalize them so that the first year-quarter is equal to one (i.e. B_0). Then, for each cell:

1. identify the first year-quarter with a record of fishing. This can be done with the raw or with the filtered dataset (below shown with filtered dataset)
2. for each year-quarter in the time-span 1960-2014, classify the cell as “never fished”, “fished in the current quarter”, “currently unfished but fished before”
3. assign standardized CPUE for each cell as 1 (i.e. equal to the first year of the region indices) if the cell has never been fished, or assign region index for that quarter if the cell is currently fished, or has been fished in the past

At this stage, each cell within the region has a relative abundance for each quarter (1 or that of the region indices). We removed all cells that have never been fished and assume abundance in those cells must be zero so that they are not included in the adjusted indices.

The new CPUE indices are then calculated, as usual, as the mean relative abundance of all cells in the region for each quarter. This series will converge with the region indices as the proportion of unfished cells goes to zero (see top panel with the two series converging over time, and middle panel with total catch for reference).

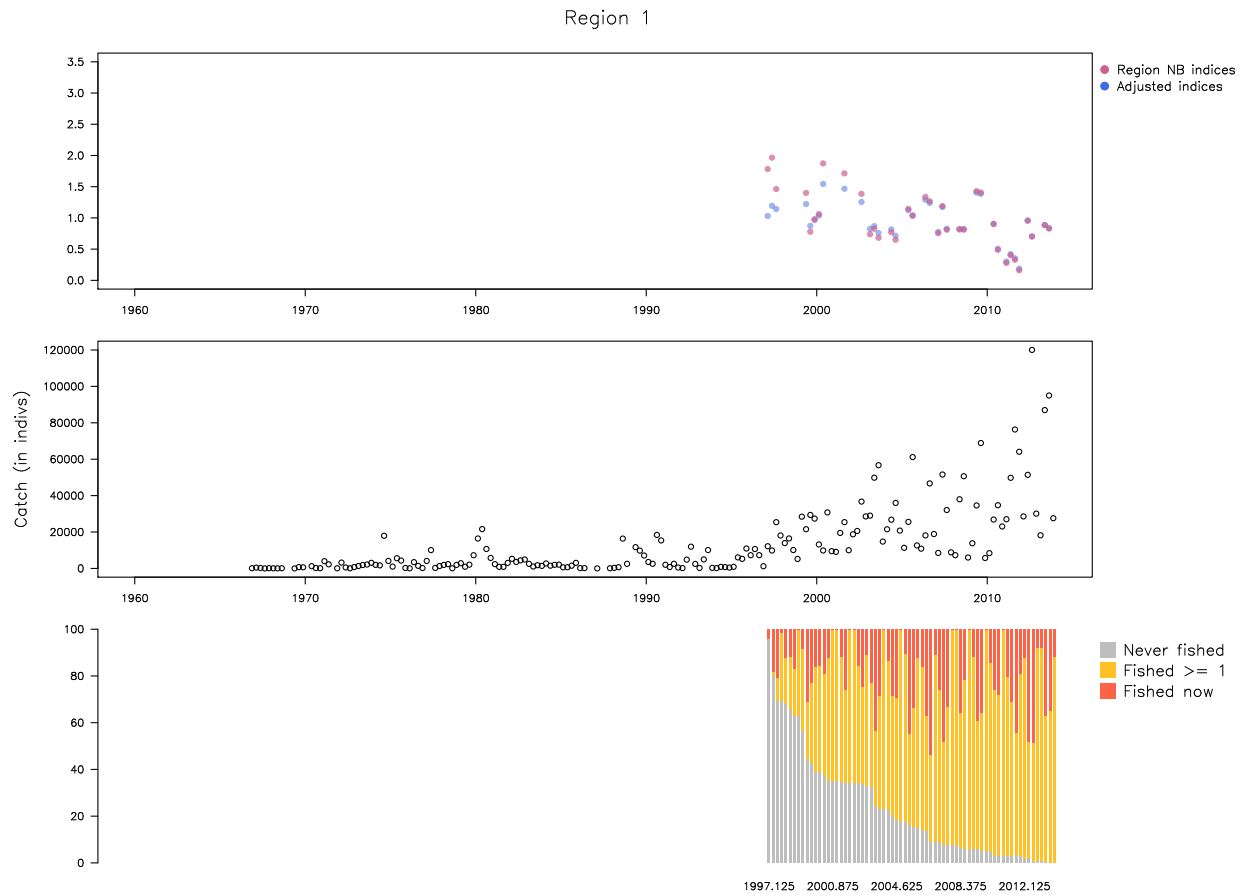


Figure 75: Summary of standardized CPUE series for region 1 corrected for limited sampling in early years. Top: Standardized indices (negative binomial) (pink) *vs.* corrected indices in blue. Middle: Catch by year in albacore individual for the region. Bottom: Relative status of cells over the history of the fishery, with cells never fished throughout excluded.

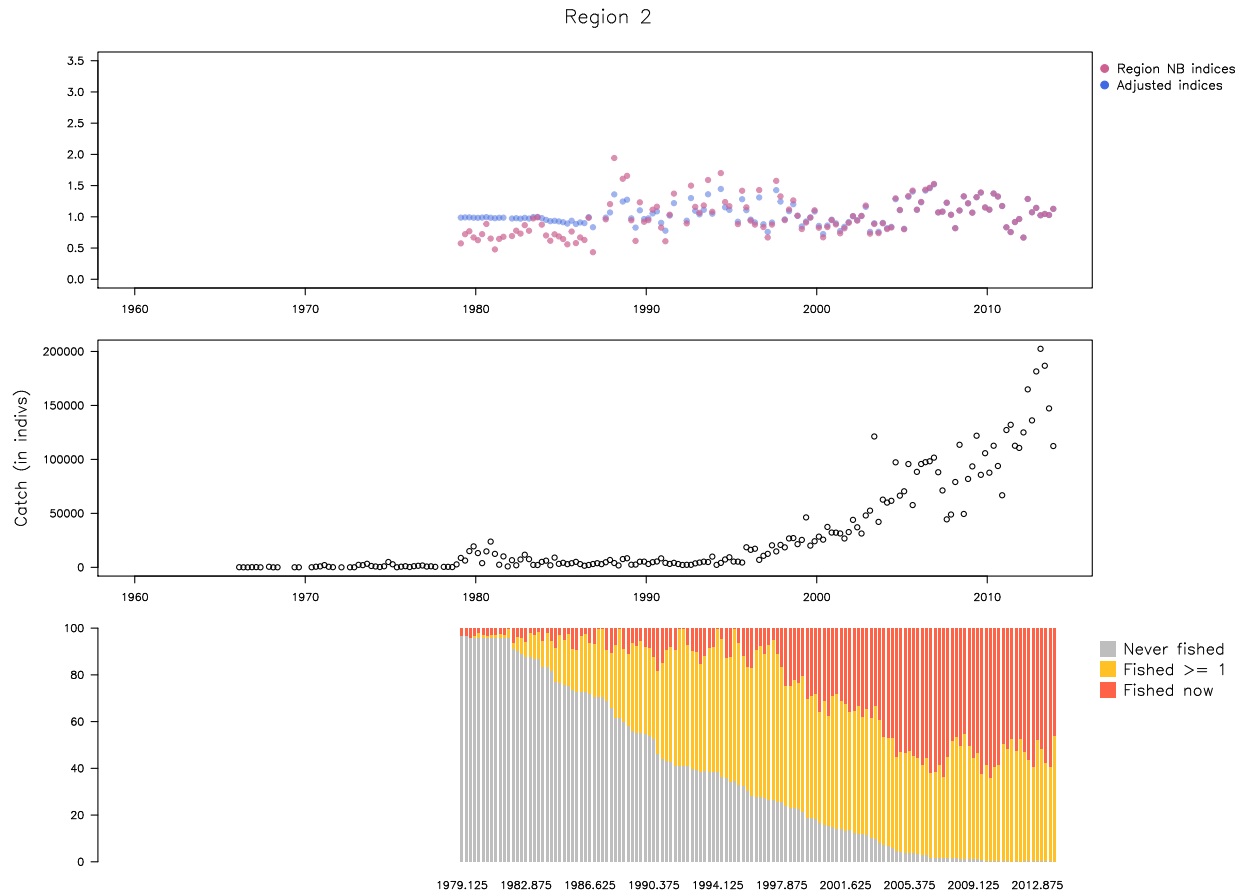


Figure 76: Summary of standardized CPUE series for region 2 corrected for limited sampling in early years. Top: Standardized indices (negative binomial) (pink) *vs.* corrected indices in blue. Middle: Catch by year in albacore individual for the region. Bottom: Relative status of cells over the history of the fishery, with cells never fished throughout excluded.

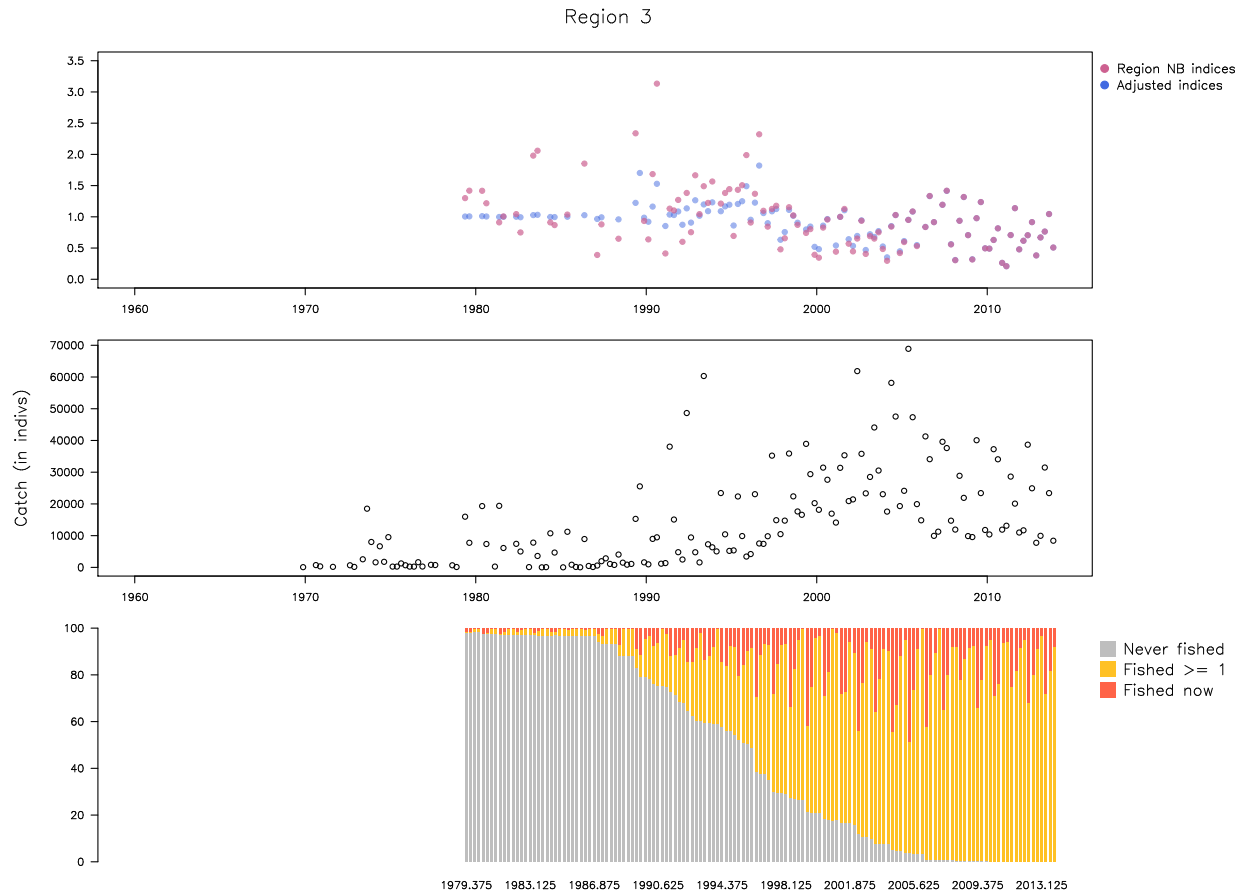


Figure 77: Summary of standardized CPUE series for region 3 corrected for limited sampling in early years. Top: Standardized indices (negative binomial) (pink) *vs.* corrected indices in blue. Middle: Catch by year in albacore individual for the region. Bottom: Relative status of cells over the history of the fishery, with cells never fished throughout excluded.

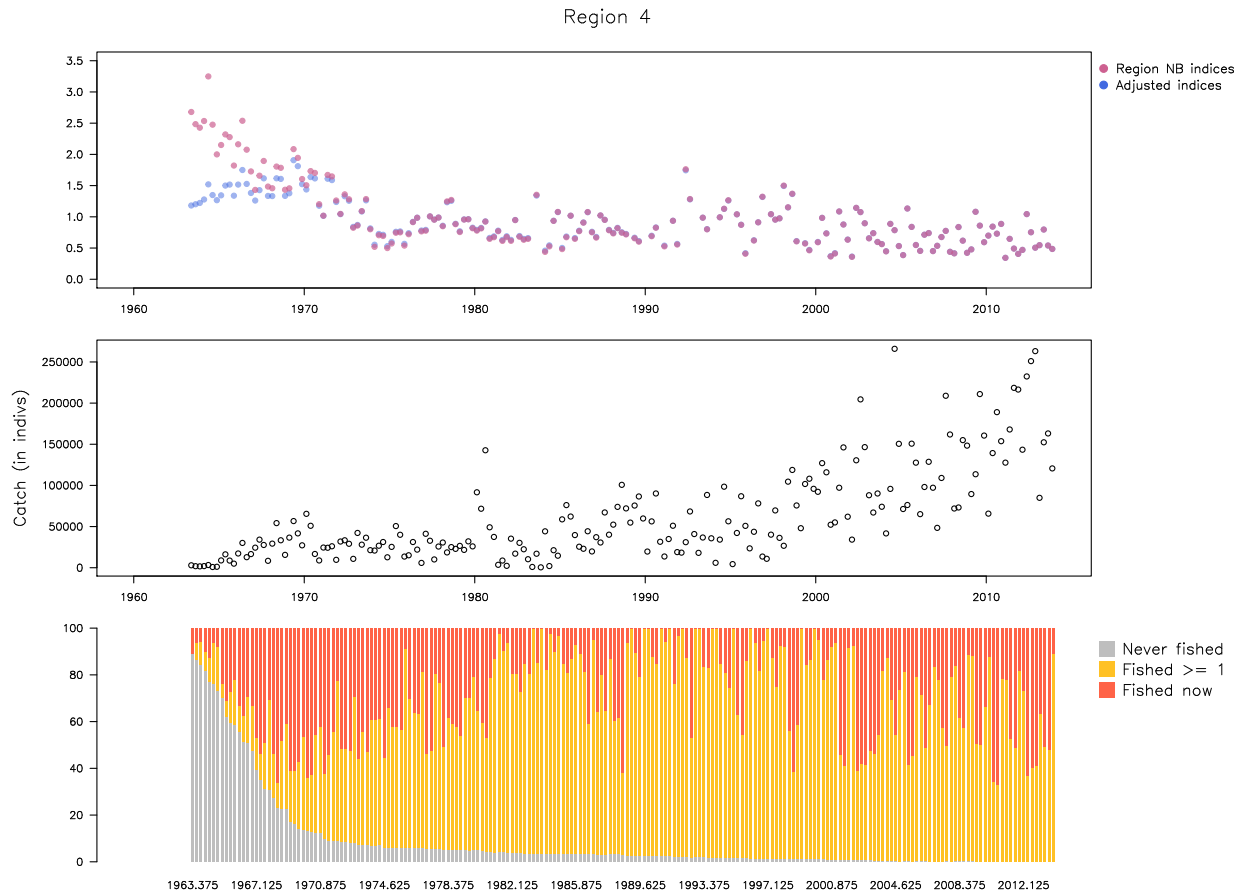


Figure 78: Summary of standardized CPUE series for region 4 corrected for limited sampling in early years. Top: Standardized indices (negative binomial) (pink) *vs.* corrected indices in blue. Middle: Catch by year in albacore individual for the region. Bottom: Relative status of cells over the history of the fishery, with cells never fished throughout excluded.

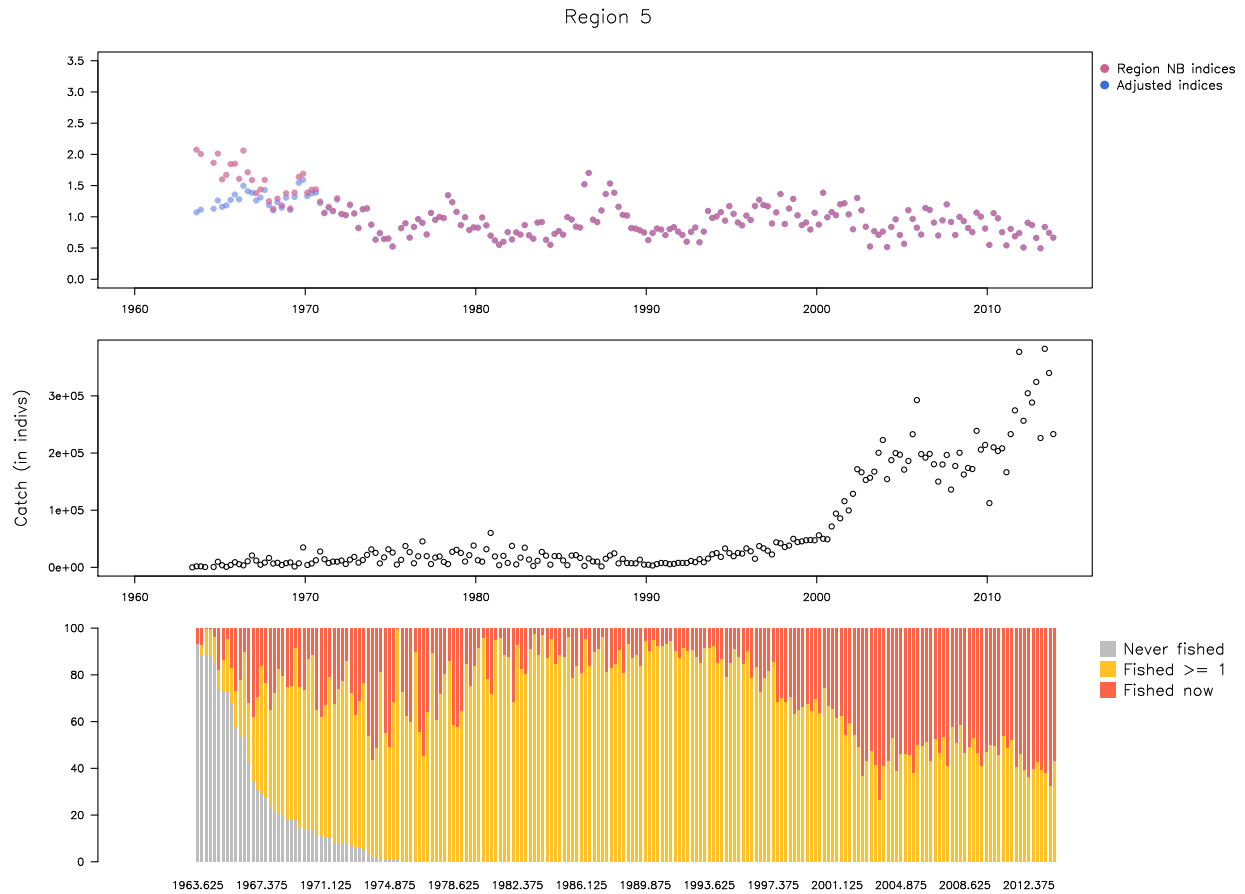


Figure 79: Summary of standardized CPUE series for region 5 corrected for limited sampling in early years. Top: Standardized indices (negative binomial) (pink) *vs.* corrected indices in blue. Middle: Catch by year in albacore individual for the region. Bottom: Relative status of cells over the history of the fishery, with cells never fished throughout excluded.

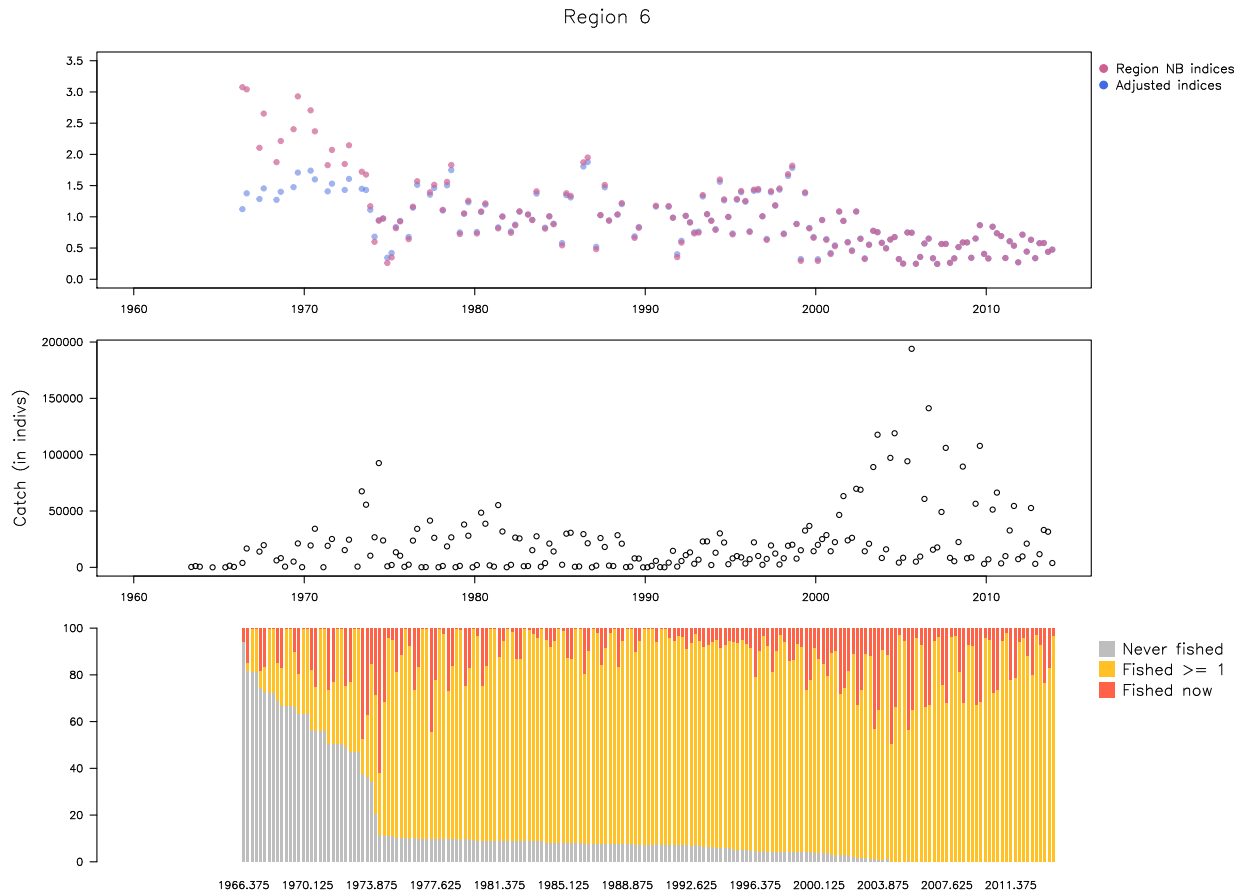


Figure 80: Summary of standardized CPUE series for region 6 corrected for limited sampling in early years. Top: Standardized indices (negative binomial) (pink) *vs.* corrected indices in blue. Middle: Catch by year in albacore individual for the region. Bottom: Relative status of cells over the history of the fishery, with cells never fished throughout excluded.

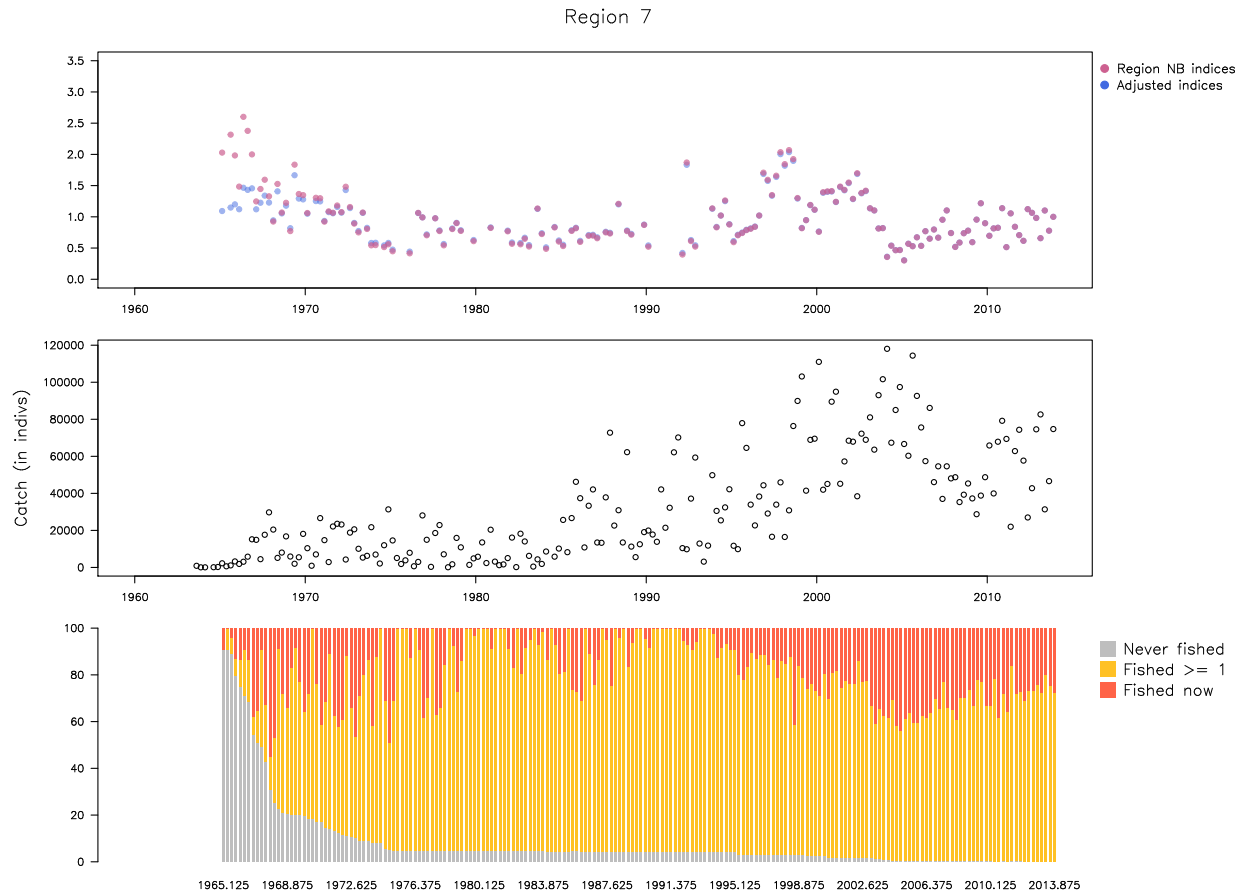


Figure 81: Summary of standardized CPUE series for region 7 corrected for limited sampling in early years. Top: Standardized indices (negative binomial) (pink) *vs.* corrected indices in blue. Middle: Catch by year in albacore individual for the region. Bottom: Relative status of cells over the history of the fishery, with cells never fished throughout excluded.

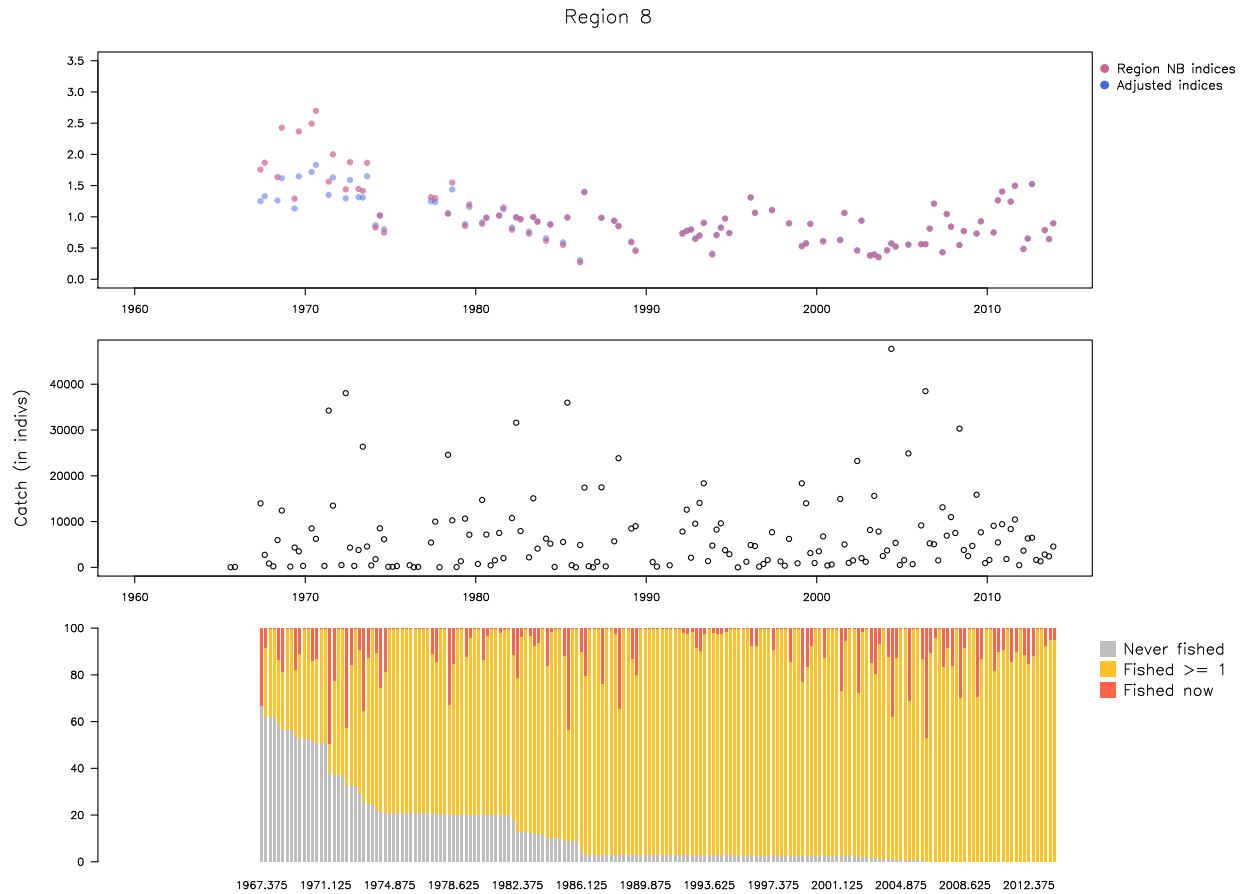


Figure 82: Summary of standardized CPUE series for region 8 corrected for limited sampling in early years. Top: Standardized indices (negative binomial) (pink) *vs.* corrected indices in blue. Middle: Catch by year in albacore individual for the region. Bottom: Relative status of cells over the history of the fishery, with cells never fished throughout excluded.